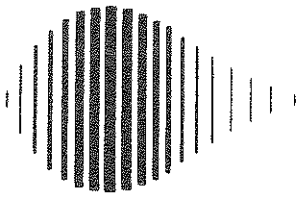

NATIONAL CENTER FOR EARTHQUAKE
ENGINEERING RESEARCH
State University of New York at Buffalo

PRELIMINARY STUDIES OF THE EFFECTS OF DEGRADING INFILL WALLS ON THE NONLINEAR SEISMIC RESPONSE OF STEEL FRAMES

by

C. Z. Chrysostomou, P. Gergely and J. F. Abel
Department of Structural Engineering
School of Civil and Environmental Engineering
Cornell University
Ithaca, New York 14853

Technical Report NCEER-88-0046

December 19, 1988

This research was conducted at Cornell University and was partially supported by the National Science Foundation under Grant No. ECE 86-07591.

NOTICE

This report was prepared by Cornell University as a result of research sponsored by the National Center for Earthquake Engineering Research (NCEER). Neither NCEER, associates of NCEER, its sponsors, Cornell University or any person acting on their behalf:

a. makes any warranty, express or implied, with respect to the use of any information, apparatus, method, or process disclosed in this report or that such use may not infringe upon privately owned rights; or

b. assumes any liabilities of whatsoever kind with respect to the use of, or the damage resulting from the use of, any information, apparatus, method or process disclosed in this report.

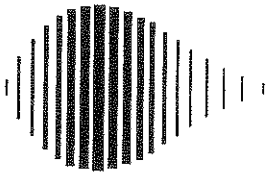

PRELIMINARY STUDIES OF THE EFFECTS OF DEGRADING INFILL WALLS ON THE NONLINEAR SEISMIC RESPONSE OF STEEL FRAMES

by

Christis Z. Chrysostomou,[1] Peter Gergely[2] and John F. Abel[3]

December 19, 1988

Technical Report NCEER-88-0046

NCEER Contract Numbers 86-4011, 87-1008 and 88-1005

NSF Master Contract Number ECE 86-07591

1 Graduate Research Assistant, Department of Structural Engineering, School of Civil and Environmental Engineering, Cornell University

2 Professor, Department of Structural Engineering, School of Civil and Environmental Engineering, Cornell University

3 Professor, Department of Structural Engineering, School of Civil and Environmental Engineering, Cornell University

NATIONAL CENTER FOR EARTHQUAKE ENGINEERING RESEARCH
State University of New York at Buffalo
Red Jacket Quadrangle, Buffalo, NY 14261

PREFACE

The National Center for Earthquake Engineering Research (NCEER) is devoted to the expansion and dissemination of knowledge about earthquakes, the improvement of earthquake-resistant design, and the implementation of seismic hazard mitigation procedures to minimize loss of lives and property. The emphasis is on structures and lifelines that are found in zones of moderate to high seismicity throughout the United States.

NCEER's research is being carried out in an integrated and coordinated manner following a structured program. The current research program comprises four main areas:

- Existing and New Structures
- Secondary and Protective Systems
- Lifeline Systems
- Disaster Research and Planning

This technical report pertains to Program 1, Existing and New Structures, and more specifically to system response investigations.

The long term goal of research in Existing and New Structures is to develop seismic hazard mitigation procedures through rational probabilistic risk assessment for damage or collapse of structures, mainly existing buildings, in regions of moderate to high seismicity. The work relies on improved definitions of seismicity and site response, experimental and analytical evaluations of systems response, and more accurate assessment of risk factors. This technology will be incorporated in expert systems tools and improved code formats for existing and new structures. Methods of retrofit will also be developed. When this work is completed, it should be possible to characterize and quantify societal impact of seismic risk in various geographical regions and large municipalities. Toward this goal, the program has been divided into five components, as shown in the figure below:

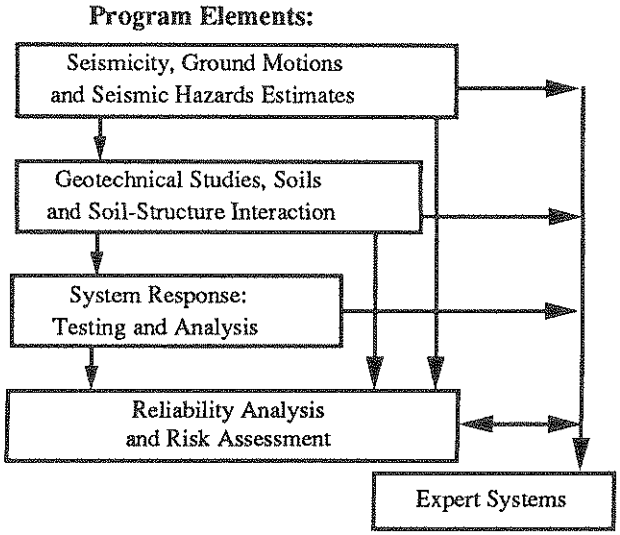

System response investigations constitute one of the important areas of research in Existing and New Structures. Current research activities include the following:

1. Testing and analysis of lightly reinforced concrete structures, and other structural components common in the eastern United States such as semi-rigid connections and flexible diaphragms.
2. Development of modern, dynamic analysis tools.
3. Investigation of innovative computing techniques that include the use of interactive computer graphics, advanced engineering workstations and supercomputing.

The ultimate goal of projects in this area is to provide an estimate of the seismic hazard of existing buildings which were not designed for earthquakes and to provide information on typical weak structural systems, such as lightly reinforced concrete elements and steel frames with semi-rigid connections. An additional goal of these projects is the development of modern analytical tools for the nonlinear dynamic analysis of complex structures.

One important problem in the systems response area is the response of buildings containing infill walls and moment-resisting frames. This report summarizes a preliminary study of the effects of infill on response. The walls are degrading and the steel frames are analyzed in the nonlinear range. This study revealed a lack of experimental data on the degradation of infill walls and, at the same time, showed needed improvements in analytical capabilities. Thus the project has provided a link between the experimental and analytical NCEER projects. After improvements are made in modeling, the analysis of various types of frames and walls will lead to a much needed understanding of the behavior of interacting walls and frames after the walls degrade, and will provide information on the period shift and on recommended values for the response modification factors.

Abstract

The effects of infills on the nonlinear response of steel frames was studied. The primary goals of this preliminary investigation were: (1) to incorporate degrading infill wall models into a nonlinear steel frame analysis program, (2) to compare the nonlinear response of a series of frames with and without infills, and (3) to utilize the Capacity Spectrum method to estimate the demand for several earthquake spectra.

The equivalent strut model was adopted to represent degrading infill walls which did not have any openings. A nonlinear static analysis program was used to calculate the load-displacement curves of a variety of steel frames.

As expected, the walls increased the capacity of the frames and decreased their initial periods. The number of hinges in the frame decreased significantly. Most of the peak lateral displacement was caused by deformations in the first story if the frame had infills at all levels.

The analysis performed in this study provided good preliminary estimates of the effects of infills on frame response. Additional experimental data is needed to refine the models and to extend their applicability to walls with openings and to evaluate the effects of walls on local frame member behavior.

TABLE OF CONTENTS

LIST OF ILLUSTRATIONS

LIST OF TABLES

SECTION 1
INTRODUCTION

1.1 Goals of the Study

Buildings consist of various types of elements. Some of them are called structural elements, for example beams and columns, which resist the loads applied to the structure and compose the structural system of a building. Others are called nonstructural elements and are usually architectural features of a building, such as partitions; these elements are not counted on carrying any loading.

A simple definition of an infill wall is a wall that occupies the space between two columns and two floors. Infills may or may not be connected to the surrounding frame elements. Infill walls are sometimes classified as structural elements but in most cases they are considered as nonstructural partitions. It was found experimentally [1], that infill walls significantly strengthen and stiffen frames. This is one of the reasons why the study of infill walls and infilled frames is important, especially for lateral dynamic loading. However, they may increase the forces induced by earthquakes. Therefore, whenever they are present and connected to the frame, it is advisable to take advantage of their strength and stiffness and consider them as load resisting elements. A second equally important reason for studying their effects is that infill walls may be used for strengthening existing buildings which have low earthquake resistance.

To be able to model and use infill walls effectively, their behavior should be first understood. Since infill walls stiffen frames, the period of the frame decreases and the seismic forces generally increase. When the wall fails during an earthquake under the increased inertia forces, there will be a rapid force transfer from the degrading wall to the frame. The frame may not be able to resist the larger forces induced by the stiff wall and may fail. Not much is known about this force transfer from infill walls to boundary frames, but studies of earthquake damage have indicated that frames have failed after the loss of their infills. The precise failure sequence has not been studied extensively, partly because the idealization of the frame-wall system is difficult. The amount of reinforcement in the wall, if any, the connection of the wall to the frame, and the properties of the frame all affect the interaction and behavior.

The purpose of this study was to gain an understanding of the behavior of infilled frames under dynamic loading. This was achieved by performing a sensitivity study of infilled steel frames using a material nonlinear model for steel and a degrading model for the infill walls. Parameters, such as the relative stiffness between the frame members and infill wall were studied and their effects on the behavior of infilled frames were examined. The problem is complex and the number of factors is large; therefore only a pilot study of this important problem is performed.

1.2 Brief Description of the Approach

Since the purpose of the study is to shed some light on the effects of infill and the load transfer during the degradation of the walls, approximate idealizations are used for the walls and for the seismic loading. Subsequent studies will utilize more sophisticated approaches.

The study consists of two distinct parts. The first part deals with the modelling and idealization of infill walls. The second with the use of the Capacity Spectrum Method for analyzing various infilled and non–infilled frames.

1.2.1 Strut Model for Infill Wall.

The infill is idealized as an equivalent strut that can resist only compression. Using empirical equations [13], an infill wall can be reduced to a strut which has the appropriate properties. The strut follows a force displacement curve which consists of a linear part until the wall crushes and then a decaying part, which idealizes the degradation of the infill. Experimental evidence is so sparse that more accurate models cannot yet be developed. The model used is described in Section 2.

1.2.2 Capacity Spectrum Method

The basic idea of the method is to develop the capacity spectrum of a structure as shown in figure 1-1. To achieve this, the period shift of the structure as it approaches collapse and the corresponding acceleration levels are calculated. By comparing this capacity spectrum with earthquake spectra, one can assess the response of the structure as well as get a measure of the damage expected under a particular earthquake. The advantage of this method is that no dynamic analysis is required. Also, once the capacity spectrum for a particular structure has been obtained, various input spectra can be used for testing the structure without doing any further analysis. The method only requires the performance of nonlinear static analyses and a way for obtaining the change in the fundamental period of the structure as it undergoes strength and stiffness degradation. The method is summarized in Section 3.

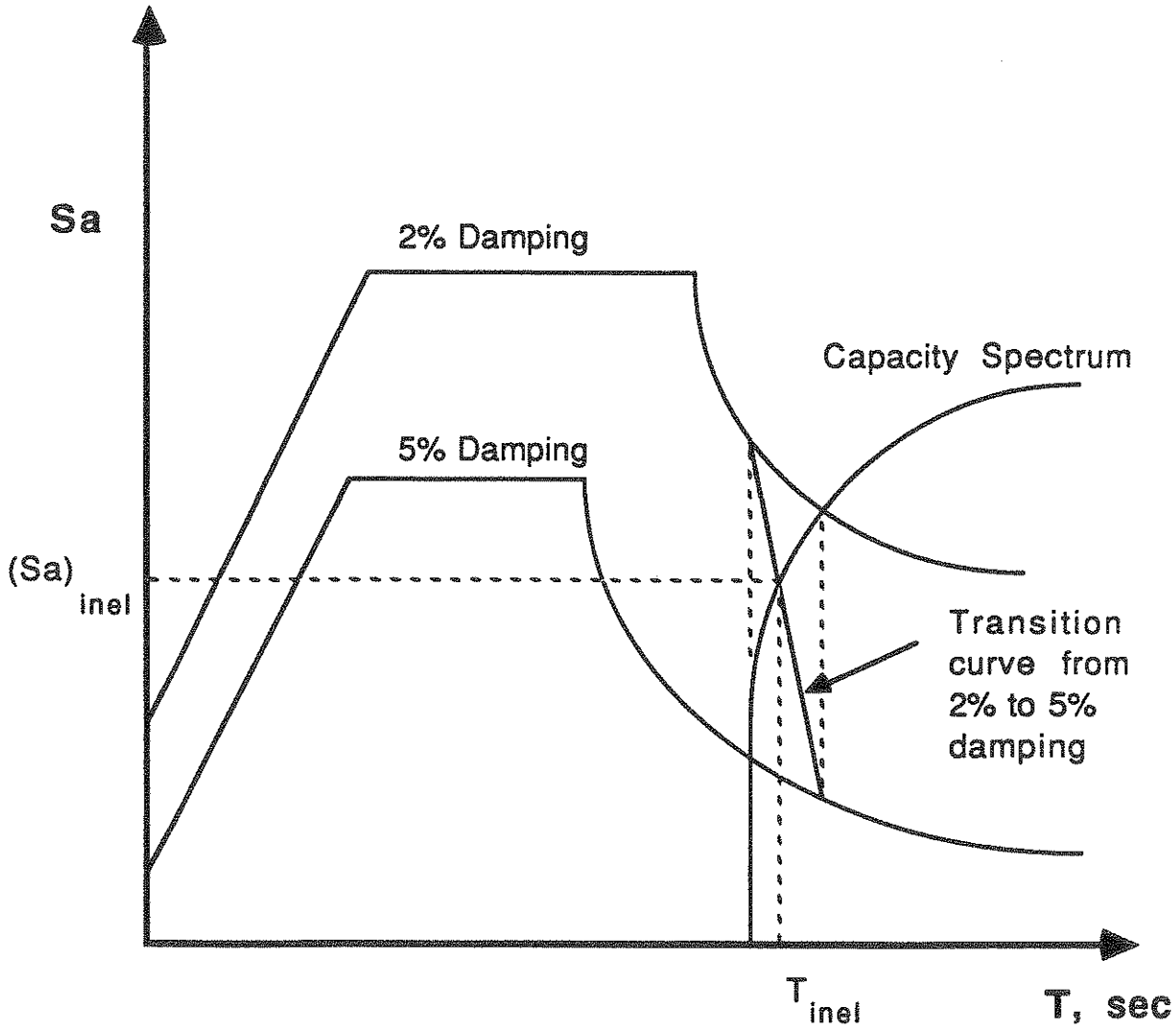

FIGURE 1-1

Capacity and Demand Spectra.

1.2.3 STAND for nonlinear steel frames.

Both the modelling of the infill wall and the capacity spectrum method were implemented in the previous version of the Static Analysis and Design program (STAND), developed at Cornell University. The input to this program comes from the Preprocessor for Framed structures (PREPF) which has also been developed at Cornell University. STAND is an interactive program for analyzing and designing steel structures using the AISC Load and Resistance Factor Design (LRFD) specification. The user can perform both linear elastic and nonlinear analysis and use the results from either for designing a structure to meet the requirements of the LRFD specification. The program STAND is described briefly in Section 4.

1.3 Description of Example Structures

The major problem in the study was the lack of sufficient experimental results for steel infilled frames. Nearly all of the experimental results are for concrete infilled frames. Therefore it was decided to perform a parametric study, and compare the overall behavior of the frames with that observed in the experimental work.

Two sets of frames were used for the analysis. The first set is for evaluating the model for the infill walls and the second for studying the effects of infill walls on the nonlinear seismic response of steel frames using the Capacity Spectrum Method. For the first case two frames were used:

1. A two–story structure loaded laterally. For this structure the wall is much stiffer than the frame. The dimensions of the frame and the lateral loading, as well as the properties of the concrete block wall are shown in figure 1-2.
2. A one–story structure loaded laterally. For this structure the frame is stiffer than

the wall. Various wall thicknesses are used. All the relevant information is shown in figure 1-3.

For the second case three steel frames were analyzed, both with and without concrete infill walls; these were the so called Lehigh frames which are described in detail in [3]. A description of the dimensions, loading and member sizes of the buildings is given in figure 1-4 and Tables 1–I, 1–II, and 1–III.

1.4 Description of the Input Used.

Two design spectra were used for the analysis of the Lehigh frames.

1. NBK0.1

   This input consists of two elastic Newmark spectra, obtained using an acceleration of 0.1g, and damping ratios of 2% and 5%.

2. NBK0.2

   This input consists of two elastic Newmark spectra, obtained using an acceleration of 0.2g and damping ratios of 2% and 5%.

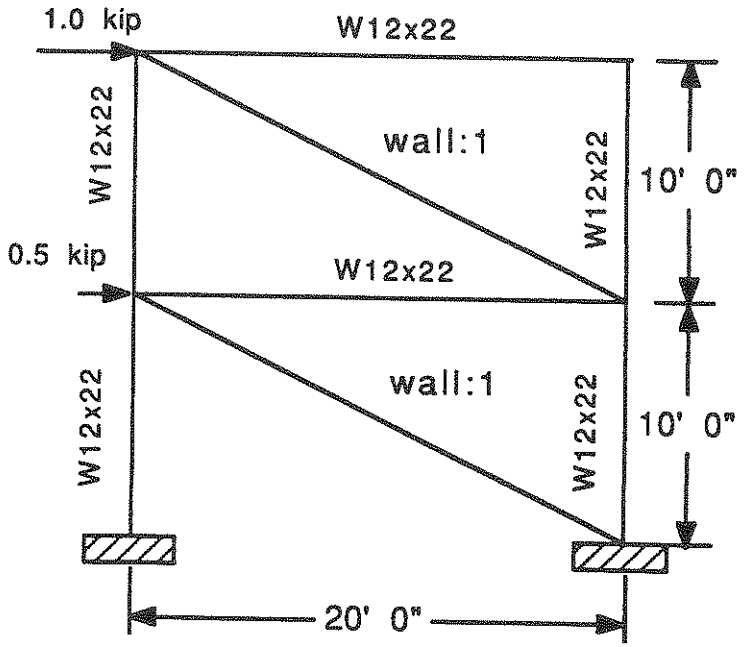

Wall properties:

A = 117.8 sq. inches

E' = 1000 ksi

fc = 1.3 ksi

t = 4.5 inches

FIGURE 1-2

Dimensions, Section Properties and Loading of Two–Story structure.

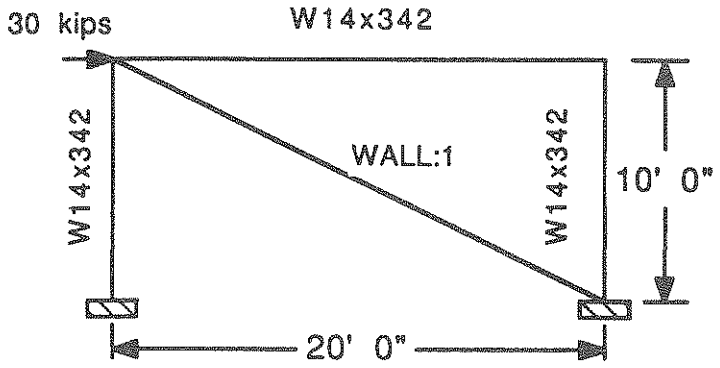

Wall properties:

A = 394.8, 274.1, 211.6, 113.4 sq. inches

E' = 1200 ksi

fc = 3.4 ksi

t = 12, 8, 6, 3 inches

FIGURE 1-3

Dimensions, Section Properties and Loading of One–Story Structure.

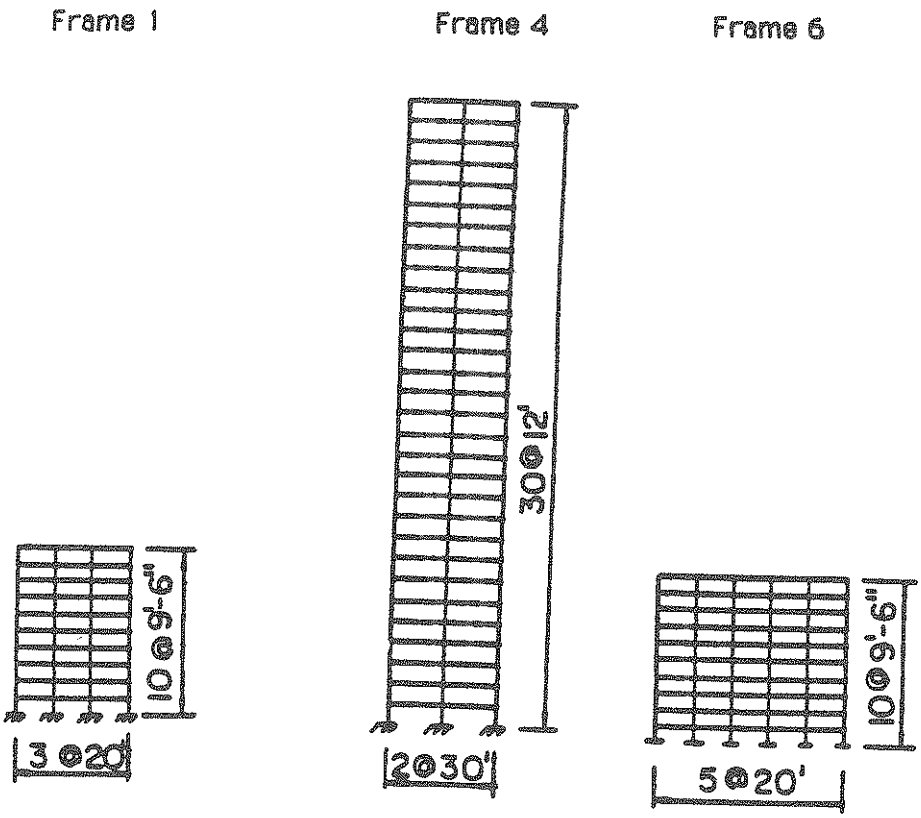

	Frame 1	Frame 4	Frame 6
Story-Bay	10-3	30-2	10-5
Spacing	20 ft	30 ft	20 ft
Roof load			
Live 30 psf		30 psf	30 psf
Dead 40 psf		40 psf	40 psf
Floor load			
Live 40 psf		75 psf	40 psf
Dead 55 psf		50 psf	55 psf
Wall(Story)	9.5 kips	18 kips	9.5 kips

FIGURE 1-4

Dimensions and Loading of Lehigh Structures.

Beams					Columns				
Levels	Design I	Design II	Design III	Design IV	Levels	Design I	Design II	Design III	Design IV
1	W12x22	W12x22	W12x22	W14x26	1-3 EXT	W8x20	W8x24	W8x20	W8x20
2	W14x22	W14x22	W14x22	"	INT	W8x17	W8x17	W8x15	W8x17
3	"	"	"	W16x31	3-5	W8x31	W8x35	W8x31	W8x31
4	"	"	"	"		W8x28	W8x31	W8x28	W8x28
5	W14x26	W14x26	W14x26	"	5-7	W8x40	W8x48	W8x40	W8x40
6	"	"	"	"		W8x40	W8x48	W8x40	W8x40
7	W14x30	W14x30	W14x30	W18x35	7-9	W8x48	W8x58	W8x48	W8x48
8	"	"	"	"		W8x58	W8x58	W8x58	W8x58
9	W16x31	W16x31	W16x31	W18x40	9-11	W8x58	W8x67	W8x58	W8x58
10	"	"	"	"		W8x67	W10x66	W8x67	W8x67

TABLE 1-I

Section Properties for Frame 1

Note: Design IV was used

Beams

Levels	Design I	Design II	Design III	Design IV
1	W21x44	W21x44		W24x76
2	W21x55	W21x55		W27x84
3	"	"		"
4	"	"		"
5	W24x61	W24x61		W30x99
6	W24x68	W24x68		W30x108
7	"	"		"
8	W24x76	W24x76		W30x116
9	"	"		"
10	"	"	Same as Design I	"
11	W24x84	W24x84		W33x118
12	"	"		"
13	W27x84	W27x84		W36x135
14	"	"		"
15	W27x94	W27x94		W36x150
16	"	"		"
17	"	"		"
18	W30x99	W30x99		W36x170
19	"	"		"
20	"	"		"
21	"	"		"
22	W30x108	W30x108		W36x182
23	"	"		"
24	"	"		"
25	W30x116	W30x116		W35x194
26	"	"		"
27	"	"		"
28	"	"		"
29	"	"		"
30	"	"		"

Columns

Levels	Design I	Design II	Design III	Design IV
1-3 EXT	W10x54	W10x60		W10x66
INT	W10x33	W10x39		W10x39
3-5	W14x68	W14x78		W14x84
	W14x68	W14x68		W14x84
5-7	W14x95	W14x103		W14x119
	W14x95	W14x103		W14x119
7-9	W14x119	W14x127		W14x142
	W14x127	W14x142		W14x158
9-11	W14x142	W14x150		W14x176
	W14x158	W14x176	Same as Design I	W14x193
11-13	W14x167	W14x184		W14x202
	W14x193	W14x211		W14x237
13-15	W14x193	W14x211		W14x237
	W14x219	W14x237		W14x264
15-17	W14x219	W14x246		W14x264
	W14x246	W14x287		W14x287
17-19	W14x246	W14x287		W14x287
	W14x287	W14x314		W14x342
19-21	W14x287	W14x314		W14x342
	W14x314	W14x342		W14x370
21-23	W14x314	W14x342		W14x370
	W14x342	W14x370		W14x398
23-25	W14x342	W14x370		W14x398
	W14x398	W14x426		W14x455
25-27	W14x370	W14x398		W14x426
	W14x426	W14x455		W14x500
27-29	W14x398	W14x455		W14x455
	W14x455	W14x500		W14x550
29-31	W14x500	W14x500		W14x605
	W14x550	W14x550		W14x665

TABLE 1-II

Section Properties for Frame 4

Note: Design IV was used

Beams					Columns				
Levels	Design I	Design II	Design III	Design IV	Levels	Design I	Design II	Design III	Design IV
1	W12x22	W12x22	W12x22	Same as Design I	1-3 EXT	W8x20	W8x24	W8x20	Same as Design I
2	W14x22	W14x22	W14x22		INT	W8x17	W8x17	W8x13	
3	"	"	"		3-5	W8x28	W8x35	W8x28	
4	"	"	"			W8x28	W8x28	W8x24	
5	"	"	"		5-7	W8x35	W8x48	W8x35	
6	"	"	"			W8x35	W8x40	W8x35	
7	W14x26	W14x26	W14x26		7-9	W8x48	W8x58	W8x48	
8	"	"	"			W8x48	W8x48	W8x48	
9	"	"	"		9-11	W8x58	W8x67	W8x58	
10	"	"	"			W8x58	W8x67	W8x58	

TABLE 1-III

Section Properties for Frame 6

Note: Design IV was used

SECTION 2

IDEALIZATION OF INFILL WALLS

The behavior of infill walls and their modes of failure is a very complex problem. The reason for this is that their behavior depends on many parameters, some of which are:

- type of material used as infill, and whether it is reinforced or unreinforced,
- interface conditions between the infills and the surrounding frame,
- relative strength and stiffness between the frame and the infill wall.

Having the above parameters in mind, many researchers developed experimental procedures to study the behavior of infilled frames and then proposed analytical models to simulate their behavior on computers.

2.1 Present knowledge of the behavior of infilled frames

One of the most important pieces of information required in dynamic analysis is the load-displacement relationship on which an analytical model is based. This relationship can be obtained by testing infilled frames under monotonic loading. The experimental work of various researchers, who tested frames under monotonic loading, is presented below.

The studies of the behavior of infilled frames goes back to the 1950's. One of the first to do research in the subject was Wood [4], who investigated the effects of brick, clinker

block, and hollow clay block infill on the lateral strength and stiffness of multistory steel frames. He concluded that in all the tests the infill strengthened and stiffened the frame and failed by sudden cracking along the compressional diagonal.

Benjamin and Williams [5,6] studied the behavior of one-story reinforced concrete and brick masonry shear panels loaded through a distributing member at the top of the wall (either a beam or a floor diaphragm). Two basic modes of failure were observed:

1. tension column failure; sudden failure by tension and shear originating at the connection between the tension column and the foundation and propagating along the base of the wall towards the compression column. This type of failure is associated with walls surrounded by very weak frames;
2. diagonal cracking in the tensile stress region along the compression diagonal. For unreinforced or lightly reinforced panels the cracking pattern depends on the amount of column reinforcement, while for moderately reinforced walls it is a function of the amount of panel reinforcement. This type of failure is associated with walls surrounded by frames strong enough to withstand tension in the windward column and shear in the leeward column.

The ultimate strength of an infilled frame was found to be a function of the extent to which the panel exhibited distributed diagonal cracking and the ability of the compression column to withstand combined shear, flexural, and compressive stresses.

Holmes [7] introduced the concept of the equivalent strut for idealizing infills. In his method he assumed a constant area for the equivalent strut and developed a simple procedure for calculating the ultimate load and the side-sway deflection of a steel frame with brickwork or concrete infilling.

Stafford Smith [8] studied the behavior of model masonry walls bounded by structural

steel frames and loaded in the vertical and lateral directions. It is reported that when the infilled frame is subject to lateral shear, two modes of failure are possible:

1. compressive failure generating from a loaded corner of the infill;
2. tension cracking along the compression diagonal of the infill.

The introduction of vertical loading, in addition to the lateral one, provided two more possible modes of infill failure:

3. vertical tension cracks from the beam to the foundation, and
4. a general compressive failure of the whole infill, roughly along a horizontal plane.

Along with his experimental investigations, Stafford Smith refined considerably the equivalent strut approach [9,10,11,12,13]. Instead of assuming constant effective width of the diagonal strut as it was the case with Holms, as mentioned above, he suggested that the effective width of an infill acting as a diagonal strut is influenced by the following factors [13]:

a. the relative stiffness of the column and the infill;
b. the length to height proportions of the infill;
c. the stress–strain relationship of the infill material
d. the value of the diagonal load acting on the infill.

Assuming no bonding between the infill and the frame and using the beam on elastic foundation approach, he derived an empirical equation for the contact length between the infill and the frame.

Mallick and Severn [14] tested a series of model steel frames infilled with plaster. Their work seems to be supporting Stafford Smith's conclusions regarding failure

criteria for plain infill panels. They concluded that the less frequent cause of failure was due to diagonal cracking and that the most common one due to crashing of one of the corners of the infill. They also noted that in prototype frames they would expect the diagonal tension cracking to be the most frequent failure mode, since the tensile strength of concrete is half that of plaster.

The latest work on the equivalent strut approach was done by Mainstone [2,15,16]. He used the same approach as Stafford to calculate the length of contact between the infill and the frame and, in addition, presents empirical equations for calculating the equivalent strut area. These are the equations that have been used in this project and are described in more detail in sections of the report to follow.

Liauw and Kwan [17,18] performed a series of experiments on scaled down models of 4–story steel frames with reinforced micro-concrete infills. They used three types of models:

1. model A in which no connectors were provided at the structural interface,
2. model B in which connectors were provided along the infill/beam interface and vertical slits of 4 mm width were provided at the infill/column interface. The function of the vertical slits was to separate the columns from the high contact pressure with the infilled panels so as to avoid premature shear failure of the columns which are considered as the most important structural elements, and
3. model C in which connectors were provided along the entire infill/frame interface to improve full structural interaction between the infilled panels and the frame.

The behavior of each of the models can be summarized as follows:

1. Models A: Separation at the tensile corners occurred almost immediately after the

models were loaded so that the panels were in contact with the frame only at the vicinity of compressive corners. However, at slightly higher loads the interface configuration became stable after the frame had gained firm contact with the panels. At greater loads, the stiffness of the models gradually decreased when the compressive corners of the panels cracked. The models reached their peak strength when the corners were crushed. Crushing of the infill appeared to occur progressively outwards from the corners and during crushing of the infill obvious signs of yielding at the steel columns were also observed. After the peak load, the models continued to sustain substantial loading (more than 85% of peak load) for a very large range of deflections.

2. Models B: These models behaved linearly at small deflection. Cracks at approximately 45° to the beams started to develop at about 1/3 peak load. Stiffness gradually decreased as the infill/beam connection was deteriorating. Peak load was reached when the infill/beam connection failed and then the load dropped rapidly. More deformation caused more contact between the infill and the columns thus enabling the models to regain part of the strength at the expense of inducing shear forces and bending moments in the columns. When the compressive corners of the panels were crushed, the models collapsed with a failure mode similar to those without connectors.
3. Models C: These models showed higher stiffness and strength. They also maintained their strength up to very large deflections leading to tremendous energy absorption before failure. Numerous cracks at 45° to the beams were developed continuously from about 1/4 peak load. In general, more cracks occurred in models C than in A or B. The stiffness dropped gradually as the compressive corners of the infilled panels and the infill/beam connection yielded. The models finally failed in shear at the infill/beam connection and by crushing of the panels at the compressive corners. Obvious yielding of the columns was observed.

Following their experimental work, Liauw and Kwan developed a plastic theory for non-

integral and integral infilled frames [19,20]. In their work they derive equations by which the collapse shear force can be calculated. The magnitude of this shear force depends on the aspect ratio of the frame, and on the relative strength between the beams, columns, and the infill wall. For the case of the non-integral frame, three modes of failure are identified and equations are developed for each one of them:

- corner crushing mode with failure in the columns(mode 1). This mode is likely to take place when the frame is weak and the panel is strong and the columns are weaker than the beams. Also in the case where the beams and the columns are of equal strength and the span is greater than the height.
- corner crushing mode with failure in the beams(mode 2). This mode is likely to take place when the frame is weak and the panel is strong and the columns are stronger than the beams, or in the case where the beams and the columns are of equal strength and the height is greater than the span.
- diagonal crushing mode(mode3). This mode is likely to take place when the infilled panel is not strong enough to develop plastic hinges in the columns or beams.

For the case of integral infilled frames, four modes of failure are identified [20]:

- corner crushing with failure in columns and infill/beam connections (mode 1),
- corner crushing with failure in beams and infill/column connections (mode 2),
- diagonal crushing with failure in infill/beam connections (mode3), and
- diagonal crushing with failure in infill/column connections (mode4)

Similar behavior of the infilled frames was observed by Zarnic and Tomazevic [21], who tested four types of specimens. All four specimens had reinforced concrete frames and the first one was with no infill, the second with unreinforced infill, the third with horizontally reinforced infill, and the fourth with horizontally reinforced infill anchored into the frame. After performing their research they concluded that:

1. "when masonry infilled reinforced concrete stiff frame is subjected to cyclic lateral loading, it behaves as a unique structural system until diagonal cracks occur in the infill. After cracking, the contribution of the infill to the lateral resistance of the infilled frame system is not diminished. However, the frame takes over a significant part of the lateral load, increasing the lateral resistance of the system, until its columns fail in shear.
2. No significant effect of relatively small amount of horizontal infill reinforcement on the lateral resistance and ductility of the infilled frame was observed. An increase in lateral resistance only has been obtained by means of anchoring the infill reinforcement into the frame".

Yorulmaz and Sozen [22] tested ten small scale frames, three of which were with no infill walls. The frames were built with reinforced concrete and filled with brick masonry. No connections were provided between the infills and the surrounding frames and three different percentages of reinforcement were used. The sections of the beams and columns were equal. They observed from their experiments that the frames with infill walls had their first cracks in the wall, approximately all at the same load. After cracking of the wall, load was transmitted to the frame and different types of mechanism were obtained according to the strength of the frame components. In the frames with low percentage of reinforcement, a tension failure (extension hinge) occurred in the beam, and the compression column of the frame developed a mechanism in itself. Final failure occurred in the extension hinge or as a "pure shear" failure in the tension column. Frames with high percentages of reinforcement failed by "pure shear" failure of the tension column.

Bertero and Klingner [23] also tested a series of reinforced concrete frames with reinforced concrete block infill wall. Unlike other researchers, they took great care in designing their test frames to provide adequate shear capacity of the columns, so as to

avoid shear failure of the columns. They also provided connection between the infill and the surrounding frame. From their experimental work they concluded that:

1. infilled walls increase significantly the stiffness of frames,
2. infilled walls increase the strength of frames,
3. infilled walls change the basic behavior from that of a bare frame, to that of a braced frame,
4. concentration of inelastic deformations and consequently the formation of a sidesway mechanism was observed in frame members bounding the panels subjected to the greatest degradation, and finally that
5. the strength and load–deflection characteristics were asymptotically approaching that of the corresponding bare frame.

It is apparent from the above that all the researchers come to similar conclusions. The interface conditions as well as the relative strength between the infill and the frame are the most important factors and control the mode of failure of the infilled frame. Therefore on trying to model the behavior of infilled frames, these factors have to be taken into account.

2.2 Modelling of infill walls in the present research

A large variety of models exist for idealizing infill walls. These vary from the simple equivalent strut approach to very complex finite element formulations, in which the infill wall is discretized into many elements and laws are defined for the interface between the wall elements themselves and between the wall elements and the surrounding frame elements. The latter models require knowledge about both the constitutive relationships at the interface between wall elements and between the wall and the frame. In addition, a fine discretization will allow the analysis of only subassemblages due to the heavy computational requirements of such an idealization.

Since the objective of this research is to study the behavior of large scale infilled frames (macro modelling) under dynamic loading, it was decided to use the equivalent strut approach. In the following section the theory of the equivalent strut approach is presented.

2.2.1 Theory of the equivalent strut approach.

According to Mainstone [2], a basic factor that affects the behavior of infills is the distribution of the reactions on the infill–frame interface. The interface distribution of forces is in turn affected by

a. the bonding between the infill and the frame along the interface,
b. whether cracking precedes crashing of the infill, and
c. initial lack of fit.

The above three cases are illustrated in figure 2-1. Figures 2-1a to 2-1d show the case when the infill fits the frame perfectly. In such a case, if there is uniform shear transfer along the interface (figure 2-1a), the infill will achieve its maximum possible contribution to resisting the load. To achieve this uniform shear transfer, the infill should be bonded to the surrounding frame. Considered as a diagonal strut, the infill may then be said to have an effective width w' (figure 2-2). On the other extreme, if the shear transfer takes place only at the diagonally opposite corners (figure 2-1b), then the infill behaves as a diagonal strut with an effective width, w'_e (figure 2-2), much smaller than in the previous case. In the case when diagonal cracking precedes crushing of the infill, the initial behavior described above is modified. In effect, two or more struts in place of the original one are formed (figure 2-1c and 2–1d). If on the other hand the infill does not fit perfectly the frame, then the alignment of the effective strut is somewhat different initially (figure 2-1e) and there is a

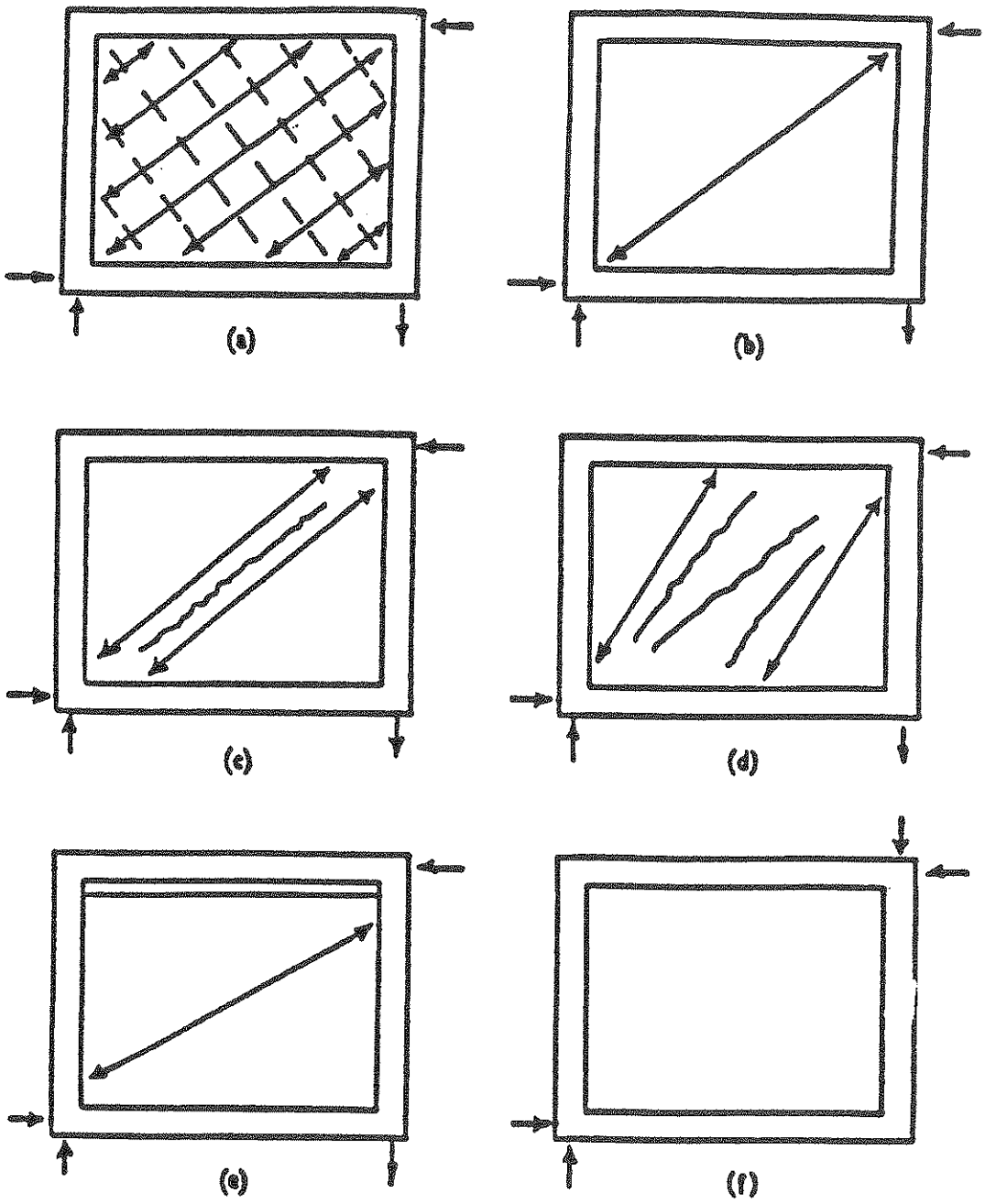

FIGURE 2-1

Behavior of Infilled Frames.

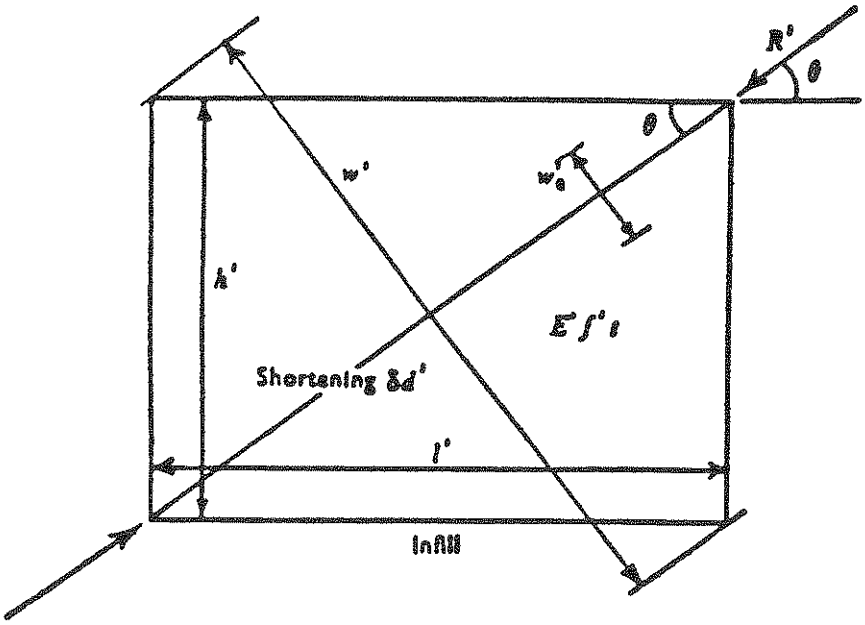

FIGURE 2-2

Definition of Parameters for Equivalent Strut.

tendency for the infill to slip and rotate until it bears on all frame members at the loaded corners.

2.2.2 Assumptions for the equivalent strut method and empirical equations for calculating equivalent strut areas.

For the equivalent strut method, as developed by Mainstone [2], the following assumptions should ideally be satisfied:

a. the infill should not be built integrally with the frame, nor should there be bonding between the two,
b. the infill should fit the frame perfectly,
c. there should be no openings in the infill (e.g. windows, doors, e.t.c.),and
d. all frame members and joints must have enough strength to develop the required infill strengths without appreciable opening of the joints.

In the same reference, the length of contact between the frame and the wall was derived using the beam on elastic foundation approach and a quantity λ_h was defined, which is given by the formula below:

$$\lambda_h = \sqrt[4]{\frac{E' t \sin 2\theta}{4 E I h'}} \qquad (2.1)$$

The definition of the parameters in the above equation is given in figure 2-3. As it can be observed from the above equation, the length of contact between the infill and the frame depends on the flexural rigidity of the surrounding columns, and the dimensions, material properties and thickness of the infill.

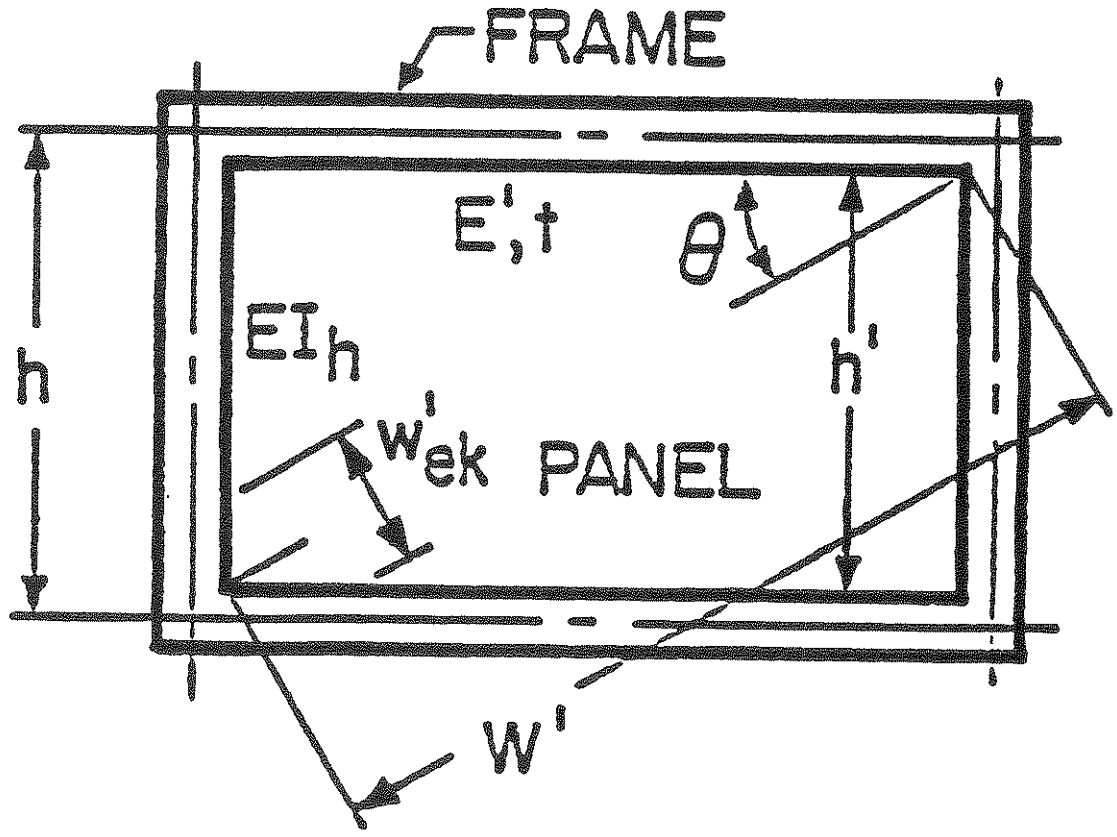

FIGURE 2-3

Definition of Parameters used to Calculate λ_h h.

From his experimental work Mainstone developed empirical equations for calculating the equivalent strut area. These equations should be used only in the case when the above mentioned assumptions are satisfied.

The equations are for two different materials, brickwork and concrete. For each of the materials there are two equations. Which one to use depends on the value of the product $\lambda_h h$.

If $4 \leq \lambda_h h \leq 5$ then

for brickwork

$$\frac{W'_e}{W'} = 0.175\ (\lambda_h\ h)^{-0.4} \qquad (2.2)$$

for concrete

$$\frac{W'_e}{W'} = 0.115\ (\lambda_h\ h)^{-0.4} \qquad (2.3)$$

If $\lambda_h h > 5$ then

for brickwork

$$\frac{W'_e}{W'} = 0.16\ (\lambda_h\ h)^{-0.3} \qquad (2.4)$$

for concrete

$$\frac{W'_e}{W'} = 0.11\ (\lambda_h\ h)^{-0.3} \qquad (2.5)$$

After calculating W'_e from the appropriate equation, the area of the equivalent strut can be obtained by multiplying W'_e by the thickness of the infill, t.

$$A_{eq} = W'_e \, t \qquad (2.6)$$

This area can be used as the area of a diagonal strut in a frame and it represents the infill material. The variation of W'_e / W' as a function of $\lambda_h h$ is shown in figure 2–4.

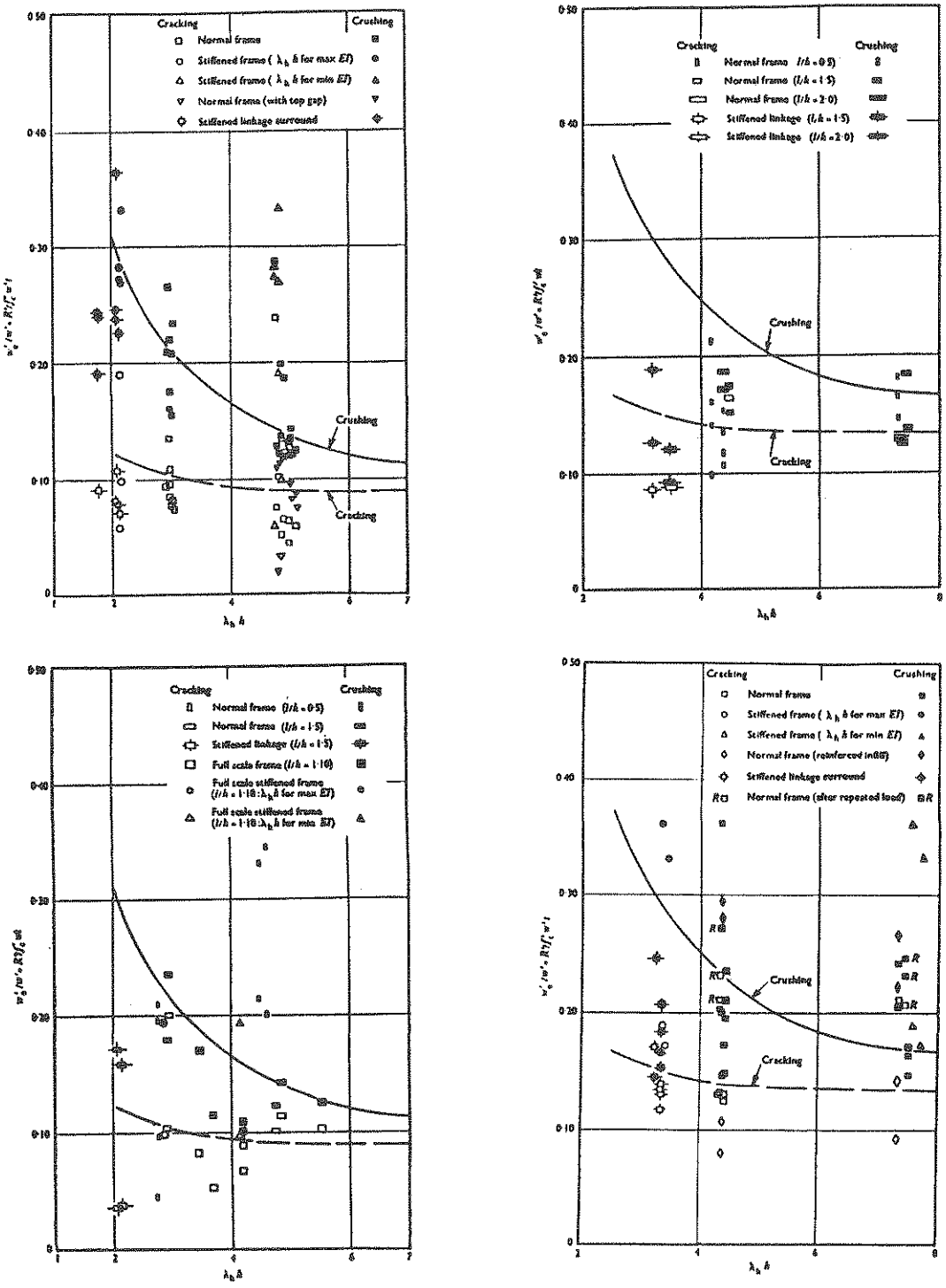

FIGURE 2-4

Variation of w'_e / w' as a function of $\lambda_h h$.

SECTION 3

REVIEW OF THE CAPACITY SPECTRUM METHOD

3.1 Description of the capacity spectrum method

To assess the dynamic characteristics of a building, one should, ideally, perform a second order inelastic dynamic analysis. By doing this, damage and force levels, as well as period shifts can be obtained for a particular building and a given earthquake input. But to perform such an analysis for a fairly large building, one has to pay a high computational toll. An alternative has been developed by Sigmund A. Freeman [24], called the Capacity Spectrum method. This is a method by which damage levels and dynamic characteristics of a structure can be obtained using a static nonlinear analysis. The capacity spectrum is a property of the structure and has nothing to do with the input. Therefore, once the capacity spectrum of a structure is obtained, it can be compared with various inputs without requiring any further analysis. One of the drawbacks of the method is that it ignores cyclic effects which can cause deterioration of the strength and stiffness of the structure. Nevertheless, it is a method by which a good estimate of the dynamic characteristics of a structure can be obtained in a relatively simple way.

To obtain the Capacity Spectrum, the base shear (V) and the roof displacement (d_R) of a structure are converted into spectral acceleration, and spectral displacement, respectively. In addition, the fundamental period and mode shape of the structure are obtained. Using the base shear and the total weight of the structure, the base shear

coefficient C_B can be calculated as

$$C_B = \frac{V}{W} \tag{3.1}$$

W is the total weight of the structure. Using the fundamental mode shape, the modal roof participation factor is

$$\frac{d_R}{S_d} = \frac{\left(\sum m \Phi\right)\left(\Phi_R\right)}{\left(\sum m \Phi^2\right)} \tag{3.2}$$

and the effective modal weight is

$$\frac{C_B}{S_a} = \frac{\left(\sum m \Phi\right)^2}{\left(\sum m\right)\left(\sum m \Phi^2\right)} \tag{3.3}$$

In the above equations m is the story mass and Φ is the story mode shape coefficient. S_a and S_d are the spectral acceleration and spectral displacement respectively. From the equations for the modal roof participation factor and the effective modal weight, the spectral acceleration and the spectral displacement can be calculated. Then the period of the structure is

$$T = 2\pi\sqrt{\frac{S_d}{(S_a)\,(g)}} \tag{3.4}$$

where g is the acceleration of gravity. The derivations for (3.2), (3.3) and (3.4) are given in Appendix A.

After calculating T and S_a for various force levels, the Capacity Spectrum of a structure can be plotted.

3.2 Implementation of the Capacity Spectrum Method

In the present research the above method was slightly modified. Instead of calculating the period of the structure using (3.4), the fundamental period and the mode shape were obtained using an eigensolver routine. Therefore there was no need to calculate the modal roof participation factor using (3.2), which is a means for obtaining the spectral displacement to be used in calculating the period of the structure. There are seven steps in the analysis which are presented below:

1. The first task is to distribute the equivalent static earthquake load over the height of the building. This is done using the SEAOC equations shown below. The base shear, V, is given by

$$V = F_t + \sum_{i=1}^{n} F_i \qquad (3.5)$$

The concentrated force, F_t, at the top, which is in addition to F_n, is given by

$$F_t = 0.07\ TV \qquad (3.6)$$

where $F_t \leq 0.25V$ and $F_t = 0.0$ if $T \leq 0.7$ sec.

In the above equations, T is the fundamental period of the structure and was obtained here using an eigenvalue routine. The magnitude of the shear force, V, was not important in this analysis, therefore an arbitrary value can be used.

The remaining portion of the base shear, i.e. $(V - F_t)$, is distributed over the height of the building in accordance to the formula:

$$F_x = \frac{(V - F_t)\, w_x\, h_x}{\sum_{i=1}^{n} w_i\, h_i} \qquad (3.7)$$

where

F_x = force at level x of the structure

h_x = height of level x from the base of the structure

w_x = weight of floor at level x

h_i = height of level i from the base of the structure

w_i = weight of floor at level i

2. After applying the load on the structure, a static first order inelastic (material nonlinear) analysis using a simple step incremental solution scheme, is performed. This is the main loop of the program. The load is increased proportionally until the stiffness matrix of the structure changes due to either yielding of an element of the frame, or deterioration of the wall stiffness. When a change in the stiffness matrix is detected, an eigenvalue analysis is performed to obtain the fundamental period, T, as well as the mode shape, $\{\Phi\}$, corresponding to this stiffness matrix. For the eigenvalue analysis, a lumped mass diagonal mass matrix is used. The mass at each floor is calculated using the full dead design load and 20% of the design live load.

3. The total base shear (V) and the total drift (d_R) of the roof of the structure is recorded.
4. Using the base shear obtained in 3, the base shear coefficient, C_B, is calculated (3.1). C_B is equivalent to the quantity

$$\frac{Z\,I\,C}{R_w} \qquad (3.8)$$

of the SEAOC code.

5. Using the eigenvector obtained for this load step, the effective modal weight C_B/S_a is calculated (3.3)
6. Using the ratio C_B/S_a and C_B, the spectral acceleration, S_a, corresponding to the response level (capacity) of the structure can be calculated.
7. The load is then incremented until a change in the stiffness is detected. Steps 2-6 are repeated until the stiffness of the structure deteriorates significantly, in which case the analysis is stopped.

After the analysis is stopped, the information shown in table 3–I is assembled for each case that a change in the stiffness of the structure is detected, and the capacity spectrum of the structure can be constructed, as shown in figure 3-1, by plotting S_a Vs T. At first the period of the structure is constant because the structure is elastic, but as the structure becomes inelastic its period increases due to the fact that its stiffness decreases. Each point on the capacity spectrum curve represents a certain damage level.

The most important piece of information that results from a Capacity Spectrum analysis is the expected damage level of the structure under a given earthquake. To obtain this information, the "inelastic" period of the structure has to first be obtained. The procedure for obtaining the expected "inelastic" period and the expected damage level are described below.

**** FR6-WALL ****

HINGE	SHEAR	dR	CB	CB/Sa	Sa	T
1	8.9008E+01	3.6207E+00	5.9369E-02	7.8513E-01	7.5617E-02	1.7935E+00
2	9.4829E+01	3.8769E+00	6.3252E-02	7.9804E-01	7.9259E-02	1.9194E+00
3	9.7747E+01	4.0444E+00	6.5198E-02	8.1841E-01	7.9664E-02	2.3436E+00
4	9.8920E+01	4.1321E+00	6.5980E-02	8.2132E-01	8.0335E-02	2.4871E+00
5	1.1124E+02	5.0799E+00	7.4195E-02	8.2101E-01	9.0371E-02	2.5051E+00
6	1.3516E+02	6.9255E+00	9.0156E-02	8.2098E-01	1.0981E-01	2.5081E+00
7	1.3776E+02	7.1269E+00	9.1887E-02	8.2000E-01	1.1206E-01	2.5147E+00
8	1.4128E+02	7.4061E+00	9.4234E-02	8.2059E-01	1.1484E-01	2.5442E+00
9	1.4222E+02	7.4834E+00	9.4860E-02	8.2314E-01	1.1524E-01	2.5965E+00
10	1.4280E+02	7.5321E+00	9.5251E-02	8.2340E-01	1.1568E-01	2.6088E+00
11	1.4632E+02	7.8250E+00	9.7598E-02	8.2340E-01	1.1853E-01	2.6104E+00
12	1.4691E+02	7.8758E+00	9.7989E-02	8.2146E-01	1.1929E-01	2.6587E+00
13	1.4732E+02	7.9128E+00	9.8263E-02	8.2003E-01	1.1983E-01	2.7097E+00
14	1.4849E+02	8.0195E+00	9.9046E-02	8.2062E-01	1.2070E-01	2.7232E+00
16	1.4967E+02	8.1311E+00	9.9828E-02	8.1980E-01	1.2177E-01	2.7845E+00
17	1.5007E+02	8.1743E+00	1.0010E-01	8.1486E-01	1.2284E-01	2.9276E+00
18	1.5183E+02	8.3742E+00	1.0127E-01	8.1234E-01	1.2467E-01	3.0052E+00
19	1.5234E+02	8.4323E+00	1.0161E-01	8.1200E-01	1.2514E-01	3.0093E+00
20	1.5328E+02	8.5439E+00	1.0224E-01	8.1211E-01	1.2589E-01	3.0771E+00
22	1.5442E+02	8.6862E+00	1.0300E-01	8.1460E-01	1.2644E-01	3.1579E+00
23	1.5473E+02	8.7265E+00	1.0321E-01	8.1542E-01	1.2657E-01	3.2302E+00
23	1.5582E+02	8.8727E+00	1.0393E-01	8.1439E-01	1.2762E-01	3.2722E+00
24	1.5640E+02	8.9536E+00	1.0432E-01	8.1375E-01	1.2820E-01	3.3085E+00
25	1.5699E+02	9.0370E+00	1.0471E-01	8.1269E-01	1.2885E-01	3.3523E+00
27	1.5753E+02	9.1161E+00	1.0507E-01	8.1542E-01	1.2886E-01	3.4003E+00
28	1.5812E+02	9.2061E+00	1.0547E-01	8.1406E-01	1.2956E-01	3.4829E+00
29	1.5979E+02	9.4675E+00	1.0658E-01	8.1397E-01	1.3094E-01	3.5127E+00
30	1.6116E+02	9.6876E+00	1.0750E-01	8.1477E-01	1.3194E-01	3.5670E+00
31	1.6218E+02	9.8546E+00	1.0818E-01	8.1593E-01	1.3258E-01	3.6051E+00
33	1.6277E+02	9.9584E+00	1.0857E-01	8.1391E-01	1.3339E-01	3:7306E+00
34	1.6394E+02	1.0168E+01	1.0935E-01	8.1401E-01	1.3434E-01	3.7504E+00
35	1.6531E+02	1.0415E+01	1.1026E-01	8.1425E-01	1.3541E-01	3.7721E+00
36	1.6641E+02	1.0619E+01	1.1099E-01	8.1521E-01	1.3615E-01	3.8255E+00
38	1.6934E+02	1.1175E+01	1.1295E-01	8.1494E-01	1.3860E-01	3.8655E+00
39	1.7202E+02	1.1737E+01	1.1474E-01	8.1727E-01	1.4039E-01	4.0894E+00
40	1.7421E+02	1.2216E+01	1.1620E-01	8.1662E-01	1.4229E-01	4.1565E+00

TABLE 3-I

Typical Output from the Capacity Spectrum Analysis.

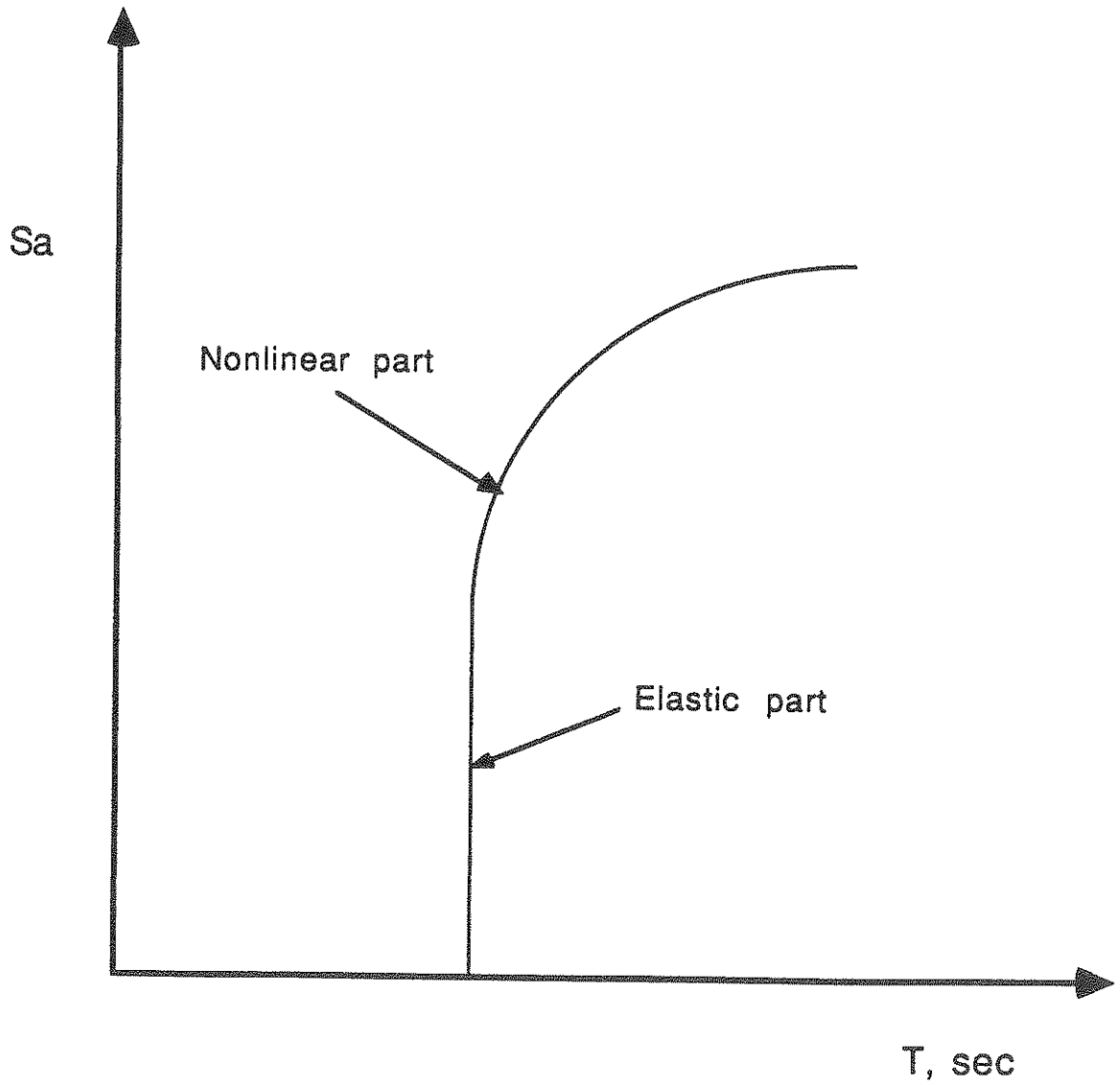

FIGURE 3-1

Capacity Spectrum.

Having obtained the capacity spectrum of a structure, design spectra can be superimposed on the same graph, which represent the demand for a particular earthquake and for a given value of damping. The intersection of the demand (design spectrum) and the capacity (capacity spectrum) gives a rough estimate of the "inelastic" period of the structure under that particular input (figure 3-2). Since damping increases with cumulative damage, one may use an elastic damping of 2% and an inelastic damping of 5% for obtaining the design spectra. In this way an upper and lower bound response spectra are obtained. These spectra are again superimposed on the capacity curve as before (figure 3-3). Since there are two spectra, a range of periods for the structure is obtained. An approximate way for obtaining the "inelastic" period of the structure in this case is as follows: extend the elastic part (vertical straight line) of the capacity spectrum until it intersects the 2% damping design spectrum (point 1). Then find the intersection of the inelastic part of the capacity spectrum with the 2% damping design spectrum. From that intersection draw a vertical line until the 5% damping design spectrum is intersected (point 2). Assuming that the effective damping varies linearly between the elastic and inelastic conditions (i.e 2% and 5% design spectra), connect points 1 and 2 with a straight line to obtain the transition from 2% to 5% damping. The point where this line intersects the capacity spectrum is the expected "inelastic" period of the structure. To this inelastic period corresponds an acceleration $(S_a)_{inel}$. From the information obtained in the analysis, a plot of S_a as a function of the shear force, V, can be obtained as shown in figure 3-4. In addition, the shear force, V, can be plotted as a function of the roof displacement, d_R (figure 3-5). From figure 3–4, the shear, V_{inel}, that corresponds to $(S_a)_{inel}$ can be obtained. Then using this value of the shear, the expected top story drift, $(d_R)_{inel}$, as well as the expected number of hinges, which gives an indication of the level of damage that the structure is expected to suffer under a particular earthquake, are obtained from figure 3-5.

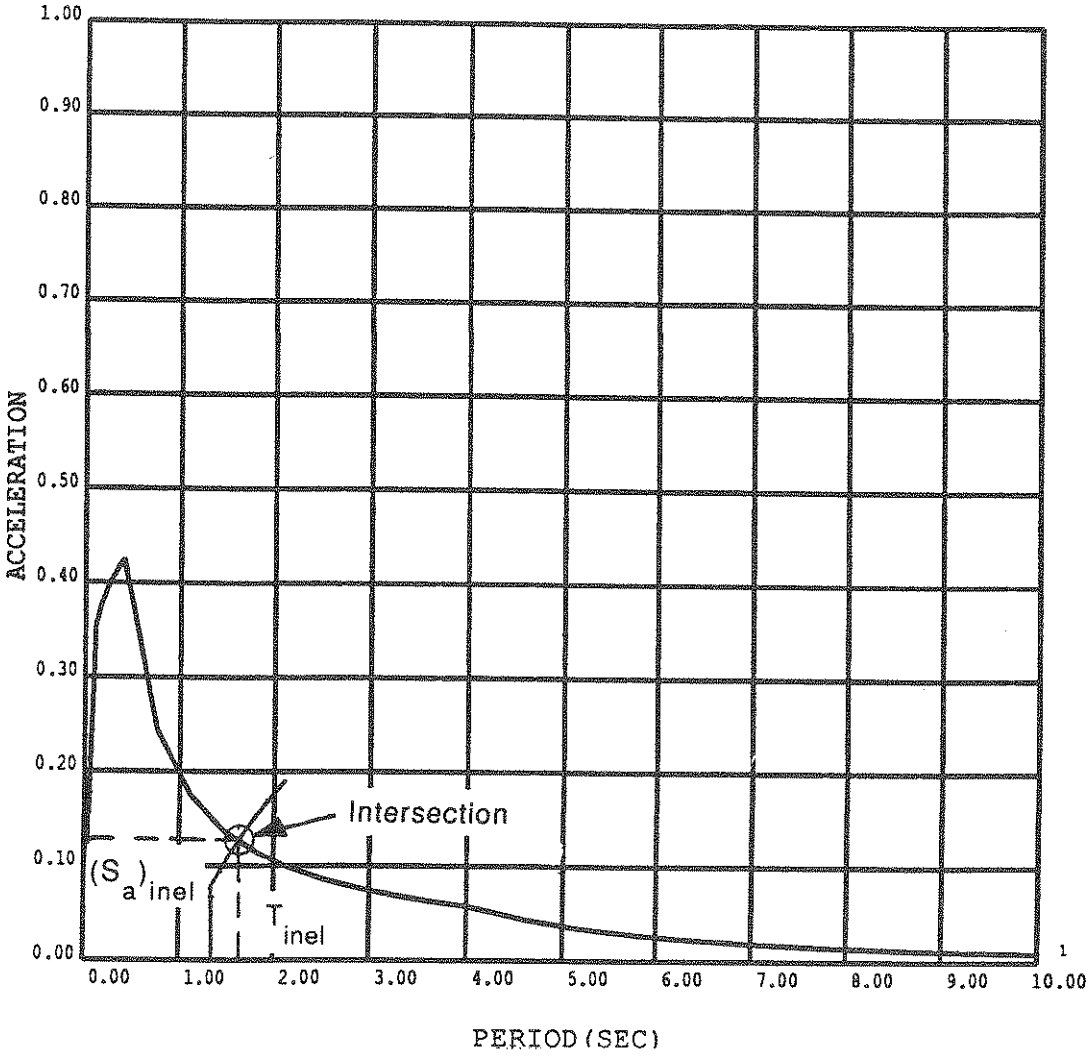

FIGURE 3-2

Capacity Spectrum with only one Damping Value for the Design Spectrum.

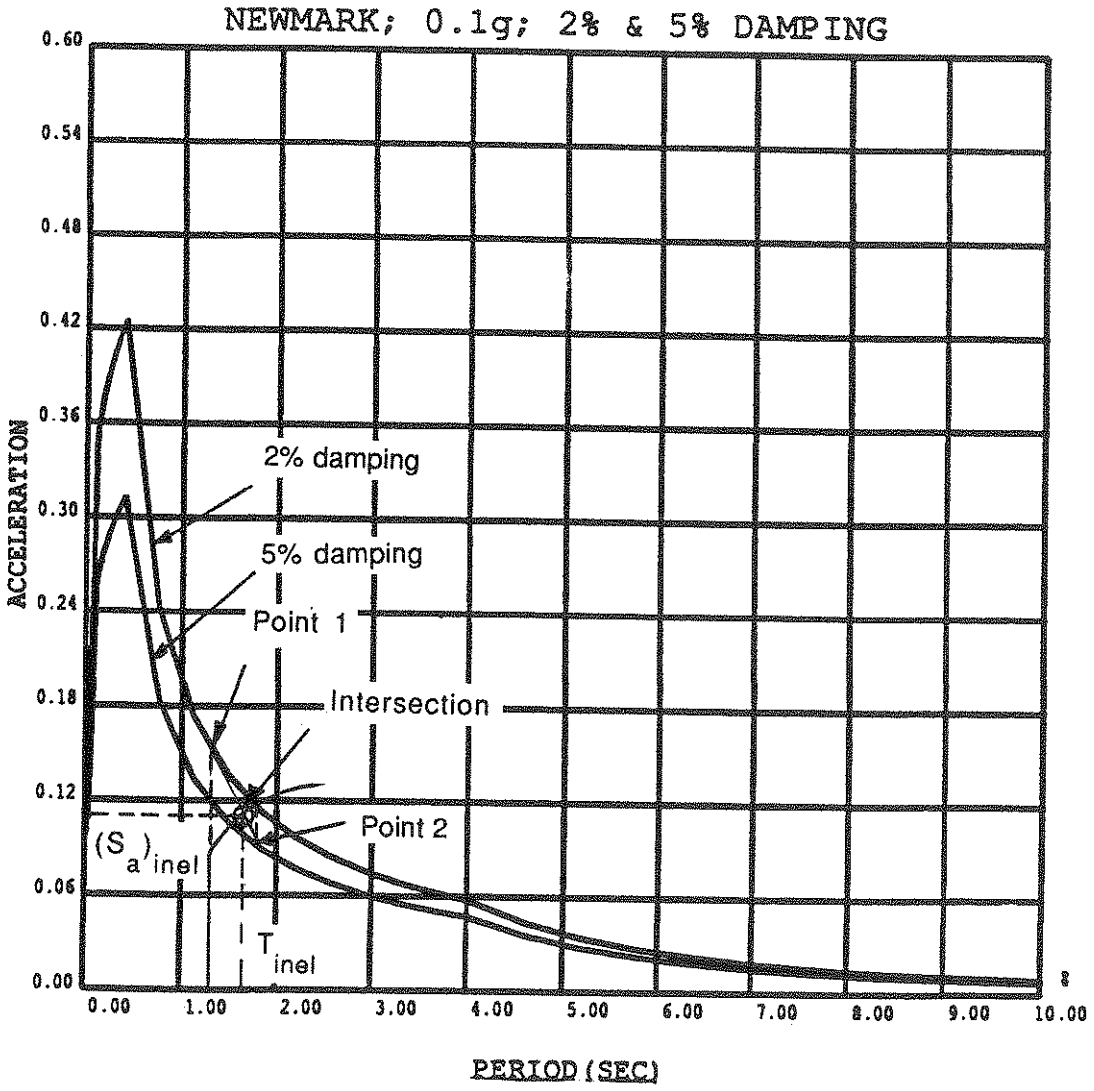

FIGURE 3-3

Capacity Spectrum with two Different Damping Values for the Design Spectrum.

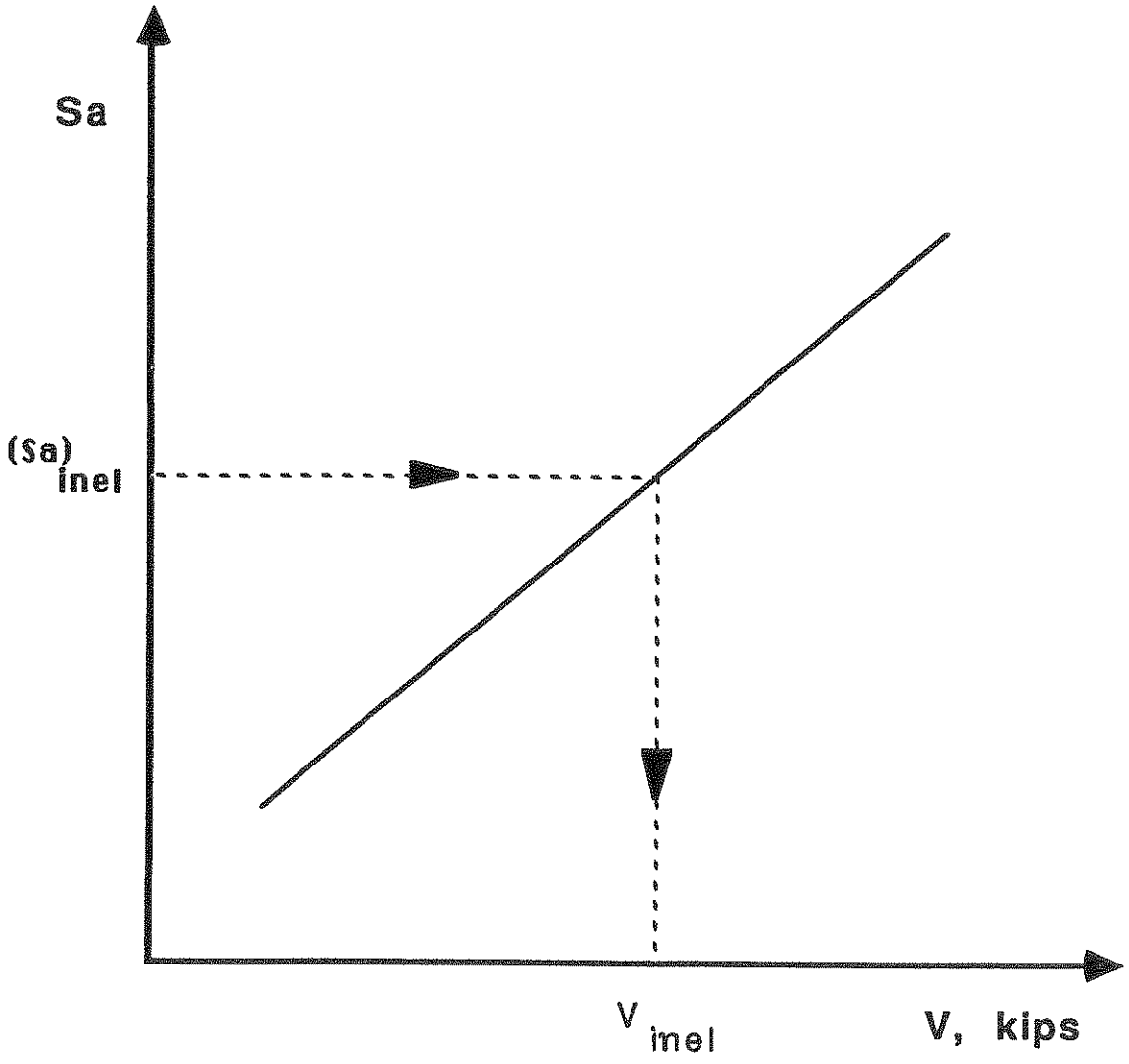

FIGURE 3-4

Plot of the Acceleration versus the Base Shear.

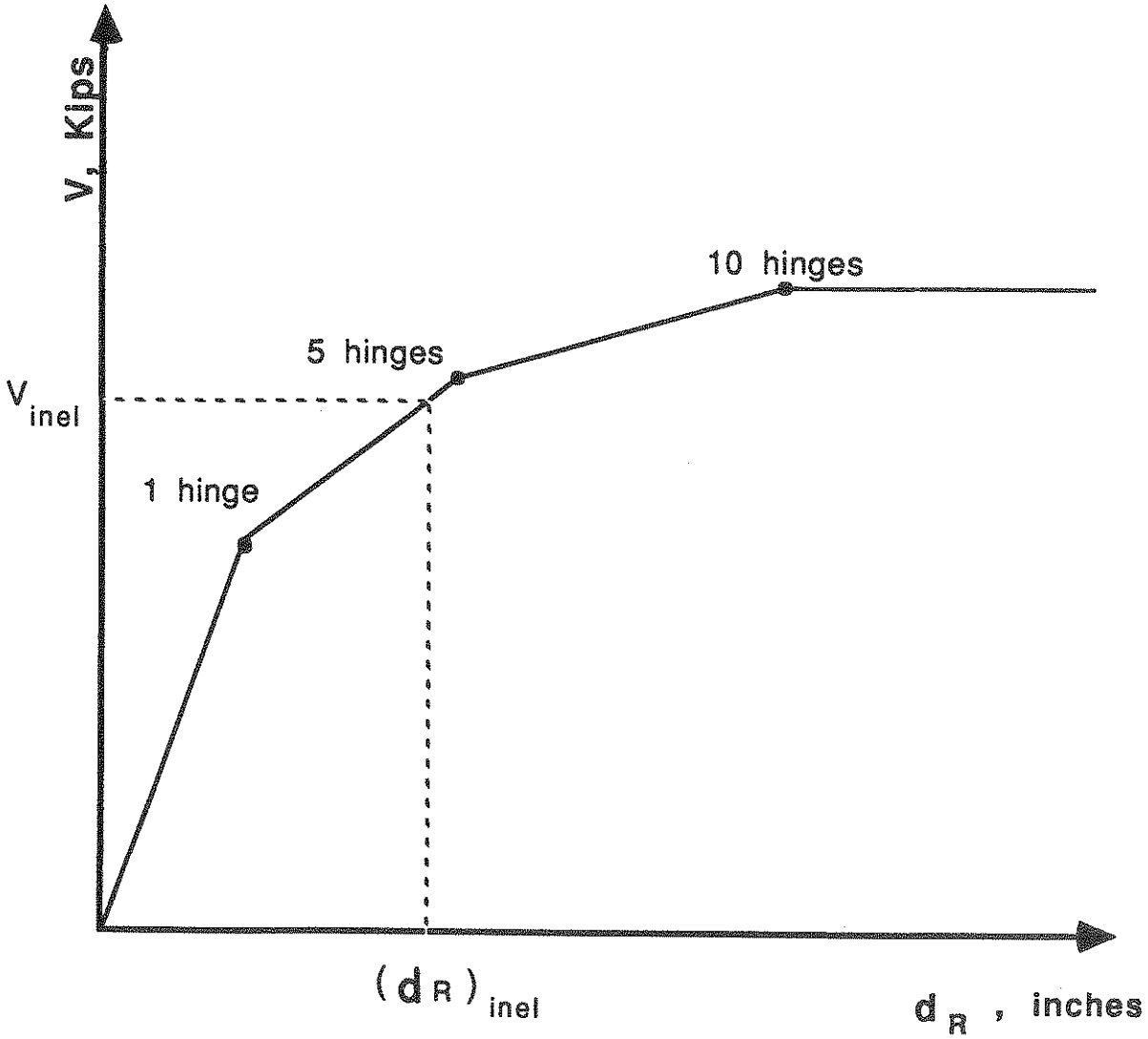

FIGURE 3-5

Plot of the Shear as a Function of the Roof Displacement.

SECTION 4

DESCRIPTION OF THE PROGRAM "STAND"

The method for idealizing infill walls using the equivalent strut approach, described in section 2, and the capacity spectrum method, described in section 3, were implemented in a computer program. Another program was also used as a preprocessor; the two programs are

1. The PREprocessor for Frames (PREPF), and
2. The STatic ANalysis and Design program (STAND).

Both programs are available in the Computer Aided Design Instructional Facility (CADIF) of Cornell University. These programs have been developed by a series of graduate students in a period of about ten years. In this section a brief description of STAND is presented. This includes a description of the main parts of STAND and some details about the material nonlinear model used to idealize steel members as well as the method for tracing post peak strength behavior. Finally, the changes made for modelling the infill walls will be described.

4.1 Brief description of STAND

STAND is an interactive graphics computer program for analyzing and designing steel frames. There are three main parts in this program:

1. Analysis

   Four types of analysis can be performed:

   a. Linear elastic or first order elastic,
   b. Material nonlinear or first order inelastic,
   c. Geometrically nonlinear or second order elastic, and
   d. Full nonlinear or second order inelastic.

   The above types of analysis can be used with any one of the following solution methods:

   a. Simple step incremental
   b. Predictor– corrector
   c. Newton–Raphson iteration

2. Strength design. A structure can be analyzed and designed according to the new LRFD specification for steel structures. The program evaluates the LRFD design equations, and in the event that any of the design equations is violated or any of the members are overdesigned, it makes suggestions as to what other members can be used. After a few iterations a set of members can be obtained which satisfy the LRFD requirements.
3. Stiffness design. In this part of the program the structure is designed to meet stiffness requirements, for example top story lateral drift limitation. An optimization algorithm is available to find the lightest structure that will satisfy lateral drift requirements.

The material nonlinear and the simple step incremental methods were employed in implementing the equivalent strut method. For the sake of completeness, a brief description of the material nonlinear model will be presented in the next subsection.

4.1.1 Material nonlinear model

The Porter and Powell model [25] is implemented in this program. The assumptions for the model are the following:

1. Linear elastic perfectly plastic material
2 Concentrated plasticity at the member ends
3. 3-D yield surface
4. Small plastic and elastic deformations.
   Joint displacements may be large.
5. Drucker's normality criterion which states that the increment in member end forces is orthogonal to the increment in plastic deformations, from which the incremental plastic deformations can be expressed as

$$\{dr_p\} = \{\Phi_{k,s}\}\,\lambda_k \qquad (4.1)$$

where

k = member end (i or j)

$\{dr_p\}$ = incremental plastic deformations

Φ = equation of the yield surface

$\{\Phi_{k,s}\}$ = vector of partial derivatives of Φ_k with respect to the forces, i.e GRADIENT VECTOR

λ_k = proportionality factor, termed the plastic deformation magnitude

> 0 loading

< 0 unloading

After some manipulations of equation (4.1), the tangent stiffness matrix for an elastic–perfectly plastic element becomes [25]

$$[\bar{K}_t] = \left[[K_e] - \left[[\Phi_{,s}]^T [K_e] \right]^T \left[[\Phi_{,s}]^T [K_e] [\Phi_{,s}] \right]^{-1} \left[[\Phi_{,s}]^T [K_e] \right] \right] \qquad (4.2)$$

where

$[K_e]$ = elastic stiffness matrix

$[\Phi_{,s}]$= matrix containing the partial derivatives of the yield surface equation with respect to the forces. In the case that none of the member ends have yielded, this matrix is equal to zero and the tangent stiffness matrix is equal to the elastic stiffness matrix.

Therefore at each load step, λ_k and $[\Phi_{,s}]$ are calculated and the tangent stiffness matrix is updated.

4.1.2. Method for tracing post peak strength behavior.

The stiffness coefficients of the geometric stiffness matrix used in STAND are a function of the axial load in a member. When a member is subjected to compressive forces, the coefficients become negative, and negative stiffness is being added to the global stiffness matrix. If these forces are large enough, the stiffness matrix may become singular or indefinite. A structure is characterized as unstable if a negative or zero term is present on the diagonal of the decomposed matrix.

In STAND [26], the diagonal terms of the decomposed matrix are checked at each load step. If a zero diagonal element is detected, the analysis is terminated with the message that collapse load has been reached. If, on the other hand, one or more negative diagonal

elements are detected, the structure is said to be in the post peak strength region. A method for tracing the post peak strength behavior of structures was proposed by Porter and Powell [25]. Referring to figure 4-1, suppose that the analysis has proceeded to point A and a negative term has been detected on the diagonal of the decomposed stiffness matrix. The equations are solved without making any changes. This will bring the solution to point B. If the sign of the calculated displacements is reversed and the increment is changed to a decrement, the solution will correctly move to point C. Following this method the post peak strength behavior of the structure can be traced.

In modelling infills, strength deterioration is taken into account which has the same effects as the geometric stiffness matrix (i.e. adds negative stiffness). Therefore the method described above is used to trace the behavior of the structure when a wall is in the region that its strength deteriorates.

A more detailed description of STAND can be obtained in [26] and [27].

4.2. Additions in STAND.

The major change that had to be made was to introduce a load–displacement curve that represented the behavior of the infilled wall. In the literature there are many such curves. Because of the large variety of materials that can be used as infills and the high variability in their properties, there are no results that can be considered as standard. Most of the experimental results, though, show the same trend. There is a more or less linear elastic part, and after a peak force is reached, deterioration of the strength of the material takes place (figure 4-2). Therefore, one way of representing these load–displacement curves is by choosing appropriate mathematical expressions that follow that behavior. Bertero and Klingner [23] suggested that the behavior of an infill

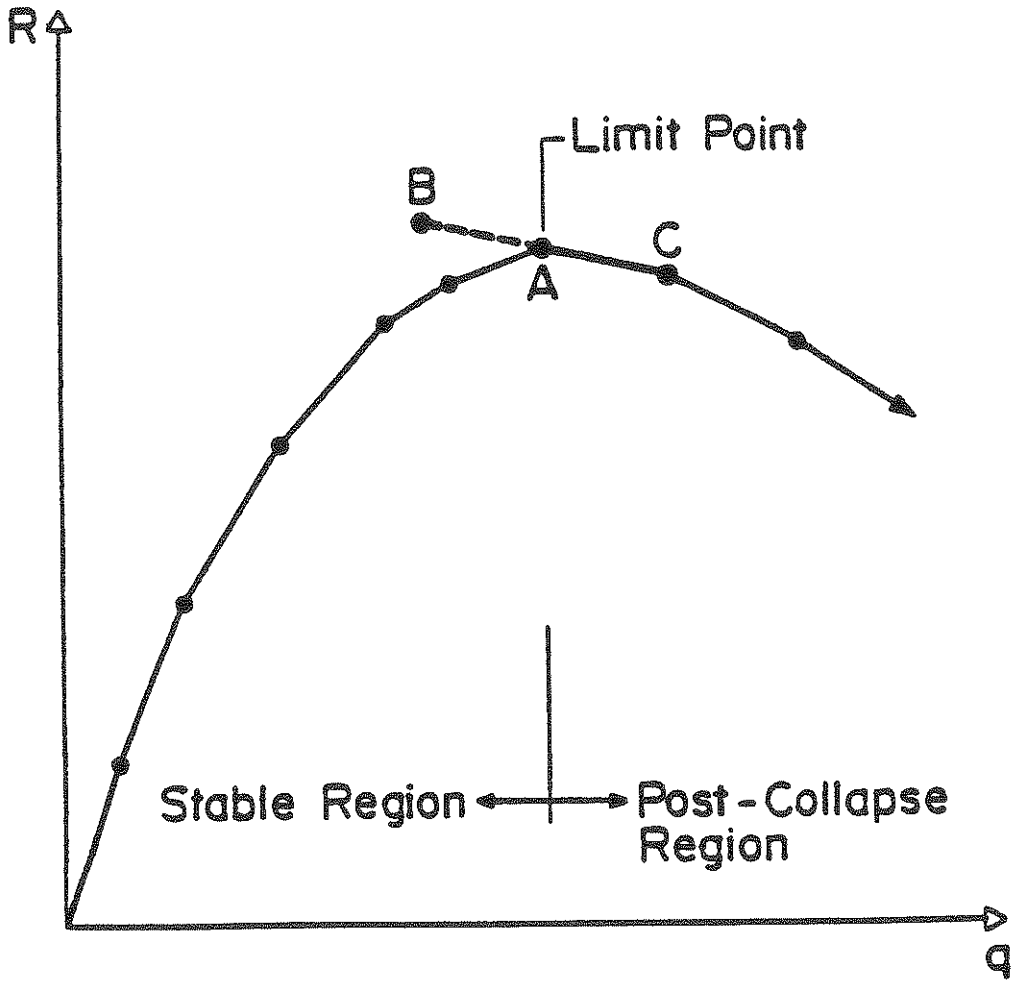

FIGURE 4-1

Method for Tracing Post Peak Strength Behavior[26].

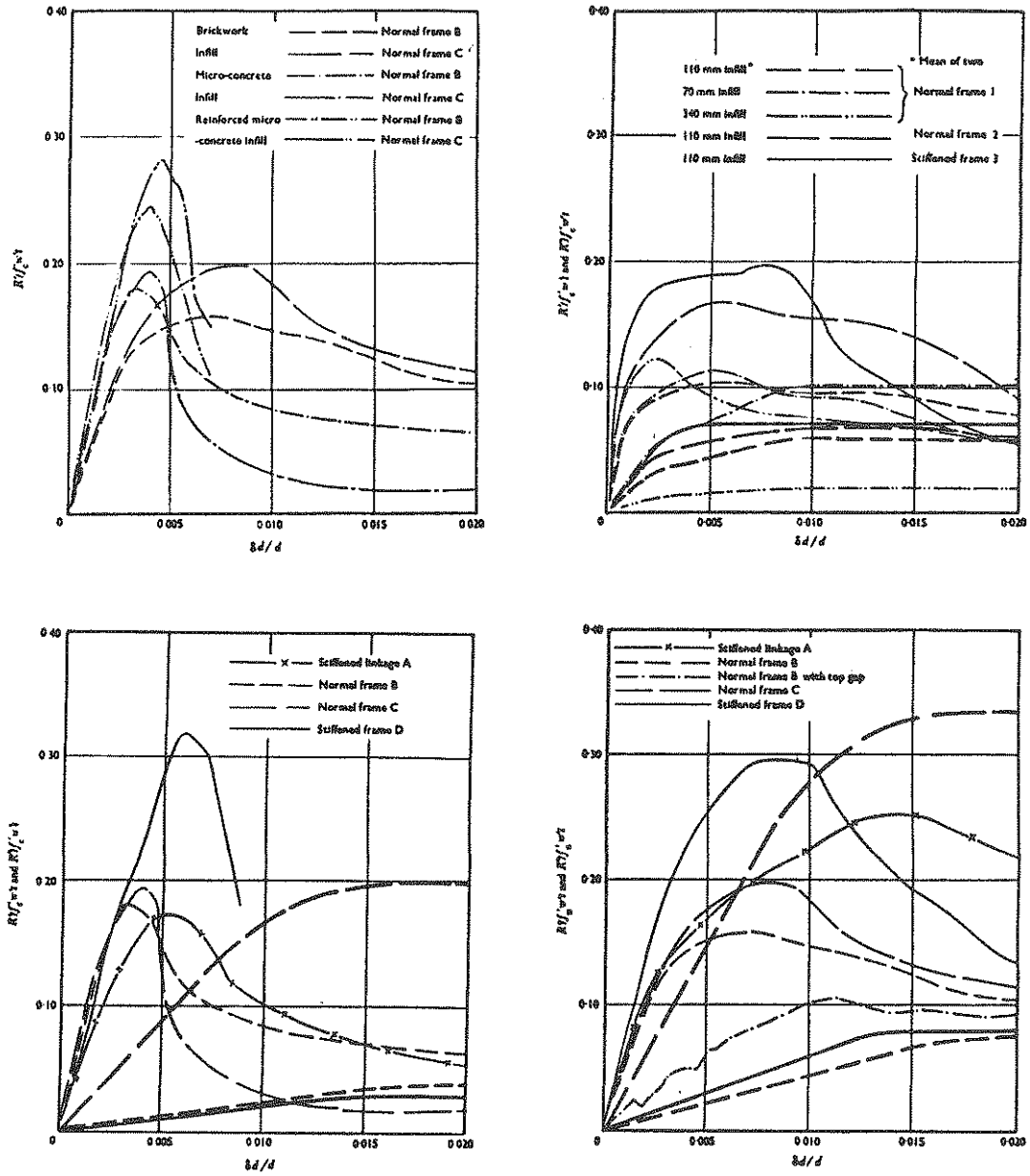

FIGURE 4-2

Experimentally Obtained Load–Displacement Curves for Infilled Walls[2].

can be represented by a combination of a straight line, for the linear elastic part, and a decaying exponential for the reduction in strength with increase in displacement (figure 4-3). The equation for the linear elastic part is

$$F = \frac{EA}{L} u \qquad (4.3)$$

where

F = axial force in the strut

E = Young's modulus of the wall

A = Equivalent area for the strut as calculated using the equations described before.

L = Length of the strut

u = axial deformation of the strut.

The equation for the strength degradation part is

$$F = f_c A e^{-u} \qquad (4.4)$$

where the symbols are as described before.

The next change was to introduce an element stiffness matrix that would represent the strut. The element stiffness matrix used is that of an axial member

$$[K] = k \begin{bmatrix} 1 & -1 \\ -1 & 1 \end{bmatrix} \qquad (4.5)$$

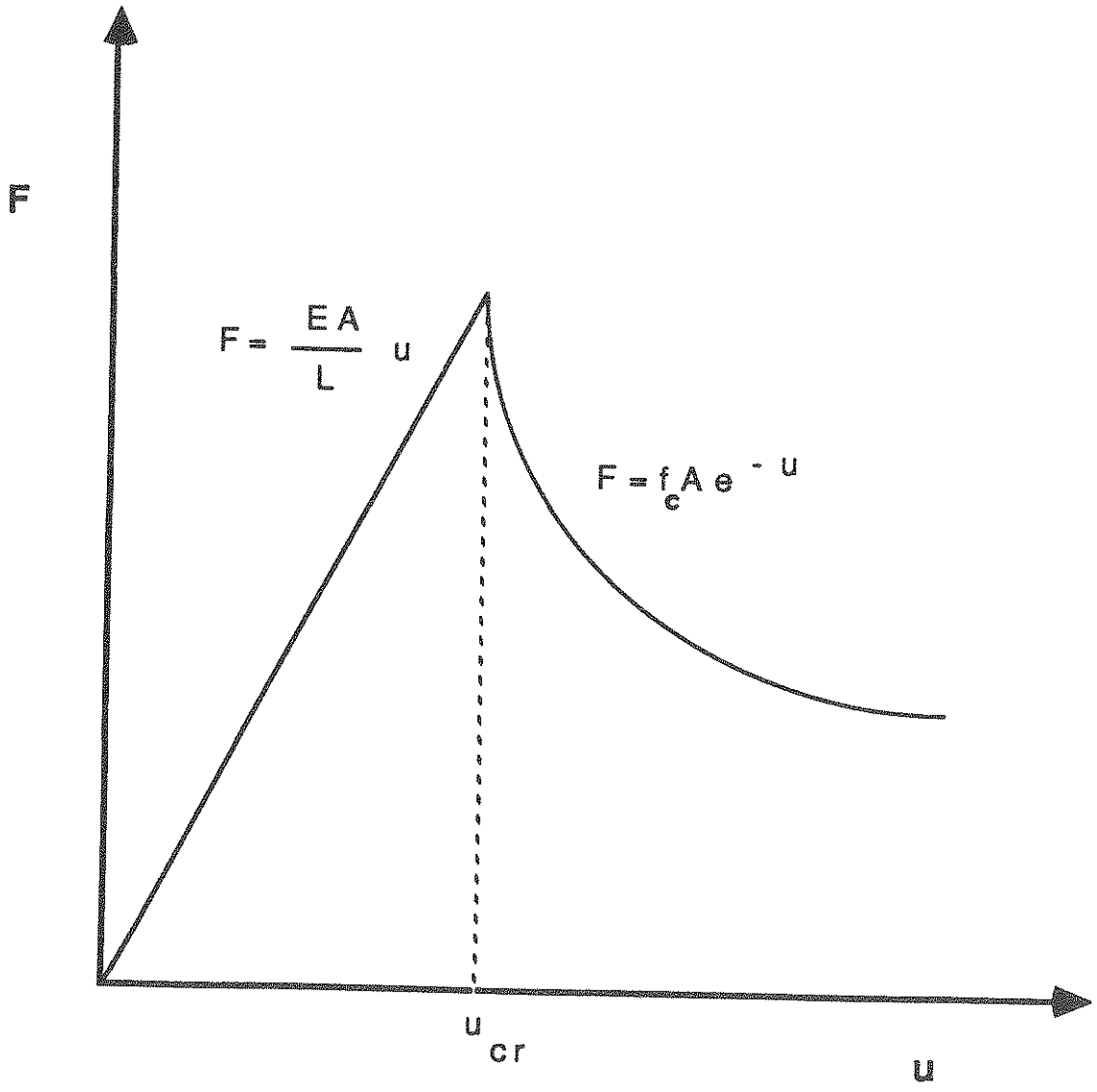

FIGURE 4-3

Model used to Idealize the Load–Displacement behavior of infill walls[23].

Let u_{cr} be the displacement at which the wall cracks.

If $u < u_{cr}$ then $k = EA/L$.

If $u \geq u_{cr}$ then $k = -f_c A e^{-u}$.

The change in stiffness is displacement controlled. After u_{cr} is reached, the stiffness and strength of the infilled wall starts degrading. As it was explained before, the addition of negative stiffness causes negative diagonal terms to appear on the diagonal of the decomposed matrix. This situation is treated in the same way as the post peak strength behavior of a frame. The details of this method were described in a previous section and will not be repeated here.

To avoid having an infilled wall fail within a load step, a check is made to find the load increment required for the wall just to reach u_{cr}. Similar checks already exist in STAND to avoid other undesirable situations (e.g. hinge formation within a load step). All the reduced load steps are compared and the smallest one is selected and used to decrease the already calculated forces and displacements.

SECTION 5

RESULTS OF ANALYSIS

The results are presented in two parts. In the first part the equivalent strut method for idealizing infill walls is evaluated, and in the second the results of the frame-wall system analyses that were performed using the Capacity Spectrum method are presented.

5.1 Evaluation of the Equivalent Strut Model.

The major difficulty was to find experimental results that provided complete data of all the structural members of the structures tested, so as to be able to input them in the computer and compare the experimental results with the ones obtained by the model under consideration. Another difficulty was that most of the experimental data referred to reinforced concrete frames, which could not be modelled by the steel material nonlinear model in STAND.

As noted by Klingner [28], the behavior of elements whose basic models of structural resistance are well known and which can be designed to respond in a stable manner, can be successfully idealized using macroscopic model; one such macroscopic model is the equivalent strut approach. A macroscopic model is expected to be capable of predicting the essential aspects of experimentally observed behavior, unlike the microscopic models (e.g. sophisticated 2–D or 3-D finite element analyses) which are required to duplicate actual behavior. In view of the above, it was decided to obtain from the literature the expected behavior of infilled frames and compare it to the behavior

obtained from the model implemented in STAND.

Bertero and Klingner [23], based on experimental observations, summarize the expected behavior of infilled frames, as it was described in Section 2.1. Those behavioral characteristics of infilled frames were used to test the model implemented in STAND. The results of the analysis for the buildings described in Section 1.3 are presented in the following sections.

5.1.1 Two-story structure loaded laterally.

The load–displacement curve obtained for this structure is shown in figure 5-1. As it can be observed, the infill increased considerably the strength and stiffness of the bare frame, as expected. Since the frame was flexible, the behavior of the infill wall dominated the response and the shape of the load–displacement curve. The strength degradation of the structure was traced successfully, and finally the load–displacement characteristics of the bare frame was approached asymptotically. Whether the bare frame behavior will be approached or not, depends on the load step used. As shown in figure 5-2, if for the same structure a larger load step is used, the response of the infilled frame during the deterioration of the wall goes below the elastoplastic response of the frame acting alone. This is one of the shortcomings of the simple step incremental method and the load step should be selected appropriately so as to avoid excessive drift from the actual response.

The deflected shapes of the infilled frame and the bare frame are shown in figures 5–3 and 5-4 respectively. The deflected shape of the infilled frame is similar to that of a braced frame as it is expected from experimental observations. The wall in the first story is in the strength deterioration part of the load–displacement curve while the wall in the second story is still elastic. Hinges have formed in the columns bounding the wall, confirming the experimental observation that the location of the panels, the strength of

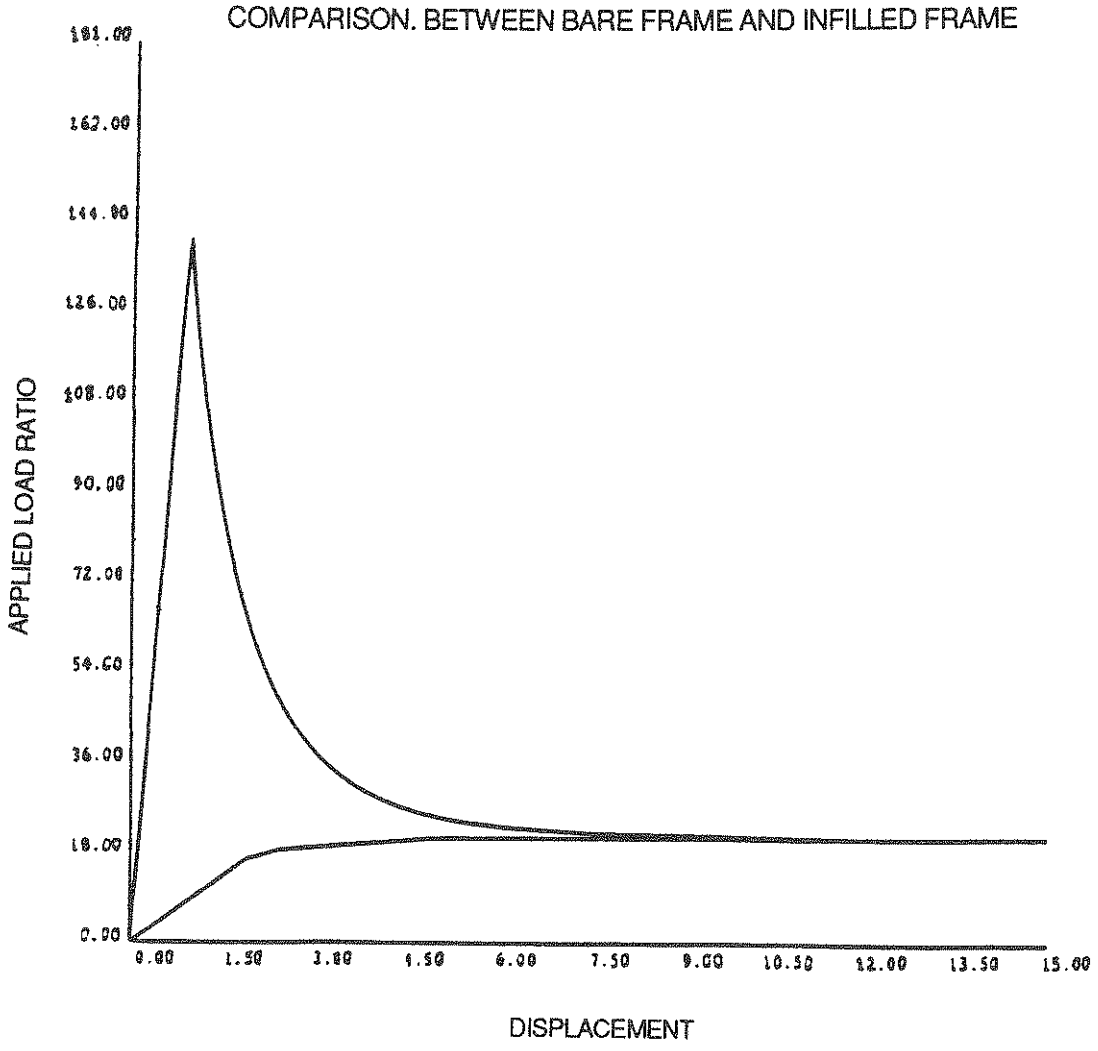

FIGURE 5-1

Load–Displacement Curve of the Two–story Structure for a Small Load Step.

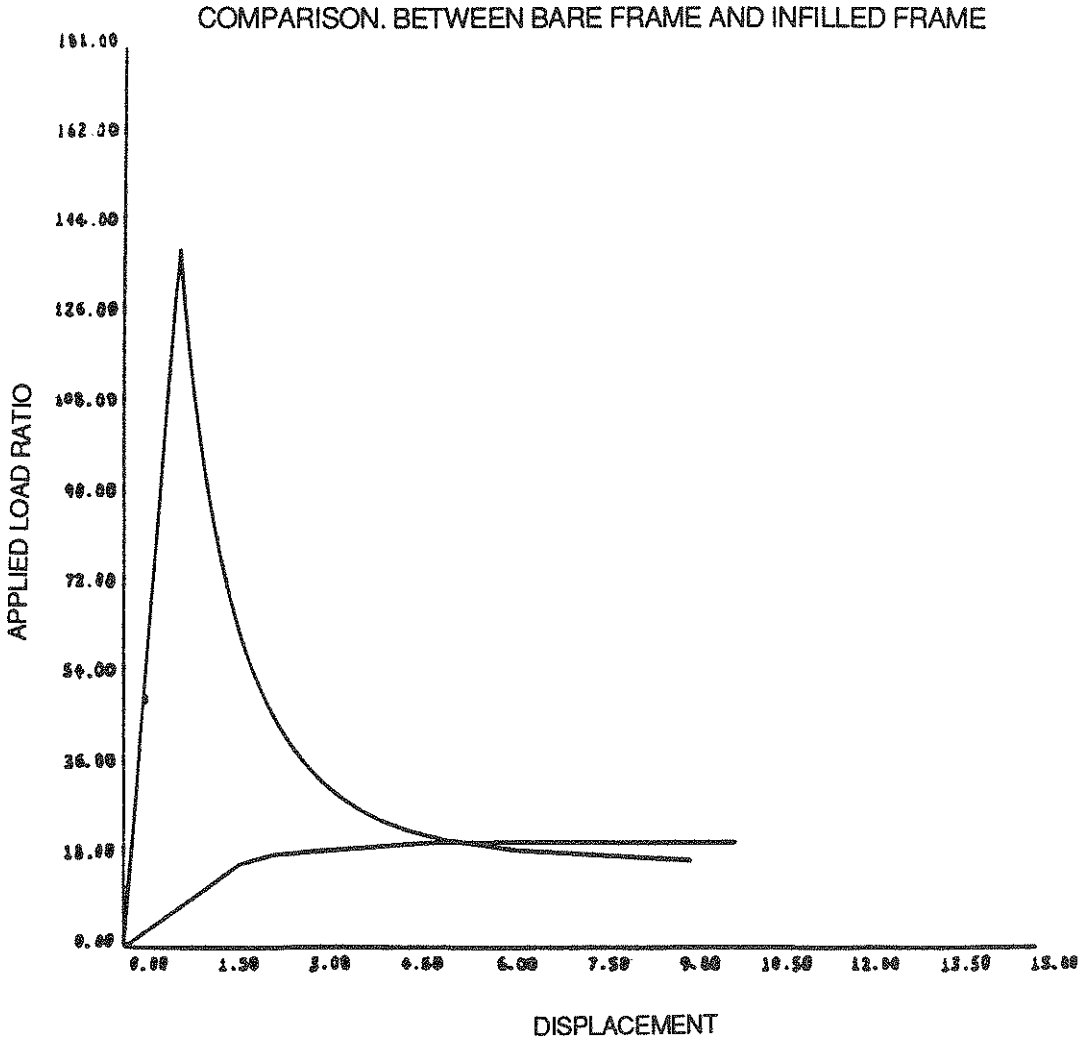

FIGURE 5-2

Effect of Load Step on the Asymptotic Behavior of the Load–Displacement curve of the infilled frame.

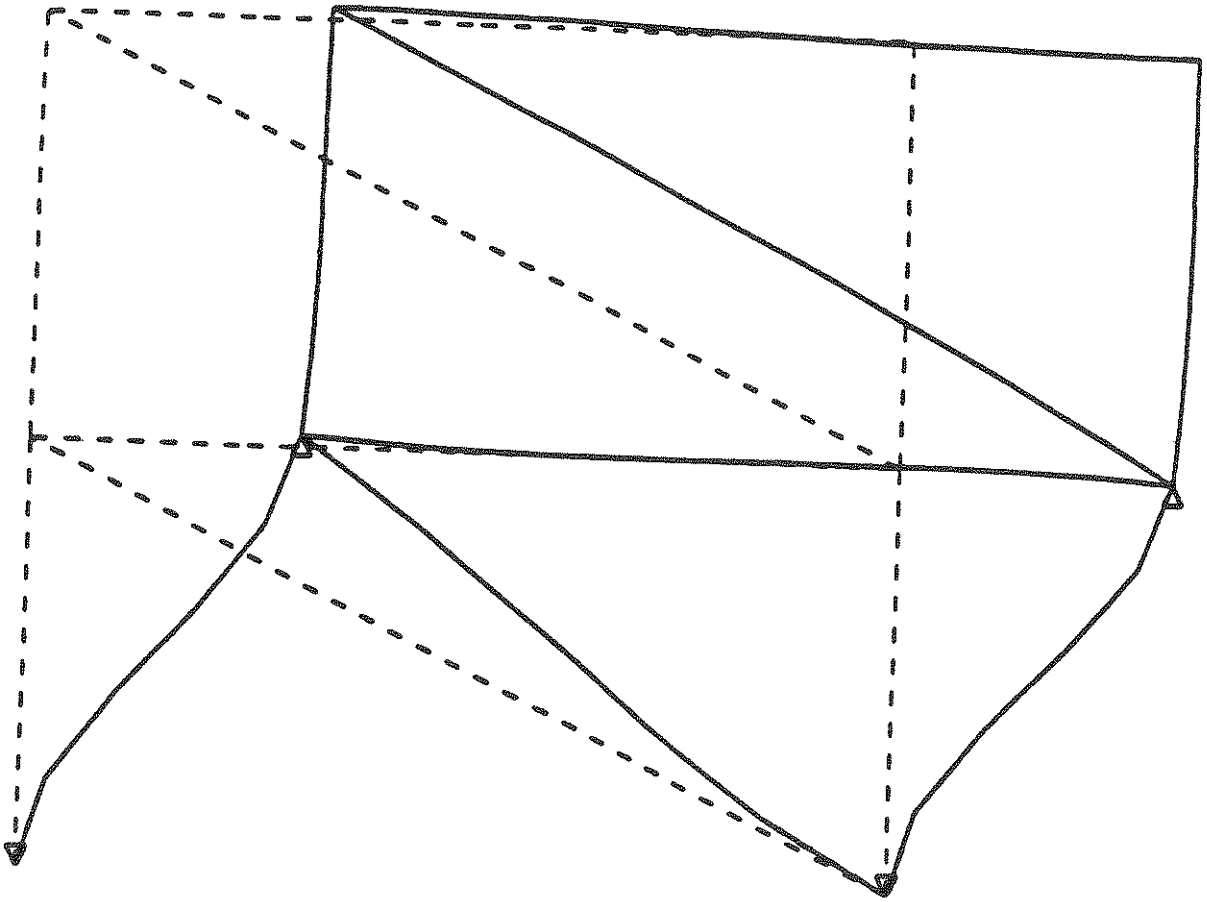

FIGURE 5-3

Deflected Shape of Two–Story infilled frame.

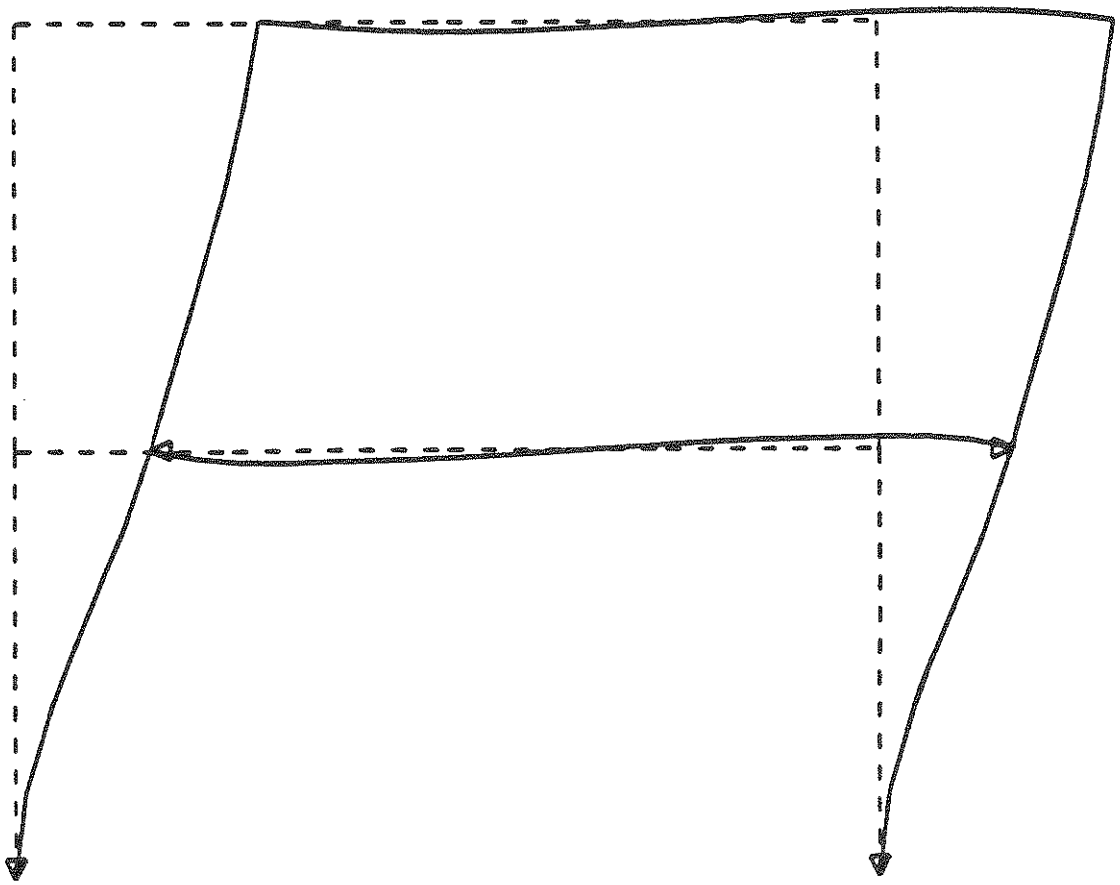

FIGURE 5-4

Deflected Shape of Two–Story Bare Frame.

which has degraded, determines the position of plastic deformations and member failures. Most of the deformations are taking place in the lower story while the top story remains practically rectangular. Comparing this behavior to that of the bare frame, it is observed that both the location of the hinges and the deflected shape are different. It should be noted that the deformations are shown to an exaggerated scale.

The axial forces, shear forces, and bending moments in the members of the structure corresponding to the deflected shape in figure 5–3 are shown in figures 5–5, 5–6, and 5–7 respectively. In figure 5-5 it can be observed that the force in the lower diagonal is small because the wall has already cracked. There is no compression force in the leeward column of the upper level because all of the compression is being transferred through the diagonal strut to the leeward column of the lower level. Both the windward and leeward columns of the lower level experience high axial forces because of the overturning moment due to the lateral load. In figure 5–6 the shear forces in the columns of the upper level are small because of the presence of the infilled wall. In the lower level, since the strength of the wall has already deteriorated, the shear in the columns is high. The moments in the members of the upper level are small, while the ones in the lower level, where the wall has deteriorated, have reached the plastic moments in the columns (figure 5-7).

Thus all experimental observations are well approximated by the results obtained by the equivalent strut method. All five points observed by Bertero and Klingner have been obtained and in addition the force distribution in the members seems to be reasonable.

5.1.2 One–story structure loaded laterally.

The only difference in the behavior of this structure compared to the previously described one, is that now, since the frame is stiffer, its overall behavior dominates the

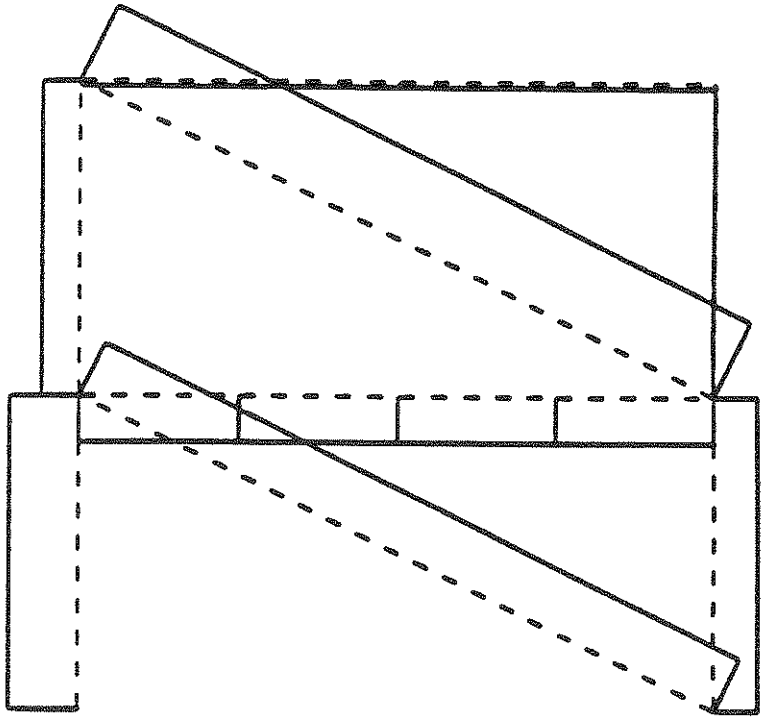

FIGURE 5-5

Axial Forces in the Members of the Two–Story Infilled Frame.

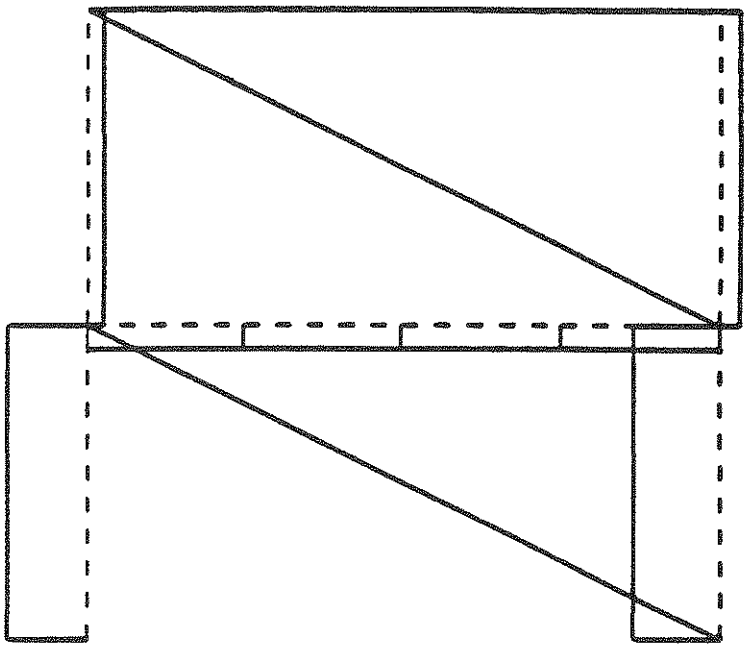

FIGURE 5-6

Shear Forces in the Members of the Two–Story Infilled Frame.

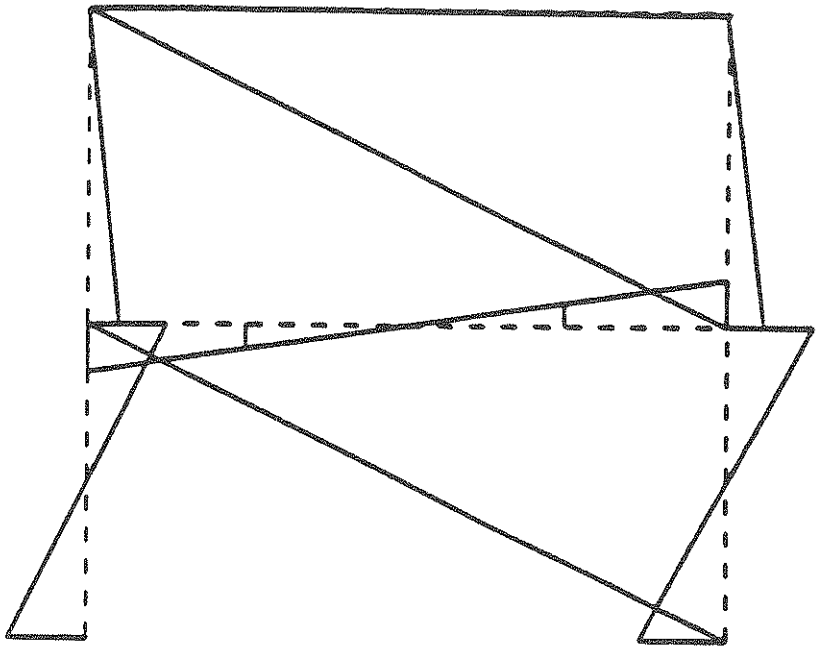

FIGURE 5-7

Bending Moments in the Members of the Two–Story Infilled Frame.

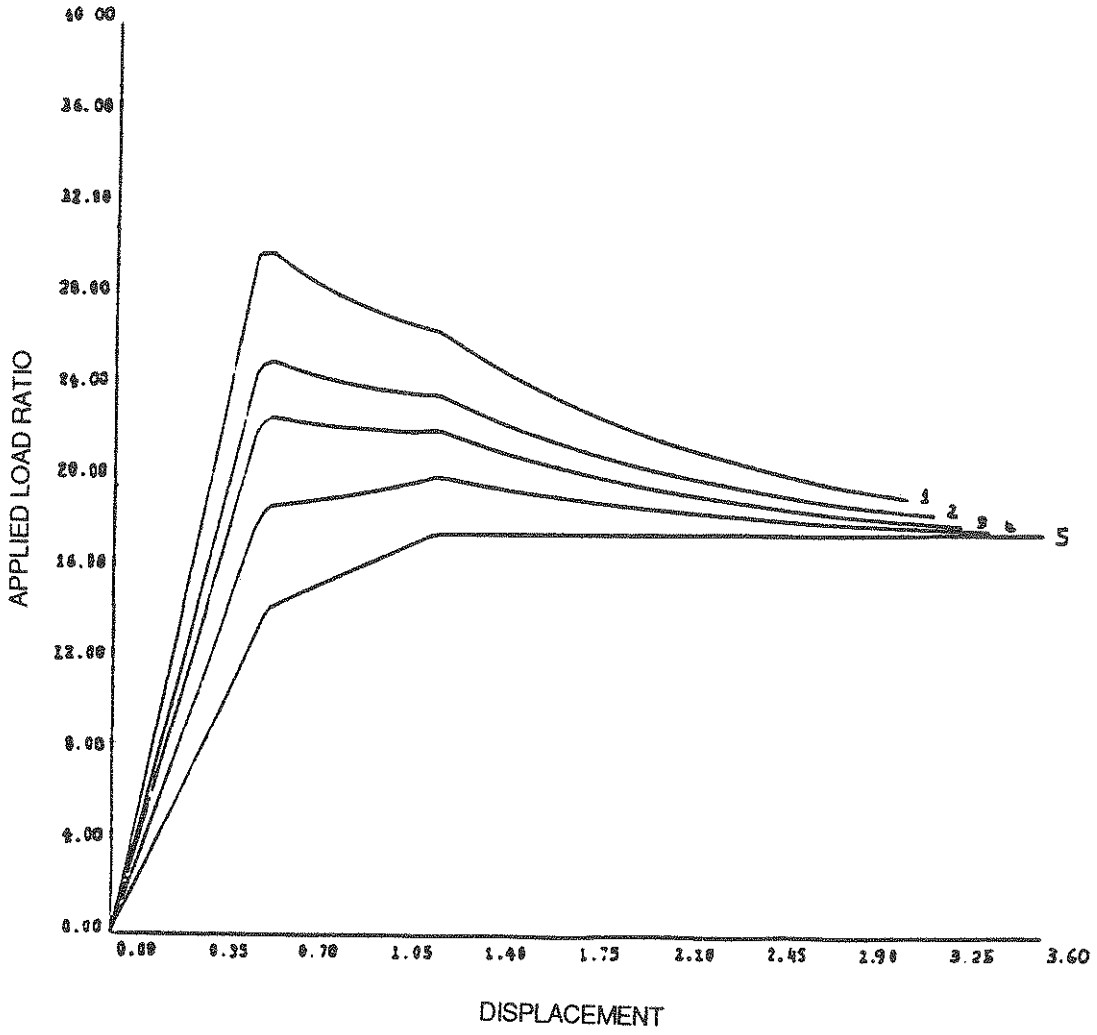

FIGURE 5-8

Load–Displacement Curve of the One–Story Structure.

response of the infilled frame (figure 5-8). In the same figure several curves appear which correspond to walls with different thicknesses. Curve 5 is the one for the bare frame. Instead of getting the shape of the load–displacement curve of the infilled wall as before, a shape which is closer to the one for the bare frame is obtained. The changes in the slope of the curve correspond to formation of hinges and occur at the same displacements as for the bare frame.

5.2 Results from capacity spectrum analysis.

Three steel structures were analyzed, each with and without concrete infill walls. The description of these structures and of the inputs used, is given in sections 1.3 and 1.4 respectively.

5.2.1 Frame 1

This is a 10-story 3-bay steel frame. The deflected shape of the structure, with and without walls, corresponding to the formation of a mechanism, is shown in figure 5–9. The small triangles show the positions of the hinges formed in the steel members. The capacity and design spectra (NBK0.1) for Frame 1 are shown in figure 5–10. The elastic period of the structure without walls is 3.04 sec while the one for the structure with walls is 1.43 sec. The infilled structure (both the wall and the frame) has the capacity to remain elastic for larger accelerations; 0.04g for the bare frame and 0.11g for the structure with infill walls. The period of the bare frame shifts from 3.04 sec to about 6 sec near collapse. The period of the infilled frame shifts from 1.43 sec to 2.3 sec. In both cases the period of the structure almost doubled as the structure was undergoing collapse.

Using the method described in section 3.2, it was found that for the bare frame the

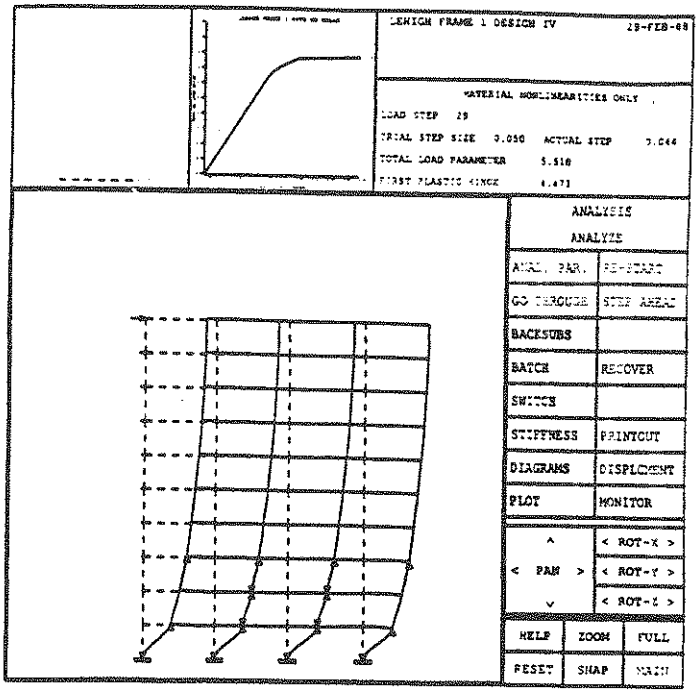

a. Frame 1 without walls

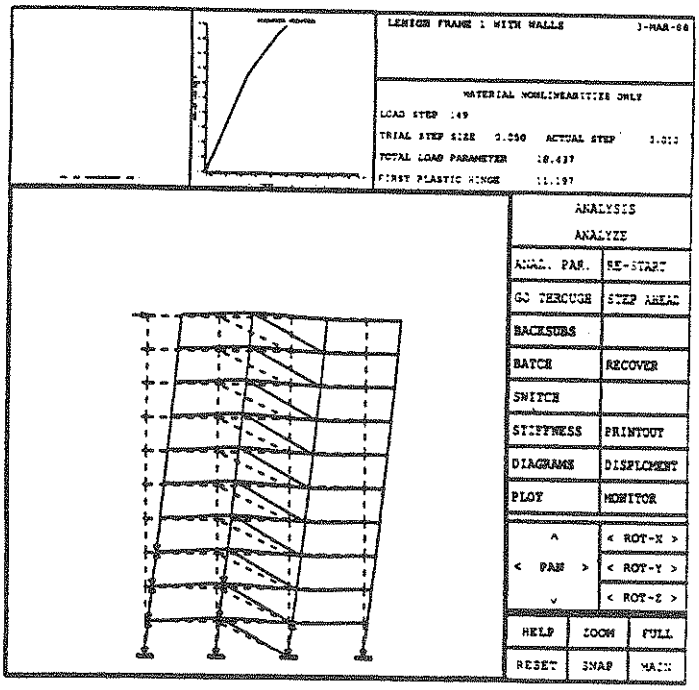

b. Frame 1 with walls

FIGURE 5-9

Deflected Shape of Frame 1 with and without Infill Walls.

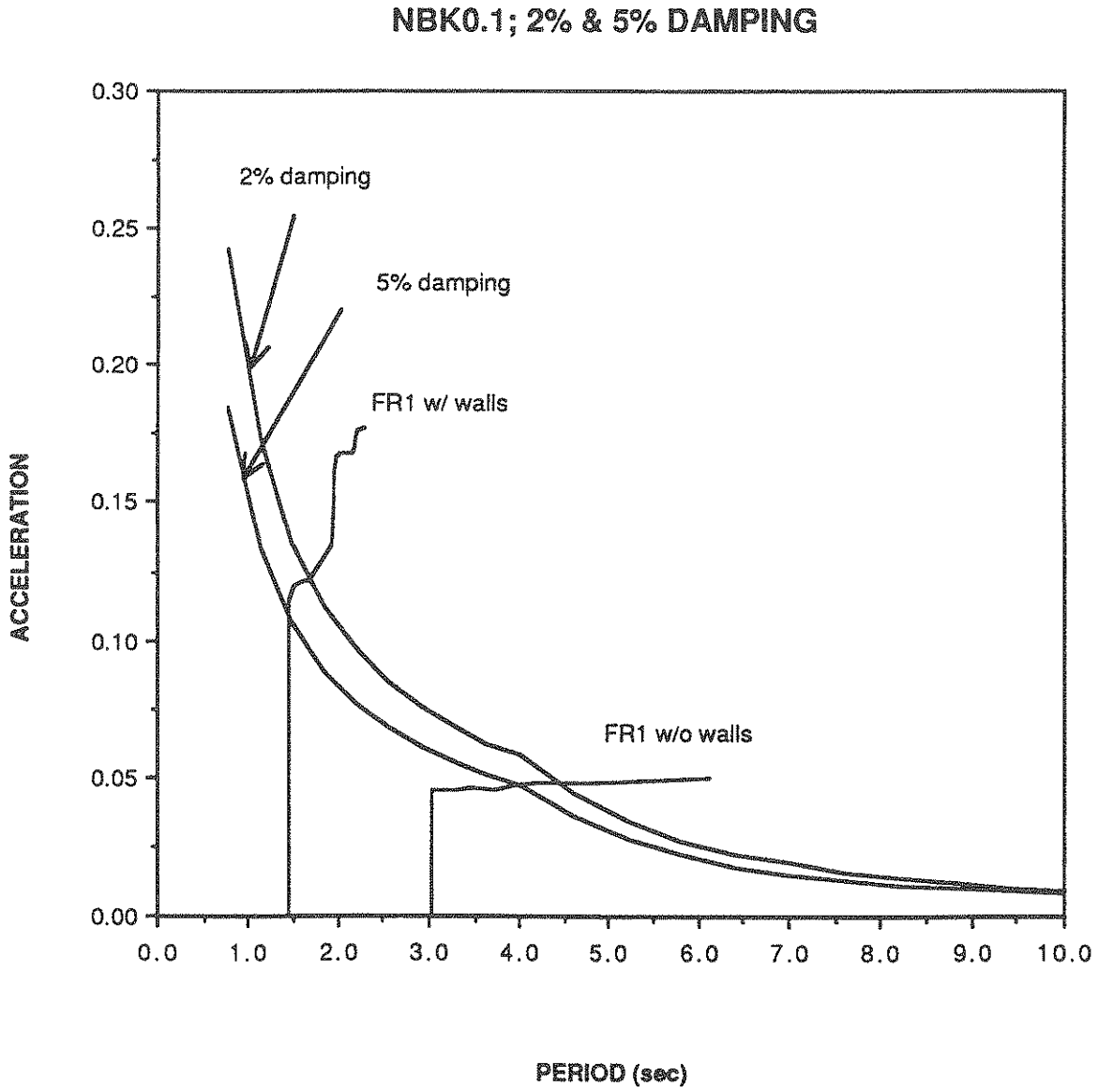

FIGURE 5-10

Capacity Spectra for Frame 1 with and without walls. The NBK0.1 input was used as a Design Spectrum.

period at the intersection of the capacity spectrum with the transition curve from the 2% to the 5% damping, was T_{inel}=4.17 sec and the corresponding acceleration, $(S_a)_{inel}$=0.048g, while for the infilled frame T_{inel}=1.6 sec and $(S_a)_{inel}$= 0.12g. These results show that the infill caused a decrease of the inelastic period of the structure and at the same time the level of forces on the structure increased. Using these values in the corresponding graphs in figure 5–11, the expected shear force, V_{inel}, is obtained as 41 kips for the bare frame and 98 kips for the infilled frame. Finally from figure 5–12, using the expected shear forces, it is determined that if the bare frame is subjected to NBK0.1, it will suffer substantial damage, about 14 hinges will form, and the roof-displacement is expected to be about 6.7 inches. On the other hand the infilled frame will suffer only minor damage, about two hinges will form, and the expected roof displacement will be 3.7 inches. Therefore, although the infill increased the level of forces on the structure, the damage of the structure for this particular earthquake will be smaller for the infilled frame than for the bare frame.

Both structures were also subjected to the NBK0.2 input. No further analysis was required except to obtain the NBK0.2 spectrum for two damping ratios and superimpose them on the capacity spectra obtained for Frame 1, with and without walls (figure 5–13). In this case, both the infilled and bare frames do not intersect the 2% damping ratio curve. This means that these structures do not have the capacity to withstand this level of forces and will fail.

5.2.2 Frame 4

Frame 4 is a 30-story 2-bay steel structure. This structure was analyzed only without infill walls and for the NBK0.1 input. The deflected shape of this structure is shown in figure 5–14. It can be observed that the first story of this structure is a "soft" one and takes all the deformation. The rest of the structure moves nearly as a rigid body.

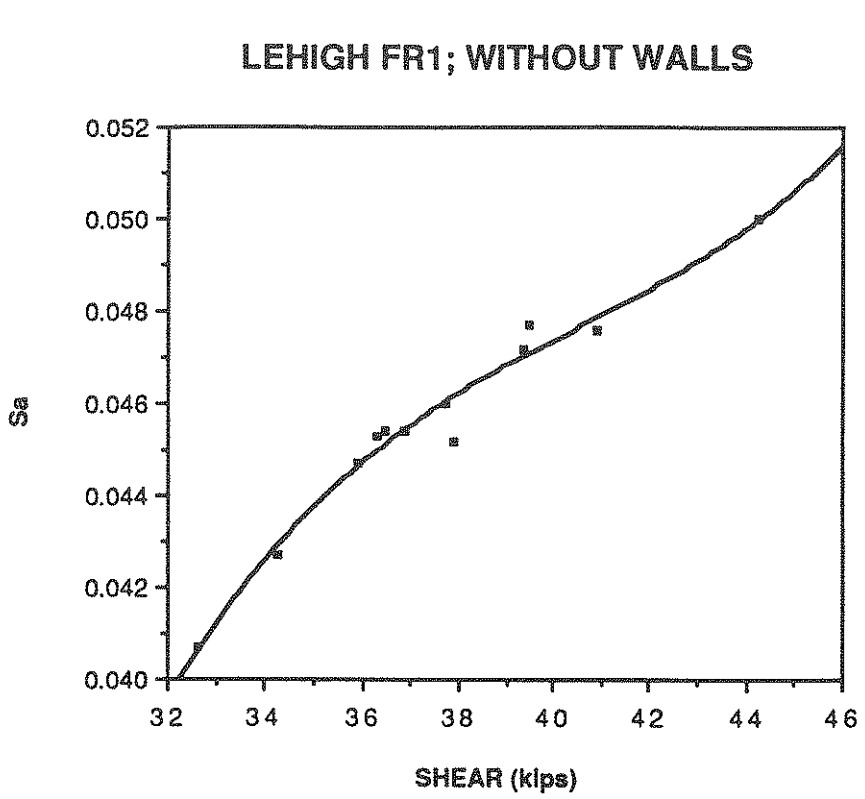

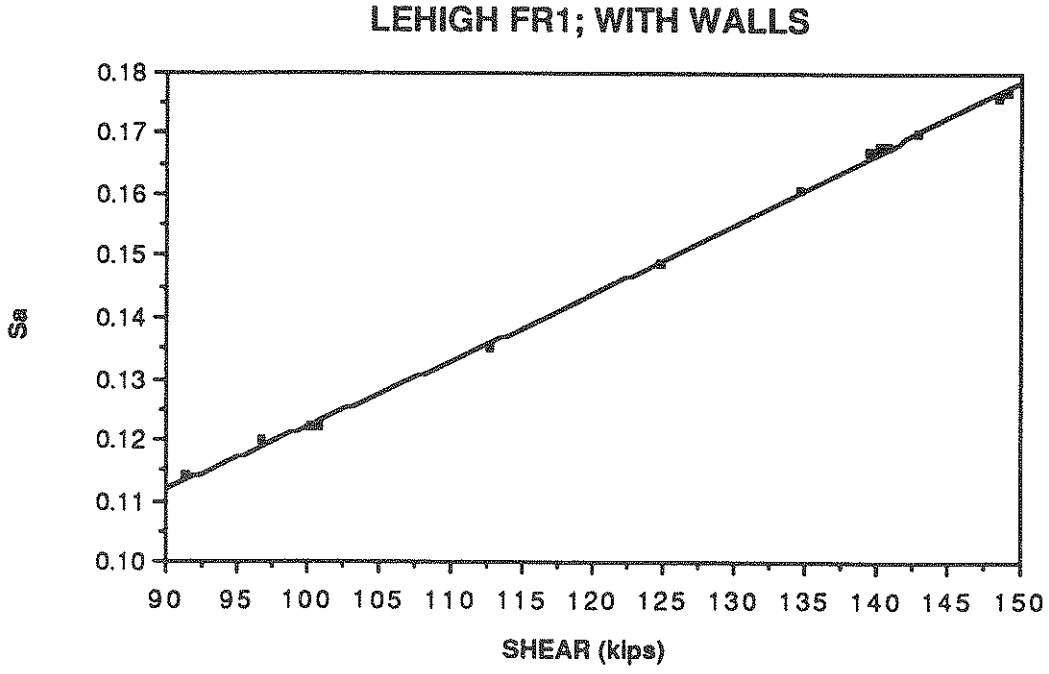

FIGURE 5-11

Plots of Acceleration versus Shear for Frame 1.

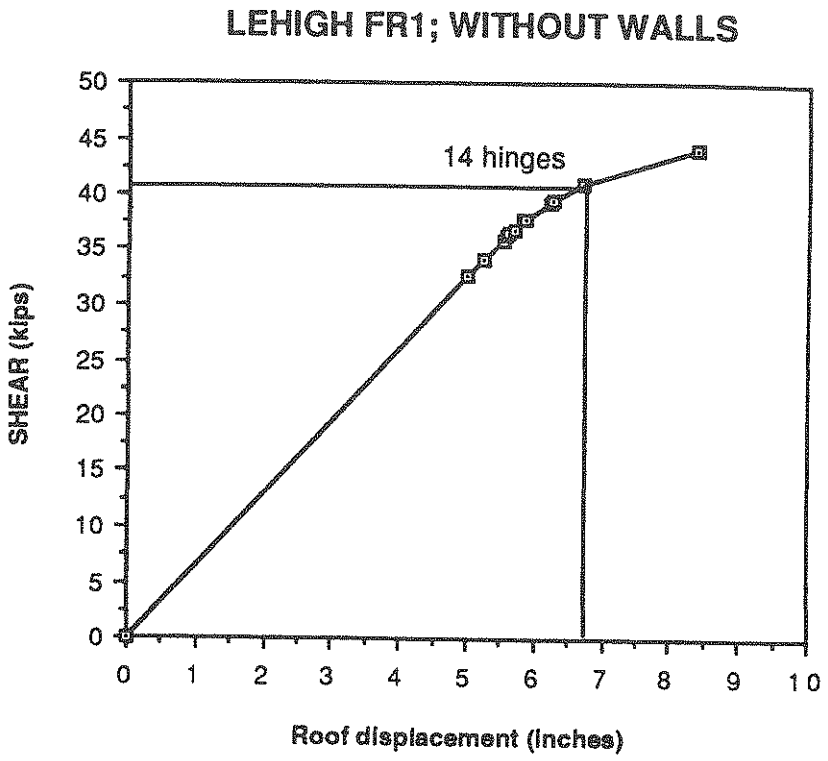

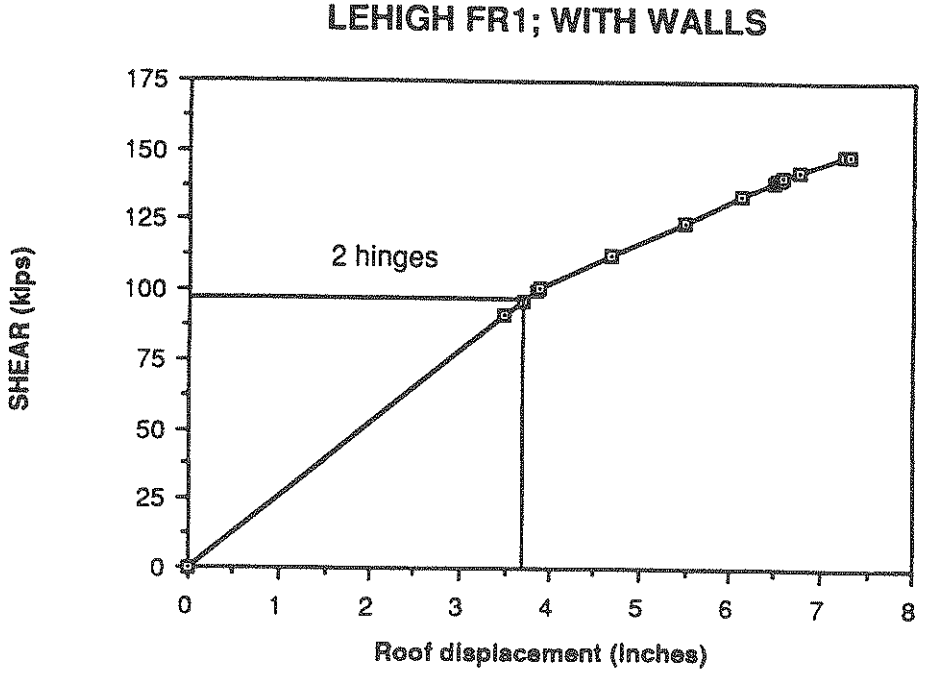

FIGURE 5-12

Plots of Shear versus Roof Displacement for Frame 1.

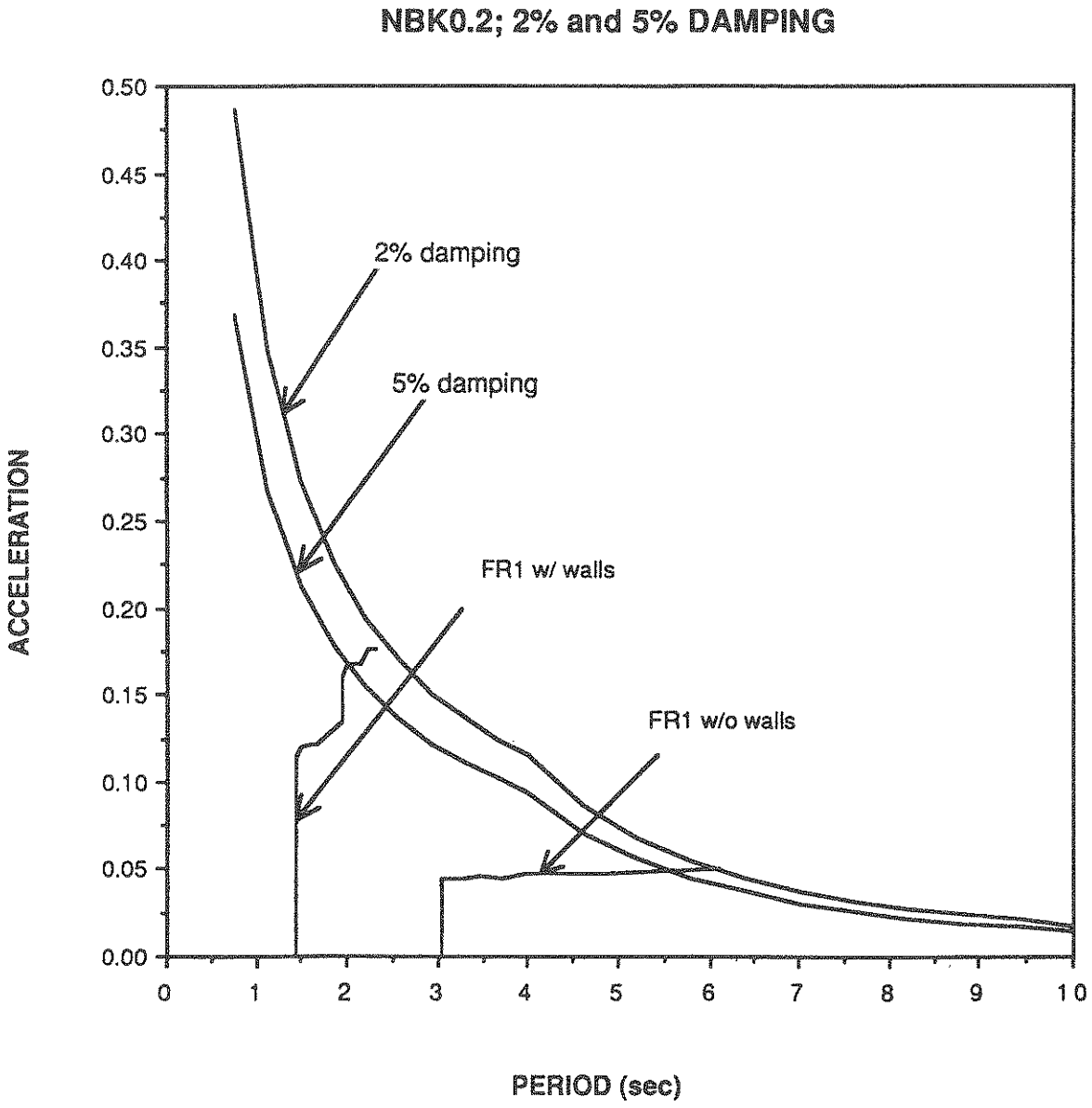

FIGURE 5-13

Capacity Spectra for Frame 1 with and without walls for the NBK0.2 input spectrum.

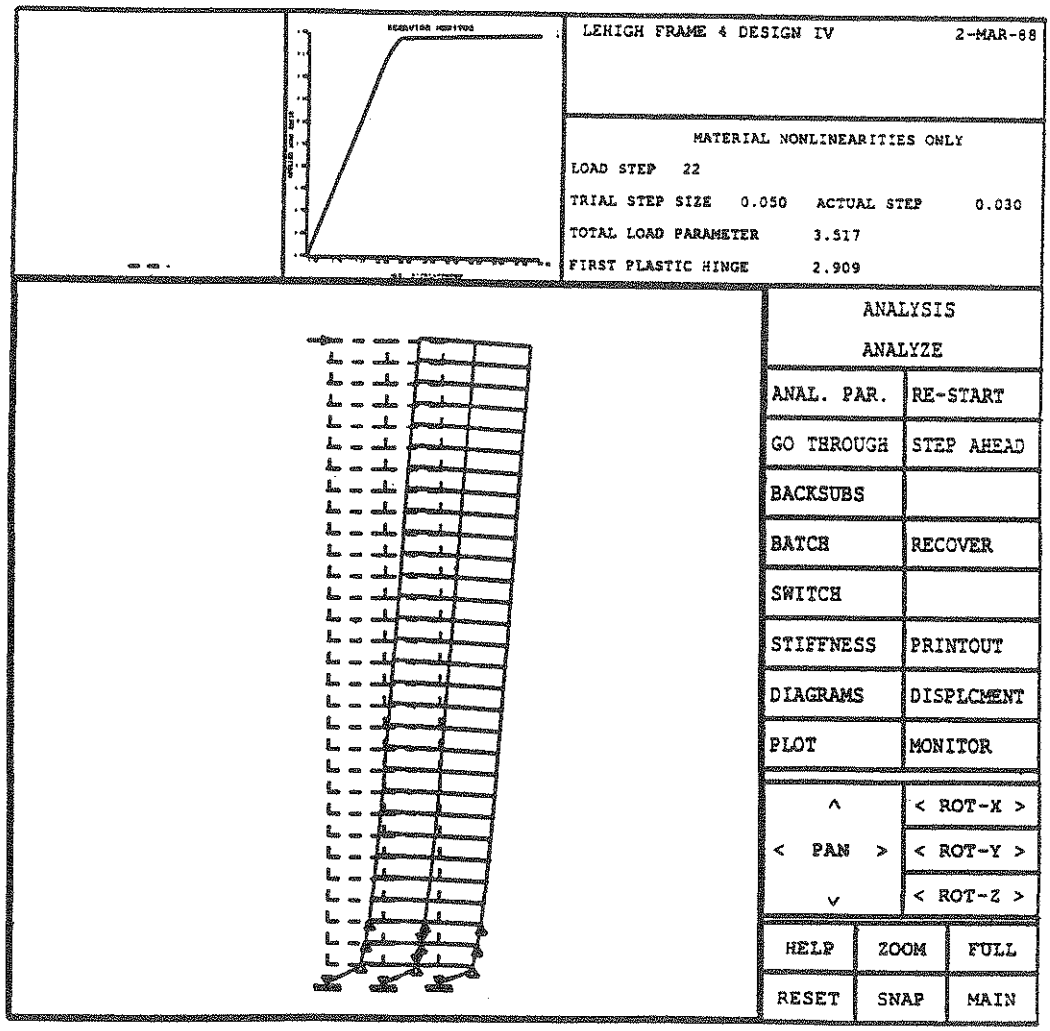

FIGURE 5-14

Deflected Shape of Frame 4.

Figure 5–15, shows the capacity spectrum superimposed on the NBK0.1 input. The elastic period for this structure is 6.6 sec. and it shifts to 12 sec at the formation of a mechanism. The inelastic period is 6.8 sec and the expected inelastic acceleration is 0.018 sec. Using these values and figures 5–16 and 5–17, it was determined that the expected inelastic base shear is 68 kips and the expected drift 12 inches. For this earthquake the structure would not suffer considerable damage since only three hinges are expected to form. The reason for this is that the structure is very flexible and the level of forces created during this level of earthquake is very small.

5.2.3 Frame 6

Frame 6 is a 10-story 5-bay structure. The deflected shape of the structure with and without walls is shown in figure 5–18. As in the case of Frame 4, the lower stories suffer most of the damage in the case of the frame without walls, while the top stories suffer no damage. The capacity spectrum superimposed on the NBK0.1 input is shown in figure 5–19. The elastic period of the structure without walls is 3.3 sec while the one with walls it is 1.79 sec. The period shifts to 13.5 sec for the structure without walls and to 4.16 sec for the structure with walls. This shows that the frame without walls is very flexible. The addition of walls makes the structure stiffer and the period is considerably reduced. The inelastic period of the structure without walls, for this demand spectrum, is 4.3 sec and of the one with walls 2.35 sec. This corresponds to an inelastic acceleration of 0.045 and 0.08 for the structure without and with walls respectively. Using these values and figures 5–20 and 5–21, it was found that the base shear for the structure without walls is 57.2 kips and the top story drift 7.2 inches, while for the one with walls 97.5 kips and 4 inches. In the case of the frame without walls, 11 hinges form while in the case of the one with walls three hinges form.

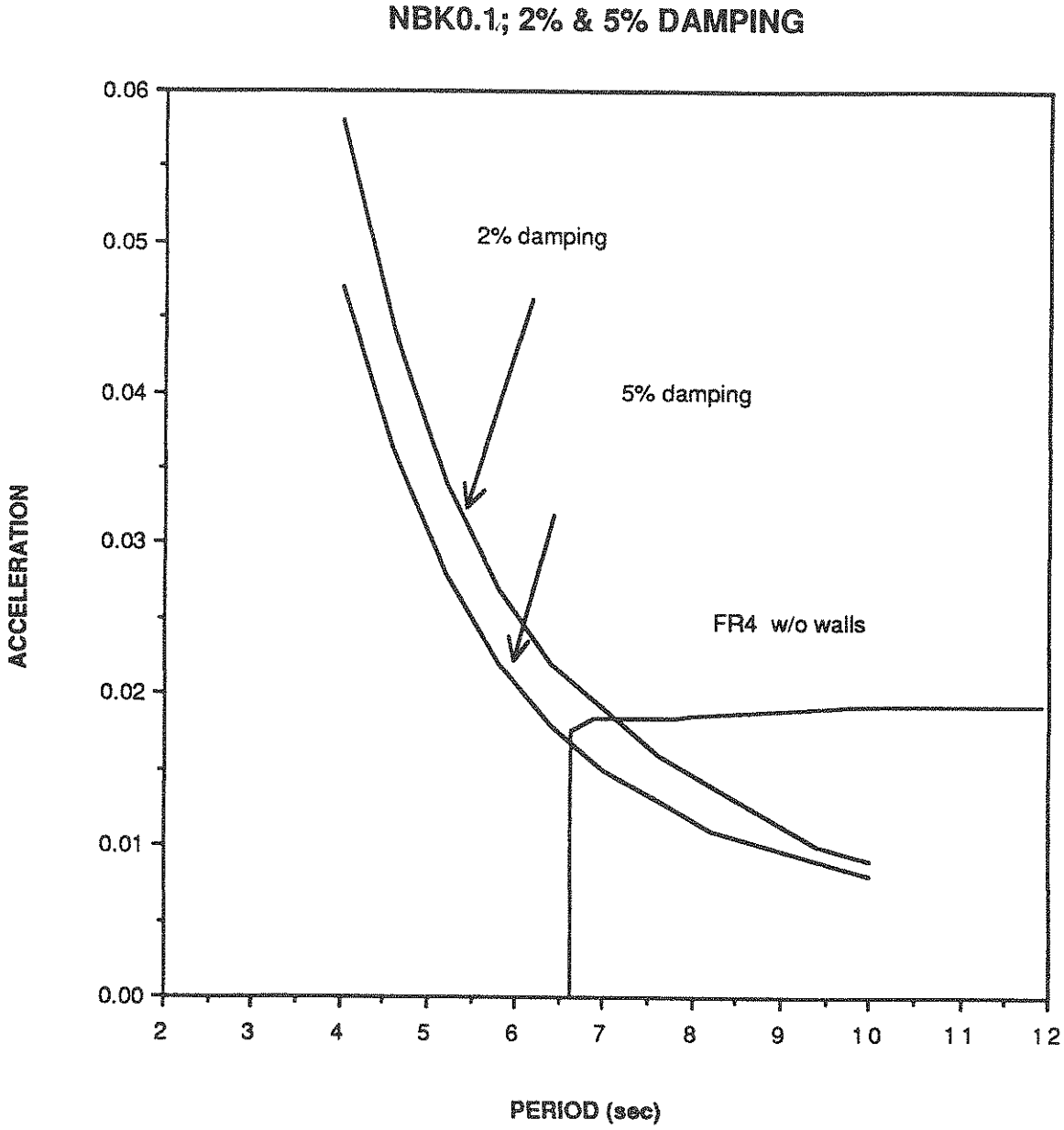

FIGURE 5-15

Capacity Spectrum for Frame 4 Without Walls with the NBK0.1 Input Spectrum.

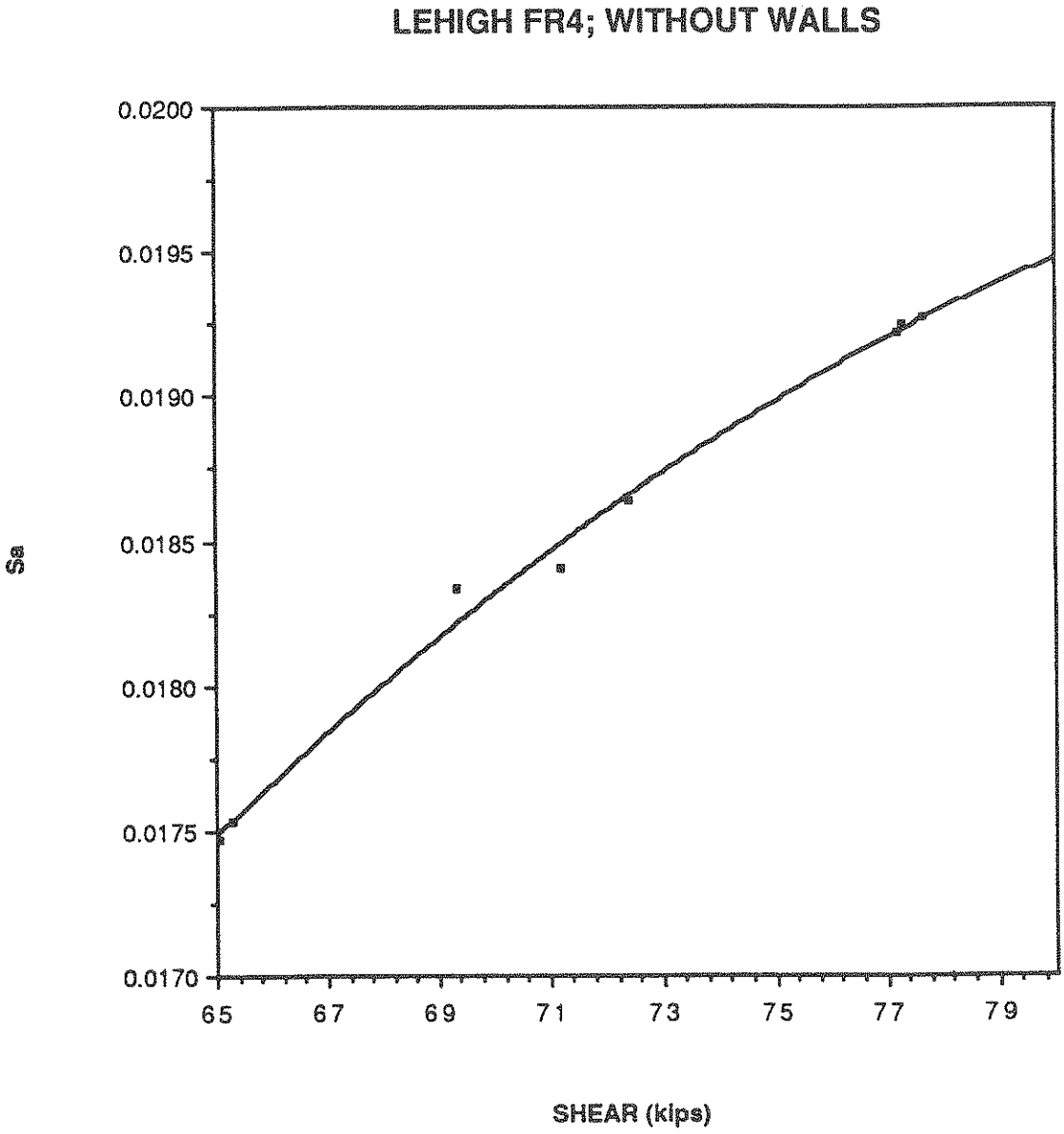

FIGURE 5-16

Plot of Acceleration versus Shear for Frame 4.

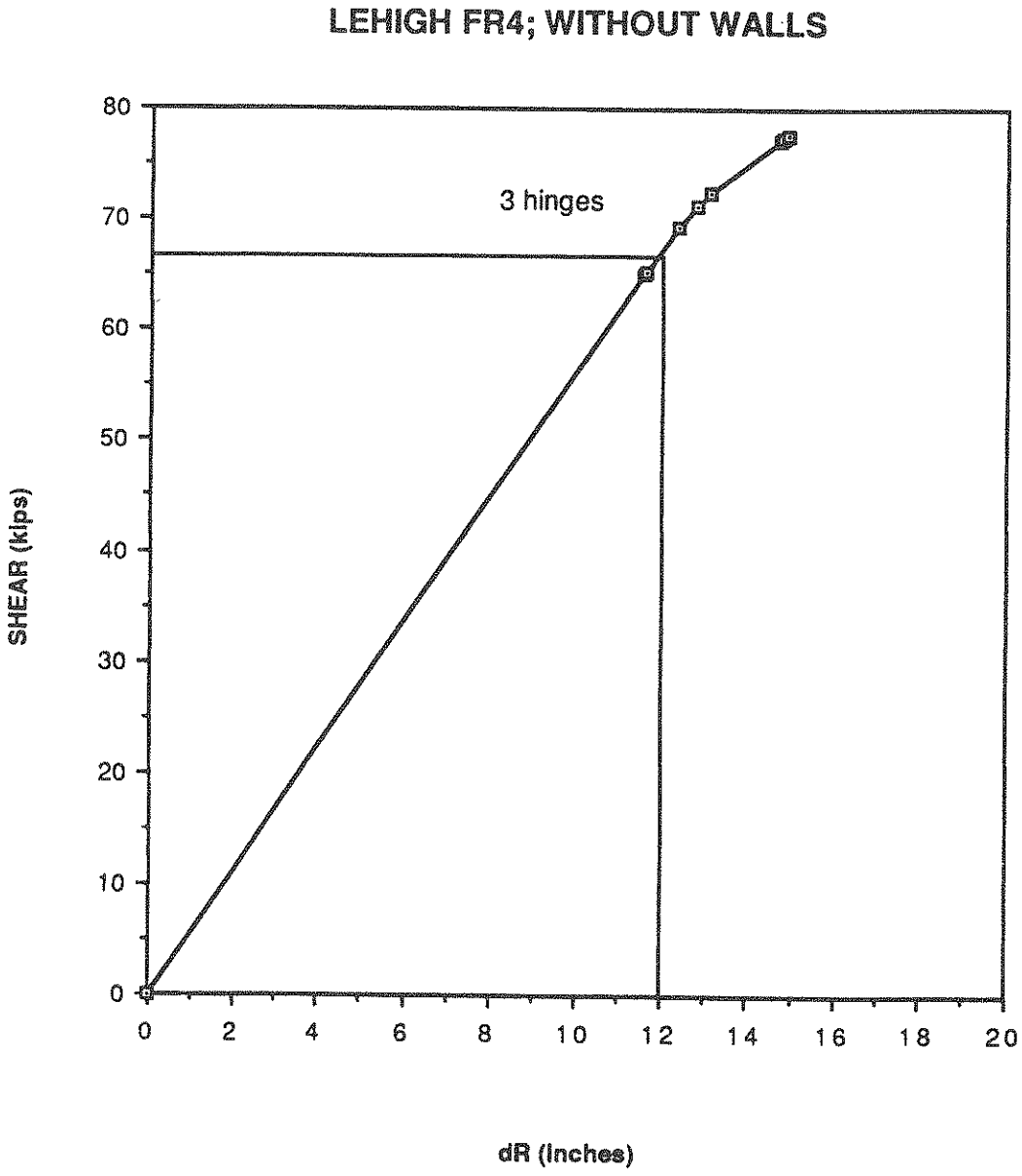

FIGURE 5-17

Plot of Shear versus Roof Displacement for Frame 4.

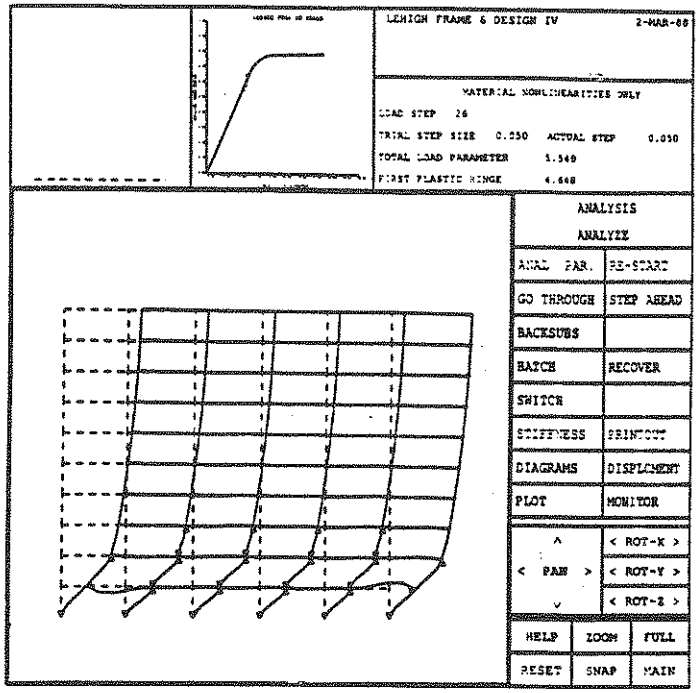

a. Frame 6 without walls

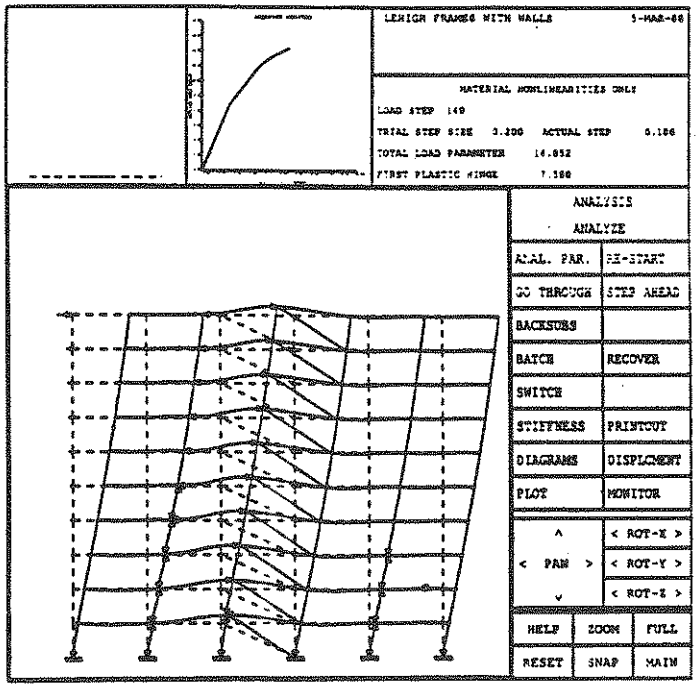

b. Frame 6 with walls

FIGURE 5-18

Deflected Shapes of Frame 6 With and Without Walls.

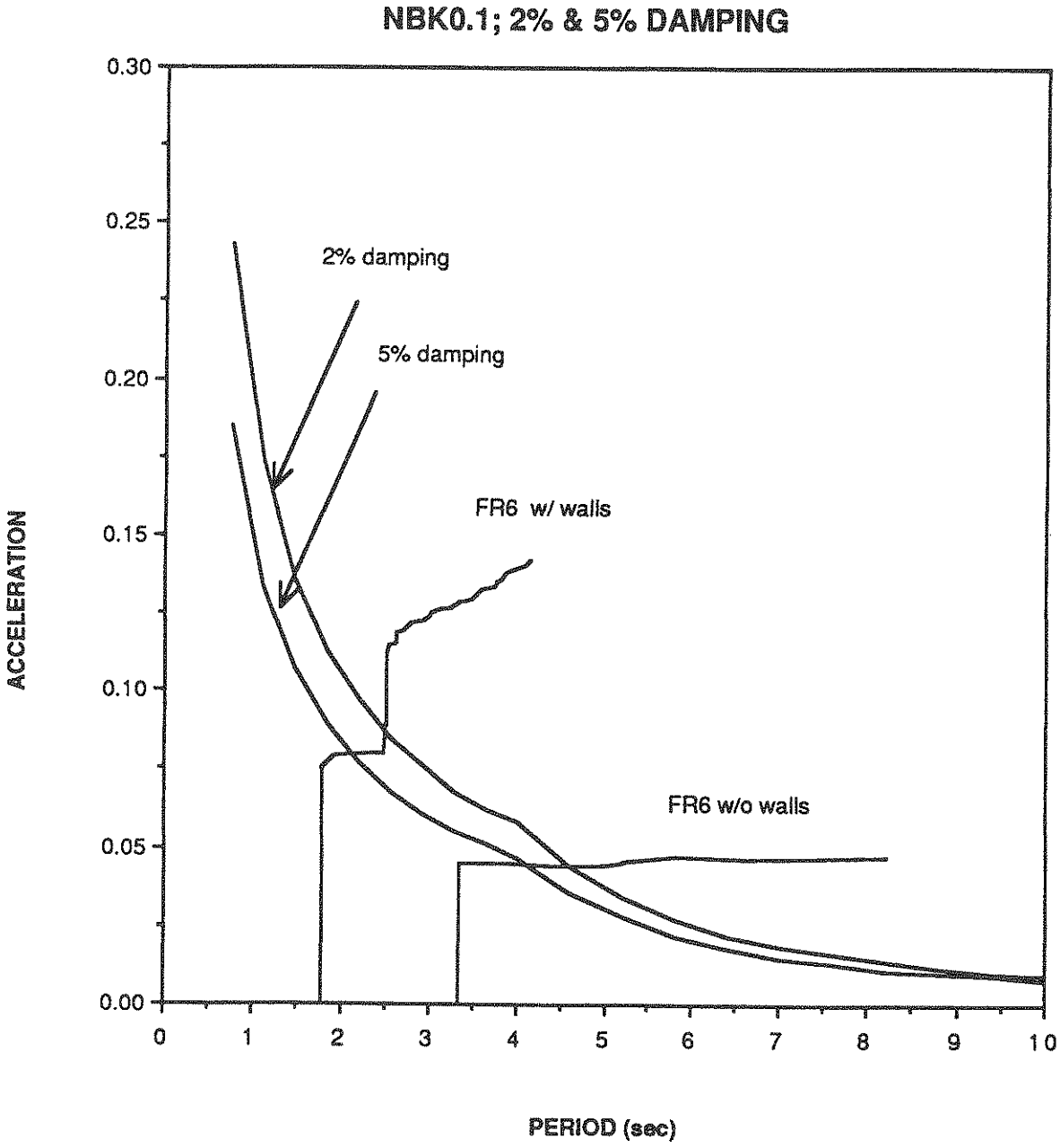

FIGURE 5-19

Capacity Spectra for Frame 6 with and without Walls for the NBK0.1 Design Spectrum.

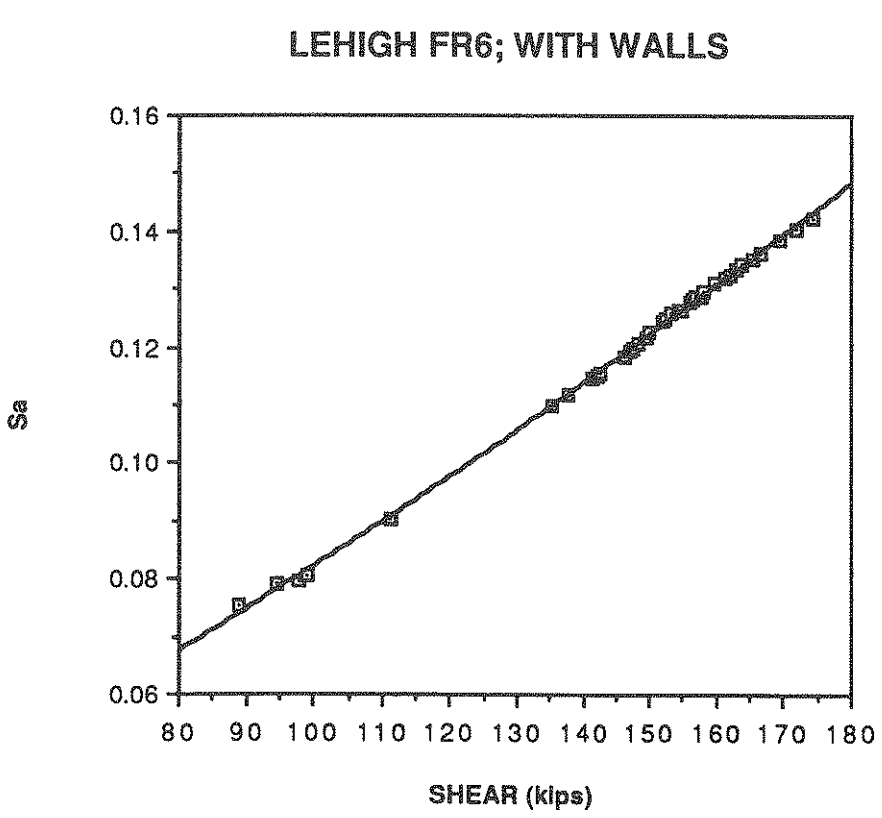

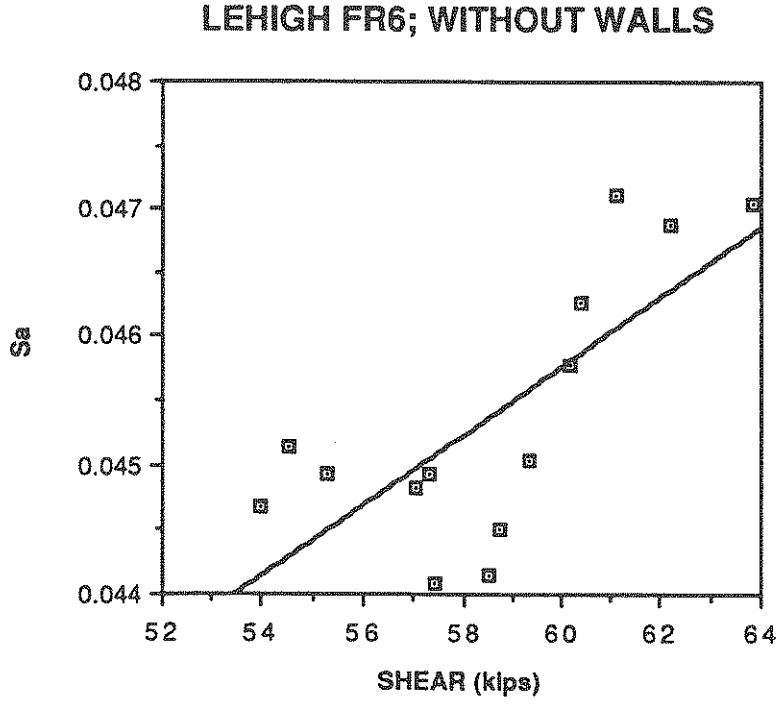

FIGURE 5-20

Plot of Acceleration versus Shear for Frame 6.

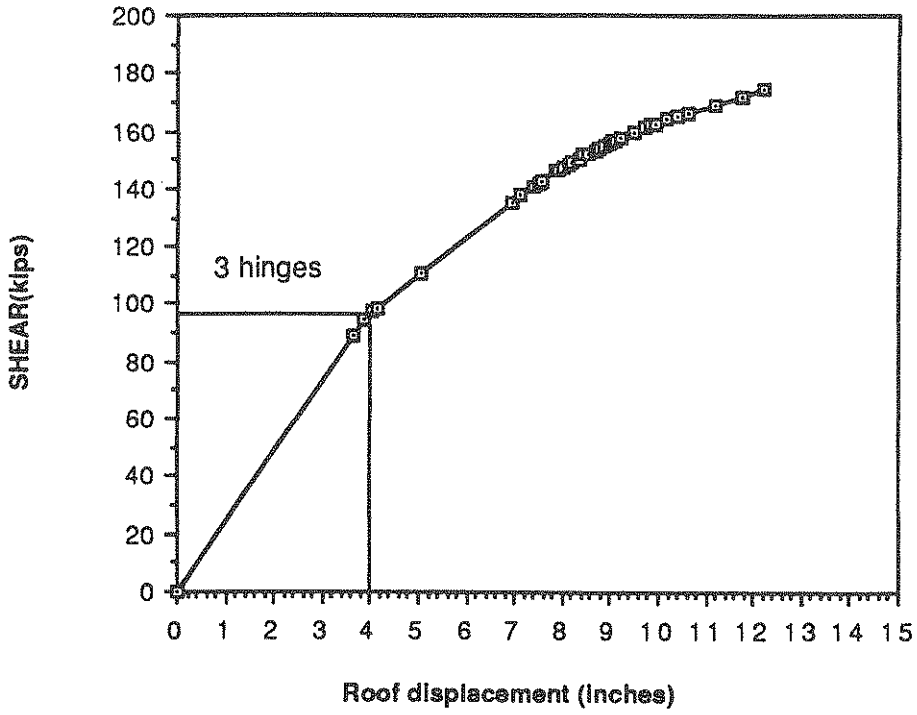

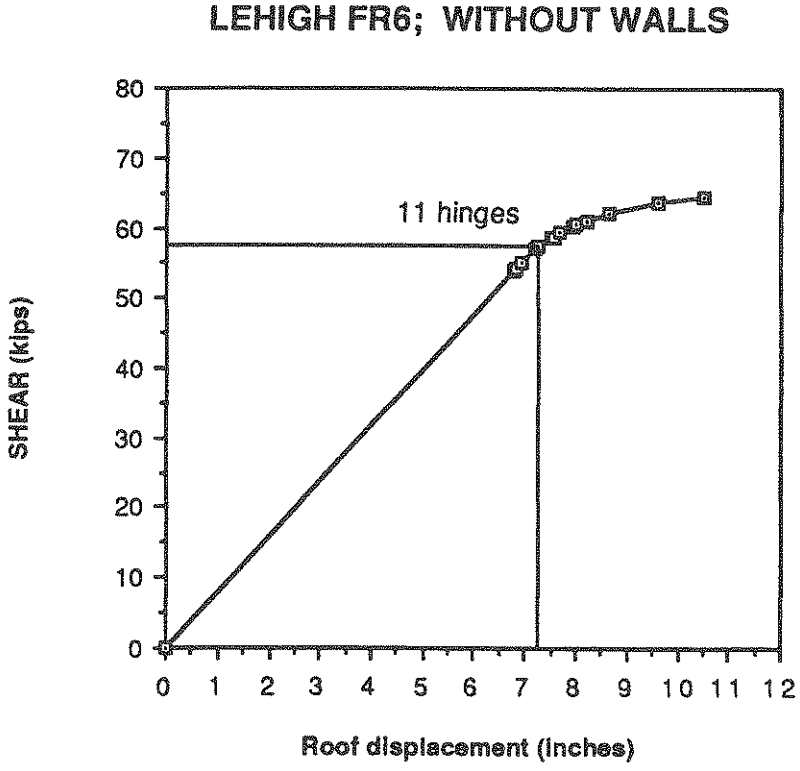

FIGURE 5-21

Plot of Shear versus Roof Displacement for Frame 6.

Frame 6 was also subjected to the NBK0.2 input (figure 5–22). Similar conclusions to the ones above can be drawn. In this case the structure is capable of withstanding this level of earthquake, but with a higher level of damage.

The results for the analyses for the NBK0.1 input are summarized in table 5–I.

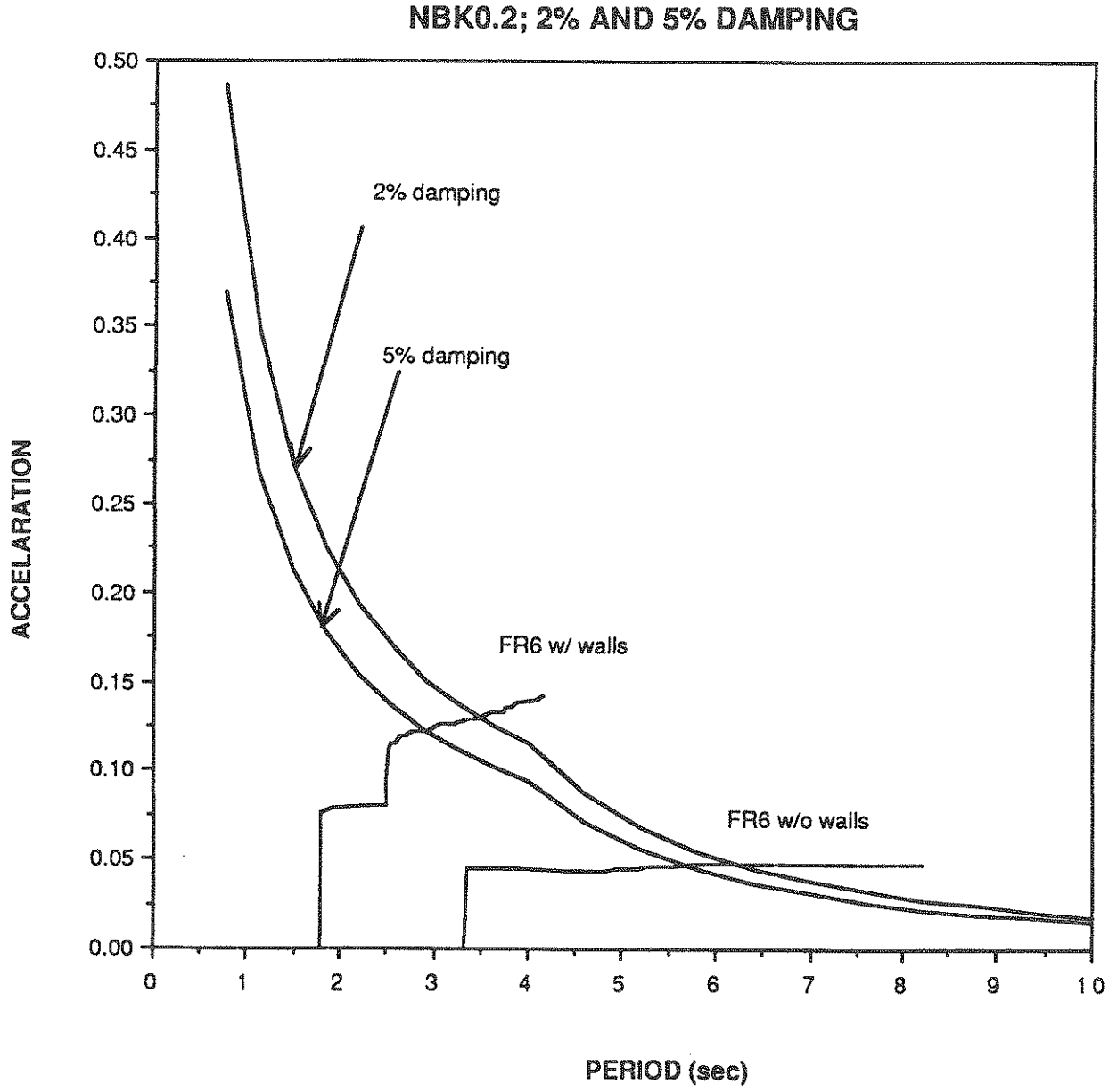

FIGURE 5-22

Capacity Spectra for Frame 6 with and without walls for the NBK0.2 Input Design Spectrum.

		ELASTIC PERIOD (sec)	ELASTIC ACCELER.	RANGE OF PERIODS (sec)	T_{inel} (sec)	$(Sa)_{inel}$	V_{inel} (kips)	$(dR)_{inel}$ (inches)	No OF HINGES
FRAME 1	bare	3.04	0.04	3.04-6	4.17	0.048	41	6.7	14
	infill	1.43	0.11	1.43-2.2	1.6	0.12	98	3.7	2
FRAME 4	bare	6.6	0.017	6.6-12	6.8	0.018	68	12.0	3
	infill	-	-	-	-	-	-	-	-
FRAME 6	bare	3.3	0.044	3.3-13.5	4.3	.045	57.2	7.2	11
	infill	1.79	0.076	1.79-4.16	2.35	0.08	97.5	4.0	3

TABLE 5-I

Results of the Analyses for NBK0.1.

SECTION 6
SUMMARY AND CONCLUSIONS

A preliminary study of the effects of infill walls on the nonlinear dynamic characteristics of infilled frames is reported. A model was implemented for idealizing infilled walls using the equivalent strut method. Two programs were used and modified: the preprocessor for frames (PREPF) and the static analysis and design program (STAND). The load–displacement curve, used to model the behavior of infilled frames under monotonic loading, consisted of a linear elastic part (straight line), and a strength degrading part (decaying exponential). The Capacity Spectrum method was used to estimate the response of structures for earthquakes using first order inelastic (material nonlinear) static analyses.

From the results it can be concluded that the equivalent strut method, as implemented here, is able to predict the overall behavior of infilled frames. All of the characteristics of infilled frames observed during experiments can be obtained using the model in STAND. Therefore, the equivalent strut method can provide a good estimate of the behavior of an infilled frame provided that the assumptions on which the method is based are satisfied. The most restrictive of the assumptions is that no openings are allowed in the infills. Since, in most of the cases, infill frames are used as partitions, they have openings such as doors and/or windows. In situations where openings are present, the equivalent strut approach will overestimate both the strength and stiffness of the infill wall and consequently that of the infilled frame. A simple way around this would be to decrease the calculated equivalent strut area by an amount equal to the percentage of the

area of the openings with respect to the total infill area. This, of course, would be a gross approximation since the failure modes of a panel with openings, are different from those of a panel without openings.

In all the analyses that were performed the structures have shown a shift of their period as the load was increased proportionally. The infills decreased the periods of the structures, but at the same time increased the level of forces that the structure had to carry. Despite this, the damage of the infilled structures analyzed was less than the one of the bare frames. For frame 1, although the infills have increased the base shear from 41 kips to 98 kips, the damage to the structure was significantly less; in the bare frame 14 hinges formed while in the infilled frame only two. Similar results were obtained for Frame 6.

Another effect of the infills was that they decreased the roof drift. This was due to the fact that infilled frames are stiffer than bare frames. In all the cases examined, the roof displacements were large. This was due to the high flexibility of the Lehigh frames, which have a soft first story. Most of the roof displacement was due to the displacement which was taking place at the first story.

The Capacity spectrum method gives to the designer an idea of how the structure will behave under a particular earthquake, without having to perform a dynamic analysis. What is attractive about this method is that once the capacity spectrum is constructed, any number of earthquake or design spectra can be superimposed, and, without any further calculations, the behavior of the structure can be examined for various earthquakes and damping values.

To improve the modelling of infill walls, load–displacement curves should be provided for the infill, with a smoother transition from the linear elastic part to the degrading strength one. As it can be observed from the results presented, the transition is rather

abrupt and a cusp is formed on the load–displacement curve of an infilled frame when an infill wall fails and the strength starts degrading. This is not in agreement with experimental results which show a much smoother and rounded transition. A way of implementing this would be to provide three curves to idealize the load–displacement behavior of an infill: the two presented here plus a third one which would idealize the transition region.

A check should be provided to avoid excessive numerical drift from the load–displacement curve of the infilled wall. Since the simple step incremental solution method was used, it is possible, if too large a step is used, to drift excessively from the assumed load– displacement curve and in this way cause a large force imbalance. This can be avoided by providing a band around the load–displacement curve; if the solution is outside this band, the load step should be decreased, so as to avoid excessive drift.

Another way to avoid excessive numerical drift is the use of another solution scheme. In STAND there already exist two more solution methods: the predictor corrector method and the Newton–Raphson iteration. Either of the schemes will follow the load–displacement curve of the infill closer than the simple step incremental solution. The Newton–Raphson iteration should practically eliminate this problem since it iterates until the unbalanced force vector disappears.

Finally, additional experimental results for steel infilled frames should be obtained to confirm the models used in the idealization. Most of the results available in the literature are for reinforced concrete frames. The material models in STAND are for steel and therefore the experimental results for concrete frames could not be used for analysis and comparison.

SECTION 7

REFERENCES

1. Laurence F. Kahn, Robert D. Hanson, "Infilled Walls for Earthquake Strengthening", Journal of the Structural Division, ASCE, Vol.105, No. ST2, FEBRUARY, 1979, pp.283–296.

2. Mainstone, R. J., "On the Stiffnesses and Strengths of Infilled Frames", Current Paper CP 2/72, Building Research Station, Feb. 1972, Reprinted from Proceedings, Institution of Civil Engineers, 1971 Supplement (iv), paper 7360 S, pp. 57-90.

3. Lu Le-Wu, Ozer E., Daniels J. H., Okten O. S., Morino S., "Frame Stability and Design of Columns in Unbraced Multistory Steel Frames", Fritz Engineering Laboratory Report No. 375.2, Lehigh University, July 1975.

4. Wood, R. H., "Stability of Tall Buildings", Proceedings ICE, Sept. 1958, pp.69–102

5. Benjamin, Jack E. and Williams, Harry A., "The Behavior of One Story Reinforced Concrete Shear Walls," Journal of the Structural Division, ASCE, May 1957, pp.1254 I–49.

6. Benjamin, Jack E. and Williams, Harry A., "The Behavior of One Story Brick Shear Walls," Journal of the Structural Division, ASCE, May 1958, pp.1723 I–30.

7. Holmes, M., "Steel Frames With Brickwork and Concrete Infilling", Proceedings Institute of Civil Engineers, 1961, vol. 19, pp. 473.

8. Stafford Smith, Bryan, "Model Test Results of Vertical and Horizontal Loading of Infilled Frames," ACI Journal, August 1968, pp. 618-624.

9. Carter, C. and Stafford Smith, B., " Structural Behavior of Masonry Infilled Frames Subjected to Racking Loads," Proceedings, International Conference on Masonry Structural Systems, Austin, Texas, 1967.

10. Stafford Smith, Bryan, "Lateral Stiffness of Infilled Frames," Journal of the Structural Division, ASCE, Dec. 1962, pp. 183-199.

11. Stafford Smith, Bryan, "Behavior of square Infilled Frames," Journal of the Structural Division, ASCE, Feb. 1966, pp. 381-403.

12. Stafford Smith, Bryan, "The composite Behavior of Infilled Frames," Proceedings, Symposium on Tall Buildings, University of Southampton, April 1966, Pergamon Press, 1967.

13. Stafford Smith, Bryan, and Carter, C., "A Method of Analysis for Infilled Frames," ICE, vol. 44, Sept/Dec. 1969, pp. 31-48.

14. Malick, D. V. and Severn, R. T., "The Behavior of Infilled Frames under Static Loading, " ICE, Sept./Dec. 1967, vol.38, pp. 639-656.

15. Mainstone, R. J. and Weeks, G. A., "The influence of a Bounding Frame on the Racking Stiffness and Strengths of Brick Walls", Current Paper CP 3/72, Building Research Station, Feb. 1972, also published in Proceedings, Second International Brick Masonry Conference (SIBMAC), 1971, pp.165-171.

16. Mainstone, R., J., "Supplementary Note on the Stiffnesses and Strengths of Infilled Frames", Current Paper CP 13/74, Building Research Station, Feb. 1974.

17. Liauw, T. C. and Kwan, K.H., "New Development in research of infilled frames",Proceedings of the Eighth World Conference on Earthquake Engineering, 1984, vol. IV, pp. 623–630.

18. Liauw, T. C. and Kwan, K.H., "Non-linear analysis of multistory infilled frames", Proc. Instn Civ. Engrs, Part2, 1982, 73, June, pp. 441-454

19. Liauw, T. C. and Kwan, K.H., "Plastic theory of non-integral infilled frames", Proc. Instn Civ. Engrs, Part2, 1983, 75, Sept., pp. 379-396

20. Liauw, T. C. and Kwan, K.H., "Plastic theory of infilled frames with finite interface shear strength", Proc. Instn Civ. Engrs, Part2, 1983, 75, Dec., pp. 707-723

21. R. Zarnic, M. Tomazevic, "The Behavior of Masonry Infilled Reinforced Concrete Frames Subjected to Cyclic Lateral Loading",Proceedings of the Eighth World Conference on Earthquake Engineering, 1984, vol. VI, pp. 863-870.

22. Yorulmaz M., Sozen M. A.: "Behavior of single-story reinforced concrete frames with filler walls", Structural Research Series No. 337, University of Illinois, 1968

23. Klingner, R. E. and Bertero, V. V., "Infilled Frames in Earthquake Resistant Construction", Report No. EERC 76-32, Earthquake Engineering Research Center, University of California, Berkeley, California, Dec. 1976.

24. Freeman, S. A., "Prediction of Response of Concrete Buildings to Severe Earthquake Motion", Douglas McHenry International Symposium on Concrete and Concrete Structures, SP-55, American Concrete Institute, Detroid, Michigan, 1978, pp. 589-605.

25. Porter, F. L., and Powell, G. H., "Static and Dynamic Analysis of Inelastic Frame Structures", Report No. EERC 71-3, Earthquake Engineering Research Center, University of California, Berkeley, California, 1971.

26. Orbison, J. G., "Nonlinear static analysis of Three–Dimensional steel frames", A Thesis presented to the faculty of Cornell University, Ithaca, New York, March 1982.

27. Pesquera Morales, C. I., "Integrated Analysis and Design of Steel Frames With Interactive Computer Graphics", A Thesis presented to the faculty of Cornell University, Ithaca, New York, March 1984.

28. Klingner, R. E., "Mathematical Modeling of Infilled Frames", American Concrete Institute, SP–63, 1980, pp. 1–25.

APPENDIX A

DERIVATION OF EQUATIONS OF CAPACITY SPECTRUM METHOD

In this appendix the derivations for equations (3.2), (3.3) and (3.4) are presented.

1. Derivation of equation (3.2).

The equation for the modal roof participation factor is

$$\frac{d_R}{S_d} = \frac{\left(\sum m \Phi\right)\left(\Phi_R\right)}{\sum m \Phi^2}$$

The generalized displacement can be expressed as

$$q_{max} = \frac{\Gamma}{\omega}(S_v) = \frac{\Gamma(S_a)}{\omega^2} = \Gamma(S_d)$$

where

q_{max} = generalized displacement

Γ = participation factor

S_a = spectral acceleration

S_v = spectral velocity

S_d = spectral displacement

ω = angular frequency

From the above we get that

$$\Gamma = q_{max} / S_d$$

The participation factor and the roof displacement, d_R, are

$$\Gamma = \frac{\sum m \Phi}{\sum m \Phi^2} \qquad q_{max} \Phi_R = d_R \quad \text{from which}$$

$$\frac{\sum m \Phi}{\sum m \Phi^2} = \frac{q_{max}}{S_d}$$

Multiplying both sides by Φ_R, the element of the eigenvector corresponding to the roof of the structure, the equation for the modal roof participation factor is

$$\frac{q_{max} \Phi_R}{S_d} = \frac{\left(\sum m \Phi\right)\left(\Phi_R\right)}{\sum m \Phi^2} \quad ==> \quad \frac{d_R}{S_d} = \frac{\left(\sum m \Phi\right)\left(\Phi_R\right)}{\sum m \Phi^2}$$

2. Derivation of equation (3.3).

The equation for the modal effective weight is

$$\frac{C_B}{S_a} = \frac{\left(\sum m \Phi\right)^2}{\sum m \sum m \Phi^2}$$

The force at each level of the structure is given by

$$\{P\} = [M]\{\Phi\}\,\Gamma S_a$$

where Γ is the participation factor, as defined on the previous page.

Assuming a diagonal mass matrix and using the above equations, the base shear, V, is then given by

$$V = \sum_{i=1}^{n} P_i = \left(\sum_{i=1}^{n} m_i \Phi_i\right) \Gamma S_a = \left(\sum m \Phi\right) \frac{\left(\sum m \Phi\right) S_a}{\sum m \Phi^2}$$

$$= \frac{\left(\sum m \Phi\right)^2 S_a}{\sum m \Phi^2}$$

The base shear is also defined as,

$$V = C_B W$$

Equating the two equations we get,

$$\frac{C_B}{S_a} = \frac{\left(\sum m \Phi\right)^2}{\sum m \Phi^2 \sum m}$$

where S_a is given as a fraction of the acceleration of gravity, g.

3. Derivation of equation (3.4)

The equation for the period of the structure is

$$T = 2\pi\sqrt{\frac{S_d}{S_a}}$$

which follows from the following relationships

$$T = \frac{2\pi}{\omega} \quad \text{and} \quad S_a = \omega^2 S_d \quad \text{hence} \quad T = 2\pi\sqrt{\frac{S_d}{S_a}}$$

NATIONAL CENTER FOR EARTHQUAKE ENGINEERING RESEARCH
LIST OF PUBLISHED TECHNICAL REPORTS

The National Center for Earthquake Engineering Research (NCEER) publishes technical reports on a variety of subjects related to earthquake engineering written by authors funded through NCEER. These reports are available from both NCEER's Publications Department and the National Technical Information Service (NTIS). Requests for reports should be directed to the Publications Department, National Center for Earthquake Engineering Research, State University of New York at Buffalo, Red Jacket Quadrangle, Buffalo, New York 14261. Reports can also be requested through NTIS, 5285 Port Royal Road, Springfield, Virginia 22161. NTIS accession numbers are shown in parenthesis, if available.

NCEER-87-0001 "First-Year Program in Research, Education and Technology Transfer," 3/5/87, (PB88-134275/AS).

NCEER-87-0002 "Experimental Evaluation of Instantaneous Optimal Algorithms for Structural Control," by R.C. Lin, T.T. Soong and A.M. Reinhorn, 4/20/87, (PB88-134341/AS).

NCEER-87-0003 "Experimentation Using the Earthquake Simulation Facilities at University at Buffalo," by A.M. Reinhorn and R.L. Ketter, to be published.

NCEER-87-0004 "The System Characteristics and Performance of a Shaking Table," by J.S. Hwang, K.C. Chang and G.C. Lee, 6/1/87, (PB88-134259/AS).

NCEER-87-0005 "A Finite Element Formulation for Nonlinear Viscoplastic Material Using a Q Model," by O. Gyebi and G. Dasgupta, 11/2/87, (PB88-213764/AS).

NCEER-87-0006 "Symbolic Manipulation Program (SMP) - Algebraic Codes for Two and Three Dimensional Finite Element Formulations," by X. Lee and G. Dasgupta, 11/9/87, (PB88-219522/AS).

NCEER-87-0007 "Instantaneous Optimal Control Laws for Tall Buildings Under Seismic Excitations," by J.N. Yang, A. Akbarpour and P. Ghaemmaghami, 6/10/87, (PB88-134333/AS).

NCEER-87-0008 "IDARC: Inelastic Damage Analysis of Reinforced Concrete Frame - Shear-Wall Structures," by Y.J. Park, A.M. Reinhorn and S.K. Kunnath, 7/20/87, (PB88-134325/AS).

NCEER-87-0009 "Liquefaction Potential for New York State: A Preliminary Report on Sites in Manhattan and Buffalo," by M. Budhu, V. Vijayakumar, R.F. Giese and L. Baumgras, 8/31/87, (PB88-163704/AS). This report is available only through NTIS (see address given above).

NCEER-87-0010 "Vertical and Torsional Vibration of Foundations in Inhomogeneous Media," by A.S. Veletsos and K.W. Dotson, 6/1/87, (PB88-134291/AS).

NCEER-87-0011 "Seismic Probabilistic Risk Assessment and Seismic Margins Studies for Nuclear Power Plants," by Howard H.M. Hwang, 6/15/87, (PB88-134267/AS). This report is available only through NTIS (see address given above).

NCEER-87-0012 "Parametric Studies of Frequency Response of Secondary Systems Under Ground-Acceleration Excitations," by Y. Yong and Y.K. Lin, 6/10/87, (PB88-134309/AS).

NCEER-87-0013 "Frequency Response of Secondary Systems Under Seismic Excitation," by J.A. HoLung, J. Cai and Y.K. Lin, 7/31/87, (PB88-134317/AS).

NCEER-87-0014 "Modelling Earthquake Ground Motions in Seismically Active Regions Using Parametric Time Series Methods," by G.W. Ellis and A.S. Cakmak, 8/25/87, (PB88-134283/AS).

NCEER-87-0015 "Detection and Assessment of Seismic Structural Damage," by E. DiPasquale and A.S. Cakmak, 8/25/87, (PB88-163712/AS).

NCEER-87-0016 "Pipeline Experiment at Parkfield, California," by J. Isenberg and E. Richardson, 9/15/87, (PB88-163720/AS).

NCEER-87-0017 "Digital Simulation of Seismic Ground Motion," by M. Shinozuka, G. Deodatis and T. Harada, 8/31/87, (PB88-155197/AS). This report is available only through NTIS (see address given above).

NCEER-87-0018 "Practical Considerations for Structural Control: System Uncertainty, System Time Delay and Truncation of Small Control Forces," J.N. Yang and A. Akbarpour, 8/10/87, (PB88-163738/AS).

NCEER-87-0019 "Modal Analysis of Nonclassically Damped Structural Systems Using Canonical Transformation," by J.N. Yang, S. Sarkani and F.X. Long, 9/27/87, (PB88-187851/AS).

NCEER-87-0020 "A Nonstationary Solution in Random Vibration Theory," by J.R. Red-Horse and P.D. Spanos, 11/3/87, (PB88-163746/AS).

NCEER-87-0021 "Horizontal Impedances for Radially Inhomogeneous Viscoelastic Soil Layers," by A.S. Veletsos and K.W. Dotson, 10/15/87, (PB88-150859/AS).

NCEER-87-0022 "Seismic Damage Assessment of Reinforced Concrete Members," by Y.S. Chung, C. Meyer and M. Shinozuka, 10/9/87, (PB88-150867/AS). This report is available only through NTIS (see address given above).

NCEER-87-0023 "Active Structural Control in Civil Engineering," by T.T. Soong, 11/11/87, (PB88-187778/AS).

NCEER-87-0024 Vertical and Torsional Impedances for Radially Inhomogeneous Viscoelastic Soil Layers," by K.W. Dotson and A.S. Veletsos, 12/87, (PB88-187786/AS).

NCEER-87-0025 "Proceedings from the Symposium on Seismic Hazards, Ground Motions, Soil-Liquefaction and Engineering Practice in Eastern North America," October 20-22, 1987, edited by K.H. Jacob, 12/87, (PB88-188115/AS).

NCEER-87-0026 "Report on the Whittier-Narrows, California, Earthquake of October 1, 1987," by J. Pantelic and A. Reinhorn, 11/87, (PB88-187752/AS). This report is available only through NTIS (see address given above).

NCEER-87-0027 "Design of a Modular Program for Transient Nonlinear Analysis of Large 3-D Building Structures," by S. Srivastav and J.F. Abel, 12/30/87, (PB88-187950/AS).

NCEER-87-0028 "Second-Year Program in Research, Education and Technology Transfer," 3/8/88, (PB88-219480/AS).

NCEER-88-0001 "Workshop on Seismic Computer Analysis and Design of Buildings With Interactive Graphics," by W. McGuire, J.F. Abel and C.H. Conley, 1/18/88, (PB88-187760/AS).

NCEER-88-0002 "Optimal Control of Nonlinear Flexible Structures," by J.N. Yang, F.X. Long and D. Wong, 1/22/88, (PB88-213772/AS).

NCEER-88-0003 "Substructuring Techniques in the Time Domain for Primary-Secondary Structural Systems," by G.D. Manolis and G. Juhn, 2/10/88, (PB88-213780/AS).

NCEER-88-0004 "Iterative Seismic Analysis of Primary-Secondary Systems," by A. Singhal, L.D. Lutes and P.D. Spanos, 2/23/88, (PB88-213798/AS).

NCEER-88-0005 "Stochastic Finite Element Expansion for Random Media," by P.D. Spanos and R. Ghanem, 3/14/88, (PB88-213806/AS).

NCEER-88-0006 "Combining Structural Optimization and Structural Control," by F.Y. Cheng and C.P. Pantelides, 1/10/88, (PB88-213814/AS).

NCEER-88-0007 "Seismic Performance Assessment of Code-Designed Structures," by H.H-M. Hwang, J-W. Jaw and H-J. Shau, 3/20/88, (PB88-219423/AS).

NCEER-88-0008 "Reliability Analysis of Code-Designed Structures Under Natural Hazards," by H.H-M. Hwang, H. Ushiba and M. Shinozuka, 2/29/88, (PB88-229471/AS).

NCEER-88-0009 "Seismic Fragility Analysis of Shear Wall Structures," by J-W Jaw and H.H-M. Hwang, 4/30/88, (PB89-102867/AS).

NCEER-88-0010 "Base Isolation of a Multi-Story Building Under a Harmonic Ground Motion - A Comparison of Performances of Various Systems," by F-G Fan, G. Ahmadi and I.G. Tadjbakhsh, 5/18/88, (PB89-122238/AS).

NCEER-88-0011 "Seismic Floor Response Spectra for a Combined System by Green's Functions," by F.M. Lavelle, L.A. Bergman and P.D. Spanos, 5/1/88, (PB89-102875/AS).

NCEER-88-0012 "A New Solution Technique for Randomly Excited Hysteretic Structures," by G.Q. Cai and Y.K. Lin, 5/16/88, (PB89-102883/AS).

NCEER-88-0013 "A Study of Radiation Damping and Soil-Structure Interaction Effects in the Centrifuge," by K. Weissman, supervised by J.H. Prevost, 5/24/88, (PB89-144703/AS).

NCEER-88-0014 "Parameter Identification and Implementation of a Kinematic Plasticity Model for Frictional Soils," by J.H. Prevost and D.V. Griffiths, to be published.

NCEER-88-0015 "Two- and Three- Dimensional Dynamic Finite Element Analyses of the Long Valley Dam," by D.V. Griffiths and J.H. Prevost, 6/17/88, (PB89-144711/AS).

NCEER-88-0016 "Damage Assessment of Reinforced Concrete Structures in Eastern United States," by A.M. Reinhorn, M.J. Seidel, S.K. Kunnath and Y.J. Park, 6/15/88, (PB89-122220/AS).

NCEER-88-0017 "Dynamic Compliance of Vertically Loaded Strip Foundations in Multilayered Viscoelastic Soils," by S. Ahmad and A.S.M. Israil, 6/17/88, (PB89-102891/AS).

NCEER-88-0018 "An Experimental Study of Seismic Structural Response With Added Viscoelastic Dampers," by R.C. Lin, Z. Liang, T.T. Soong and R.H. Zhang, 6/30/88, (PB89-122212/AS).

NCEER-88-0019 "Experimental Investigation of Primary - Secondary System Interaction," by G.D. Manolis, G. Juhn and A.M. Reinhorn, 5/27/88, (PB89-122204/AS).

NCEER-88-0020 "A Response Spectrum Approach For Analysis of Nonclassically Damped Structures," by J.N. Yang, S. Sarkani and F.X. Long, 4/22/88, (PB89-102909/AS).

NCEER-88-0021 "Seismic Interaction of Structures and Soils: Stochastic Approach," by A.S. Veletsos and A.M. Prasad, 7/21/88, (PB89-122196/AS).

NCEER-88-0022 "Identification of the Serviceability Limit State and Detection of Seismic Structural Damage," by E. DiPasquale and A.S. Cakmak, 6/15/88, (PB89-122188/AS).

NCEER-88-0023 "Multi-Hazard Risk Analysis: Case of a Simple Offshore Structure," by B.K. Bhartia and E.H. Vanmarcke, 7/21/88, (PB89-145213/AS).

NCEER-88-0024 "Automated Seismic Design of Reinforced Concrete Buildings," by Y.S. Chung, C. Meyer and M. Shinozuka, 7/5/88, (PB89-122170/AS).

NCEER-88-0025 "Experimental Study of Active Control of MDOF Structures Under Seismic Excitations," by L.L. Chung, R.C. Lin, T.T. Soong and A.M. Reinhorn, 7/10/88, (PB89-122600/AS).

NCEER-88-0026 "Earthquake Simulation Tests of a Low-Rise Metal Structure," by J.S. Hwang, K.C. Chang, G.C. Lee and R.L. Ketter, 8/1/88, (PB89-102917/AS).

NCEER-88-0027 "Systems Study of Urban Response and Reconstruction Due to Catastrophic Earthquakes," by F. Kozin and H.K. Zhou, 9/22/88, to be published.

NCEER-88-0028 "Seismic Fragility Analysis of Plane Frame Structures," by H.H-M. Hwang and Y.K. Low, 7/31/88, (PB89-131445/AS).

NCEER-88-0029 "Response Analysis of Stochastic Structures," by A. Kardara, C. Bucher and M. Shinozuka, 9/22/88.

NCEER-88-0030 "Nonnormal Accelerations Due to Yielding in a Primary Structure," by D.C.K. Chen and L.D. Lutes, 9/19/88.

NCEER-88-0031 "Design Approaches for Soil-Structure Interaction," by A.S. Veletsos, A.M. Prasad and Y. Tang, 12/30/88.

NCEER-88-0032 "A Re-evaluation of Design Spectra for Seismic Damage Control," by C.J. Turkstra and A.G. Tallin, 11/7/88, (PB89-145221/AS).

NCEER-88-0033 "The Behavior and Design of Noncontact Lap Splices Subjected to Repeated Inelastic Tensile Loading," by V.E. Sagan, P. Gergely and R.N. White, 12/8/88.

NCEER-88-0034 "Seismic Response of Pile Foundations," by S.M. Mamoon, P.K. Banerjee and S. Ahmad, 11/1/88, (PB89-145239/AS).

NCEER-88-0035 "Modeling of R/C Building Structures With Flexible Floor Diaphragms (IDARC2)," by A.M. Reinhorn, S.K. Kunnath and N. Panahshahi, 9/7/88.

NCEER-88-0036 "Solution of the Dam-Reservoir Interaction Problem Using a Combination of FEM, BEM with Particular Integrals, Modal Analysis, and Substructuring," by C-S. Tsai, G.C. Lee and R.L. Ketter, 12/31/88, to be published.

NCEER-88-0037 "Optimal Placement of Actuators for Structural Control," by F.Y. Cheng and C.P. Pantelides, 8/15/88.

NCEER-88-0038 "Teflon Bearings in Aseismic Base Isolation: Experimental Studies and Mathematical Modeling," by A. Mokha, M.C. Constantinou and A.M. Reinhorn, 12/5/88.

NCEER-88-0039 "Seismic Behavior of Flat Slab High-Rise Buildings in the New York City Area," by P. Weidlinger and M. Ettouney, 10/15/88, to be published.

NCEER-88-0040 "Evaluation of the Earthquake Resistance of Existing Buildings in New York City," by P. Weidlinger and M. Ettouney, 10/15/88, to be published.

NCEER-88-0041 "Small-Scale Modeling Techniques for Reinforced Concrete Structures Subjected to Seismic Loads," by W. Kim, A. El-Attar and R.N. White, 11/22/88, to be published.

NCEER-88-0042 "Modeling Strong Ground Motion from Multiple Event Earthquakes," by G.W. Ellis and A.S. Cakmak, 10/15/88.

NCEER-88-0043 "Nonstationary Models of Seismic Ground Acceleration," by M. Grigoriu, S.E. Ruiz and E. Rosenblueth, 7/15/88.

NCEER-88-0044 "SARCF User's Guide: Seismic Analysis of Reinforced Concrete Frames," by Y.S. Chung, C. Meyer and M. Shinozuka, 11/9/88.

NCEER-88-0045 "First Expert Panel Meeting on Disaster Research and Planning," edited by J. Pantelic and J. Stoyle, 9/15/88.

NCEER-88-0046 "Preliminary Studies of the Effect of Degrading Infill Walls on the Nonlinear Seismic Response of Steel Frames," by C.Z. Chrysostomou, P. Gergely and J.F. Abel, 12/19/88.